

# Ru(II) photosensitizers competent for hypoxic cancers by green light activation

Francisco J. Ballester,<sup>a</sup> Enrique Ortega,<sup>a</sup> Delia Bautista,<sup>b</sup> M. Dolores Santana<sup>a,\*</sup> and José Ruiz<sup>a,\*</sup>

<sup>a</sup> Departamento de Química Inorgánica, Universidad de Murcia, and Biomedical Research Institute of Murcia (IMIB-Arrixaca), E-30071 Murcia, Spain, Email: jruiz@um.es and dsl@um.es.

<sup>b</sup> SAI Universidad de Murcia, E-30071 Murcia, Spain.

## Table of content

1. Starting materials and reagents.....	1
2. Instrumentation.....	1
3. Synthesis.....	2
3.1. Synthesis of the ligands.....	2
3.2. Synthesis of the complexes.....	3
4. NMR experiments.....	7
5. Photophysical properties.....	18
6. Singlet oxygen quantum yields.....	20
7. Stability of complexes 1-5.....	22
7.1. UV-Vis.....	22
7.2. HPLC – MS.....	23
8. Octanol-H <sub>2</sub> O partition coefficient and solubility measures.....	27
9. <sup>1</sup> H-NMR aggregation experiments.....	30
10. Oxidation of NADH.....	31
11. X-ray diffraction.....	33
12. Cell-based assays.....	37
12.1. Cell culture.....	37
12.2. Cytotoxicity assays in the dark.....	37
12.3. Photocytotoxicity assays.....	40
12.4. Metal accumulation in isolated DNA and in whole cells.....	40
12.5. Determination of ROS generation in HeLa cells under hypoxia after the treatment with the Ru complexes using selective scavengers.....	41
12.6. Inhibition of global protein synthesis assay in cancer cells.....	48
12.7. Cell death induction determination by flow cytometry.....	51
13. References.....	52

## 1. Starting materials and reagents

Synthetic manipulations in the preparation of the complexes were carried out under atmosphere of dry nitrogen using Schlenk techniques. Solvents were dried by the usual method.

### Reactives:

4-chloro-3-nitrobenzoic acid, butylamine, trimethylamine, zinc in powder, ammonium formate, benzaldehyde, biphenyl-4-carboxaldehyde, 2-naphthaldehyde, trifluoroacetic acid, CDDP, magnesium sulphate, potassium acetate, potassium hexafluorophosphate, 1,10-phenanthroline monohydrate, ethylenediamine, o-phenylenediamine, sodium pyruvate, sodium azide, 4,5-dihydroxybenzene-1,3-disulfonate (tiron), D-mannitol, 1,3-diphenylisobenzofuran (DPBF), phosphate buffered saline (PBS) and  $\beta$ -Nicotinamide adenine dinucleotide, reduced disodium salt hydrate (NADH) were purchased to Sigma – Aldrich (Madrid, Spain). Nitric and sulphuric acids were purchased to Scharlau. Ruthenium dimer  $[\text{Ru}(p\text{-cymene})\text{Cl}_2]_2$  from Johnson Matthey. The solvents dimethyl sulfoxide (DMSO), N,N-dimethylformamide (DMF), acetonitrile, diethyl ether, hexane, ethyl acetate and dichloromethane were purchased to Scharlau, and ethanol and methanol from J. Baker. Deuterated solvents acetonitrile-*d*3 and chloroform-*d* were purchase to Euriso-top

## 2. Instrumentation

The  $^1\text{H}$  and  $^{13}\text{C}$  NMR spectra were recorded on Bruker AC 300E, Bruker AV 400, or Bruker AV 600 NMR spectrometer. Chemical shifts are cited relative to  $\text{SiMe}_4$  and were determined by reference to the residual  $^1\text{H}$  and  $^{13}\text{C}$  solvent peaks. UV/Vis spectroscopy was carried out on a PerkinElmer Lambda 750 S spectrometer with operating software. ESI mass (positive mode) analyses were performed on a HPLC/MS TOF 6220. The isotopic distribution of the heaviest set of peaks matched very closely that calculated for the formulation of the complex cation in every case. Excitation and emission spectra were recorded on a Jobin Yvon Fluorolog 3-22 spectrofluorometer with a 450 W xenon lamp double-grating mono-chromators and a TBX-04 photomultiplier. The solution measurements were carried out in a right angle configuration using 10 mm quartz fluorescence cells. Lifetimes were measured using an IBH FluoroHub TCSPC controller and a NanoLED pulse diode excitation source; the estimated uncertainty is  $\pm 10\%$ . The FT-IR spectra were recorded on a Perkin-Elmer 1430 spectrophotometer using potassium bromide. The C, H, N and S analyses were performed with a Carlo Erba model EA 1108 microanalyzer. Irradiation experiment where performed with photoreactor Luzchem EXPO-LED with green light led lamp ( $\lambda = 520 \text{ nm}$ ). The measures of light power where realized using Thorlabs Digital Optical Power and Energy Meter PM100D with S120VC photodiode power sensor.

### 3. Synthesis

#### 3.1. Synthesis of the ligands

The N<sup>N</sup> ligands (**dpq**) and (**dppz**) were synthesized as previously reported [1].

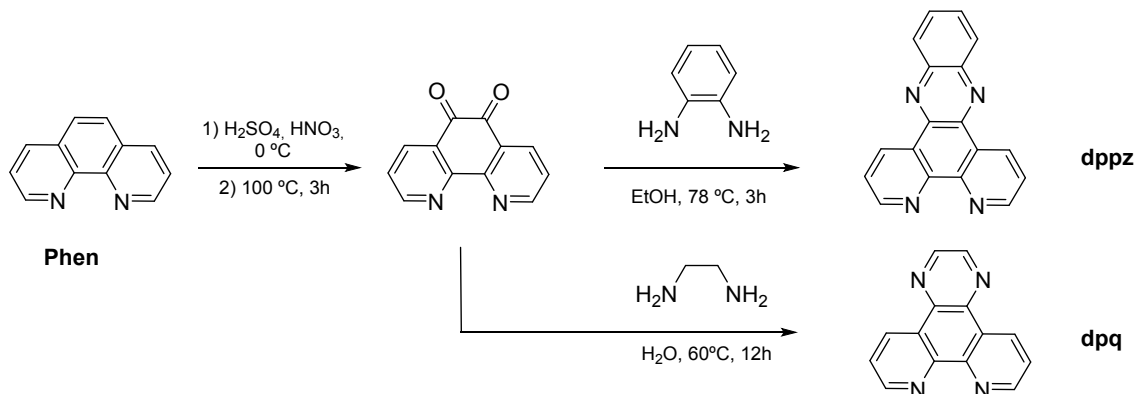


**Figure S1.** Synthetic scheme of the N<sup>N</sup> ligands

Also, the HC<sup>N</sup> proligands **HL1** and **HL2** and methyl 3-amino-4-(butylamino)benzoate were obtained as previously described [2].

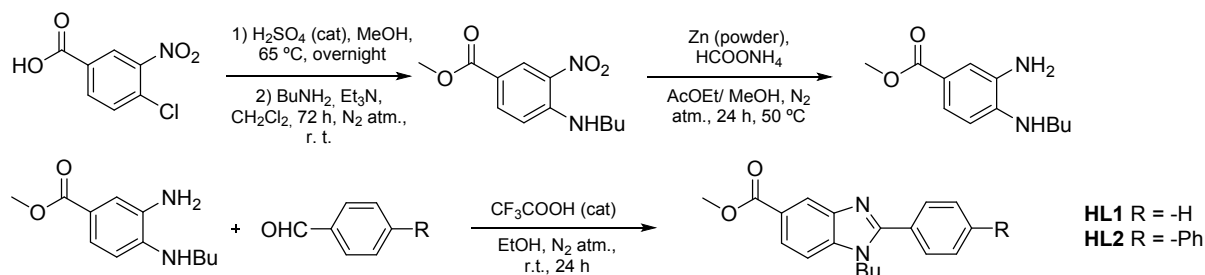


**Figure S2.** Synthetic scheme of the HC<sup>N</sup> proligands

#### Proligand HL3

The new HC<sup>N</sup> proligand **HL3** was obtained using a modification of the procedure previously described [2].

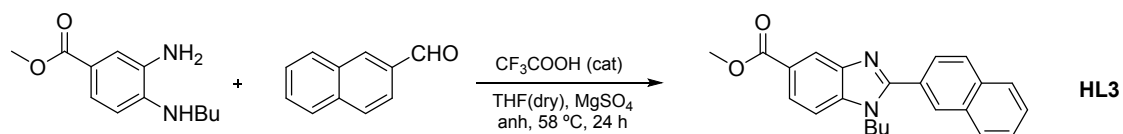
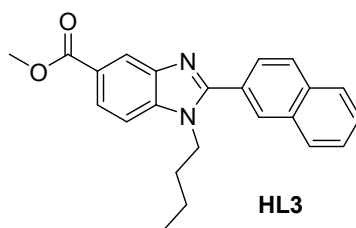


**Figure S3.** Synthetic scheme of the HC<sup>N</sup> proligands

Methyl 3-amino-4-(butylamino)benzoate (444.6 mg, 2 mmol) and 2-naphthaldehyde (1.05 eq, 327.7mg, 2.1 mmol) were dissolved in 50 ml of dry tetrahydrofuran (THF). Then, 50  $\mu$ L of trifluoroacetic acid were added and 500mg of anhydrous magnesium sulfate. The mixture was heated 24 hours at 58 °C. The mixture was filtered, the solvent was removed under reduced pressure, and the crude was purified by column chromatography using as eluent a mixture of 8/2 (v/v) of Hexane/ Ethyl Acetate.



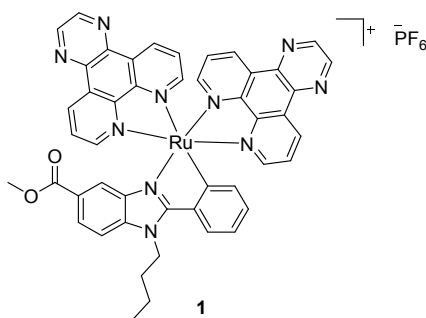
White powder. Yield = 60%.  $^1\text{H NMR}$  (300 MHz,  $\text{CDCl}_3$ )  $\delta$  (ppm) = 8.56 (d,  $J = 1.5\text{ Hz}$ , 1H), 8.24 (s, 1H), 8.06 (dd,  $J = 8.5, 1.6\text{ Hz}$ , 1H), 7.99 (d,  $J = 8.5\text{ Hz}$ , 1H), 7.96 – 7.88 (m, 2H), 7.81 (dd,  $J = 8.5, 1.7\text{ Hz}$ , 1H), 7.60 – 7.55 (m, 2H), 7.46 (d,  $J = 8.6\text{ Hz}$ , 1H), 4.33 (t,  $J = 7.7\text{ Hz}$ , 2H), 3.96 (s, 3H), 1.89 – 1.75 (m, 2H), 1.34 – 1.17 (m, 2H), 0.85 (t,  $J = 7.4\text{ Hz}$ , 3H).  $^{13}\text{C NMR}$  (75 MHz,  $\text{CDCl}_3$ )  $\delta$  (ppm) = 167.5(q), 155.2(q), 142.1(q), 138.7(q), 133.7(q), 132.9(q), 129.4, 128.7, 128.5, 127.8, 127.4, 126.9, 125.9, 124.7(q), 124.4, 122.0, 109.9, 52.1, 44.9( $\text{CH}_2$ ), 31.8( $\text{CH}_2$ ), 19.9( $\text{CH}_2$ ), 13.5. IR (KBr) = 1713.25 ( $\text{C}=\text{O}$ ) ( $\text{cm}^{-1}$ ). Mass spectra: Calc.  $[\text{M}^+\text{+H}] = 358.1681$  (m/z), Exp.  $[\text{M}^+\text{+H}] = 359.1759$  (m/z).

### 3.2. Synthesis of the complexes

In a dry Schlenk the respective proligand (0.3 mmol), potassium acetate (58.9 mg, 0.6 mmol) and potassium hexafluorophosphate (110.45 mg, 0.6 mmol) were added and then dissolved in 20 mL of degassed acetonitrile. Three cycles vacuum- $\text{N}_2$  were performed. Then,  $[\text{Ru}(p\text{-cymene})(\text{Cl})_2]_2$  (91.86 mg, 0.15 mmol) was added, and the orange solution was heated 48 hours at 40 °C under  $\text{N}_2$  atmosphere. The yellow solution was filtered, concentrated and purified by column chromatography in alumina and using as eluent a mixture 9/1 (v/v) of  $\text{CH}_2\text{Cl}_2/\text{ACN}$ . The first yellow fraction where collected and the solvent was eliminated obtaining  $[\text{Ru}(p\text{-cymene})(\text{C}^{\wedge}\text{N})(\text{NCCH}_3)](\text{PF}_6)$  intermediate<sup>[3]</sup>.

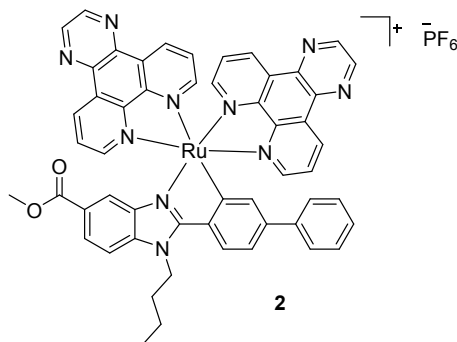
Immediately, the  $[\text{Ru}(p\text{-cymene})(\text{C}^{\wedge}\text{N})(\text{NCCH}_3)](\text{PF}_6)$  intermediate (0.15 mmol) where dissolved in 5ml of chloroform and added to 45 mL of degassed ethanol and two equivalent of the respective  $\text{N}^{\wedge}\text{N}$  ligand (**phen**, **dpq** or **dppz**) was added<sup>[4]</sup>. The mixture where heated at 65 °C for an hour. After reaching room temperature, a dark-purple precipitate appear. The solid was filtrated, dissolved in  $\text{CH}_2\text{Cl}_2$  and purified by column chromatography in alumina and using as eluent a mixture 9/1 (v/v) of  $\text{CH}_2\text{Cl}_2/\text{ACN}$ . The solvent was removed under reduced pressure, the residue was dissolved in 3 mL of dichloromethane and precipitate with hexane.

## Complex 1



Dark red powder. Yield = 49%. **<sup>1</sup>H NMR** (401 MHz, CD<sub>3</sub>CN) δ (ppm) = 9.55 (dd, *J* = 8.2, 1.3 Hz, 1H), 9.25 (dd, *J* = 8.2, 1.2 Hz, 1H), 9.22 – 9.16 (m, 2H), 9.14 – 9.10 (m, 3H), 9.08 (d, *J* = 2.1 Hz, 1H), 8.56 (dd, *J* = 5.4, 1.4 Hz, 1H), 8.50 (dd, *J* = 5.1, 1.4 Hz, 1H), 8.34 (d, *J* = 5.9 Hz, 1H), 8.15 (dd, *J* = 5.4, 1.3 Hz, 1H), 8.4 (d, *J* = 8.0 Hz, 1H), 7.87 (dd, *J* = 8.2, 5.1 Hz, 1H), 7.70 – 7.65 (m, 2H), 7.63 (dd, *J* = 8.2, 5.4 Hz, 1H), 7.58 (dd, *J* = 8.2, 5.4 Hz, 1H), 7.51 (d, *J* = 8.6 Hz, 1H), 6.90 (m, 1H), 6.82 (m, 1H), 6.45 (d, *J* = 7.3 Hz, 1H), 6.38 (s, 1H), 4.71 (t, *J* = 7.5 Hz, 2H), 3.61 (s, 3H), 2.04 – 1.97 (m, 2H), 1.51 – 1.35 (m, 2H), 0.95 (t, *J* = 7.3 Hz, 3H). **<sup>13</sup>C NMR** (101 MHz, CD<sub>3</sub>CN) δ (ppm) = 167.1(q), 163.1(q), 157.1, 154.1, 153.5, 153.0, 151.7(q), 151.4(q), 150.5(q), 149.4(q), 147.2, 147.1, 142.2(q), 141.2(q), 141.2(q), 140.9(q), 140.7(q), 137.8(q), 137.4(q), 132.9, 131.2, 130.5(q), 130.4, 130.4(q), 130.2, 129.4(q), 127.4, 127.3, 127.2, 127.0, 126.7(q), 125.7(q), 124.7, 122.4(q), 117.5, 111.5, 52.3, 46.1(CH<sub>2</sub>), 32.4(CH<sub>2</sub>), 20.7(CH<sub>2</sub>), 14.1. IR (KBr) = 1714.47 (C=O) (cm<sup>-1</sup>). Mass spectra: Calc. [M<sup>+</sup> + H] = 873.1988 (m/z), Exp. [M<sup>+</sup> + H] = 873.1996 (m/z). Elemental Analysis: C<sub>47</sub>H<sub>35</sub>N<sub>10</sub>O<sub>2</sub>PF<sub>6</sub>Ru Calc.: C = 55.46%, H = 3.47%, N = 13.76%, Exp.: C = 55.56 %, H = 3.48 %, N = 13.74 %

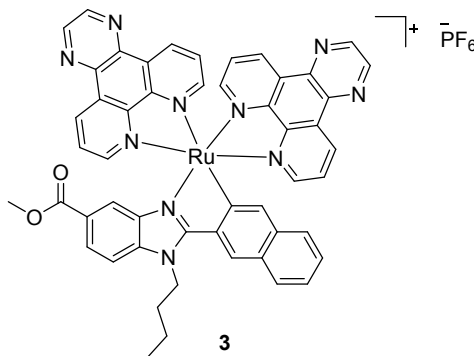
## Complex 2



Dark red powder. Yield = 70%. **<sup>1</sup>H NMR** (401 MHz, CD<sub>3</sub>CN) δ (ppm) = 9.58 (dd, *J* = 8.2, 1.4 Hz, 1H), 9.29 (dd, *J* = 8.1, 1.3 Hz, 1H), 9.26 – 9.20 (m, 2H), 9.15 – 9.12 (m, 2H), 9.11 – 9.10 (m, 1H), 8.67 (dd, *J* = 5.4, 1.4 Hz, 1H), 8.49 (dd, *J* = 5.1, 1.4 Hz, 1H), 8.39 (dd, *J* = 5.4, 1.3 Hz, 1H), 8.25 (dd, *J* = 5.4, 1.3 Hz, 1H), 8.10 (d, *J* = 8.2 Hz, 1H), 7.88 (dd, *J* = 8.2, 5.2 Hz, 1H), 7.74 (dd, *J* = 8.6, 1.6 Hz, 1H), 7.70 (dd, *J* = 8.2, 5.4 Hz, 1H), 7.64 (dd, *J* = 8.2, 5.4 Hz, 2H), 7.62 (dd, *J* = 8.4, 5.2 Hz, 1H), 7.55 (dd, *J* = 8.6, 0.6 Hz, 1H), 7.29 – 7.17 (m, 6H), 6.80 (s, 1H), 6.40 (d, *J* = 1.2 Hz, 1H), 4.75 (t, *J* = 7.5 Hz, 2H), 3.62 (s, 3H), 2.08 – 1.97 (m, 2H), 1.61 – 1.40 (m, 2H), 0.96 (t, *J* = 7.3 Hz, 3H). **<sup>13</sup>C NMR** (101 MHz, CD<sub>3</sub>CN) δ (ppm) = 167.0(q), 162.8(q), 157.3, 154.1, 153.6, 152.9, 151.6(q), 151.4(q), 150.5(q), 149.4(q), 147.2, 147.2, 147.1, 147.1, 142.2(q), 142.1(q), 141.3(q), 141.1(q), 141.1(q), 141.0(q), 140.9(q), 140.7(q), 137.0(q), 135.2, 132.9, 131.2, 130.5(q), 130.4, 130.3(q), 130.2, 129.6, 128.3, 127.8, 127.3, 127.3, 127.2, 127.0, 126.9, 125.7(q), 124.7, 121.4, 117.5, 111.5, 52.2, 46.1(CH<sub>2</sub>), 32.4(CH<sub>2</sub>), 20.7(CH<sub>2</sub>),

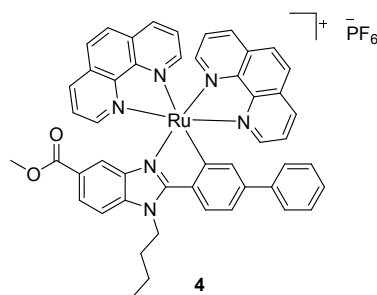
14.10. IR (KBr)= 1715.75 (C=O) (cm<sup>-1</sup>). Mass spectra: Calc. [M<sup>+</sup>] = 949.2301 (m/z), Exp. [M<sup>+</sup>] = 949.2310 (m/z). Elemental Analysis: C<sub>53</sub>H<sub>39</sub>N<sub>10</sub>O<sub>2</sub>PF<sub>6</sub>Ru Calc.: C = 58.19%, H = 3.59%, N = 12.80%, Exp.: C = 58.23%, H = 3.60%, N = 12.78%

### Complex 3



Dark red powder. Yield = 51 %. **<sup>1</sup>H NMR** (600 MHz, CD<sub>3</sub>CN) δ (ppm) = 9.61 (d, *J* = 8.0 Hz, 1H), 9.35 (d, *J* = 8.0 Hz, 1H), 9.29 (d, *J* = 8.3 Hz, 1H), 9.26 (d, *J* = 8.2 Hz, 1H), 9.20 – 9.13 (m, 4H), 8.67 (d, *J* = 5.2 Hz, 1H), 8.56 (d, *J* = 5.4 Hz, 1H), 8.52 (s, 1H), 8.46 (d, *J* = 5.2 Hz, 1H), 8.22 (d, *J* = 5.4 Hz, 1H), 7.94 – 7.86 (m, 2H), 7.79 (d, *J* = 8.9 Hz, 1H), 7.70 – 7.63 (m, 3H), 7.62 (d, *J* = 8.8 Hz, 1H), 7.27 – 7.18 (m, 2H), 7.10 (d, *J* = 7.7 Hz, 1H), 6.81 (s, 1H), 6.47 (s, 1H), 4.92 – 4.84 (m, 2H), 3.63 (s, 3H), 2.11 – 2.04 (m, 2H), 1.57 – 1.45 (m, 2H), 1.01 (t, *J* = 7.3 Hz, 3H). **<sup>13</sup>C NMR** (151 MHz, CD<sub>3</sub>CN) δ (ppm) = 167.0(q), 162.4(q), 157.0, 153.9, 153.6, 153.1, 151.7(q), 151.4(q), 150.6(q), 149.5(q), 147.3, 147.3, 147.1, 147.1, 142.3(q), 141.3(q), 141.1(q), 141.0(q), 140.9(q), 137.4(q), 134.9(q), 134.7, 132.9, 131.3, 131.0(q), 130.6, 130.5(q), 130.5(q), 130.1, 130.1, 128.1, 127.4, 127.3, 127.2, 126.9, 126.1, 125.9, 125.2, 124.2, 118.1, 111.9, 52.3, 46.2(CH<sub>2</sub>), 32.2(CH<sub>2</sub>), 20.7(CH<sub>2</sub>), 14.1. IR (KBr)= 1716.78 (C=O) (cm<sup>-1</sup>). Mass spectra: Calc. [M<sup>+</sup> + H] = 924.2223 (m/z), Exp. [M<sup>+</sup> + H] = 923.2162 (m/z). Elemental Analysis: C<sub>51</sub>H<sub>37</sub>N<sub>10</sub>O<sub>2</sub>PF<sub>6</sub>Ru Calc.: C = 57.36%, H = 3.49%, N = 13.12%, Exp.: C = 57.42%, H = 3.48%, N = 13.10%

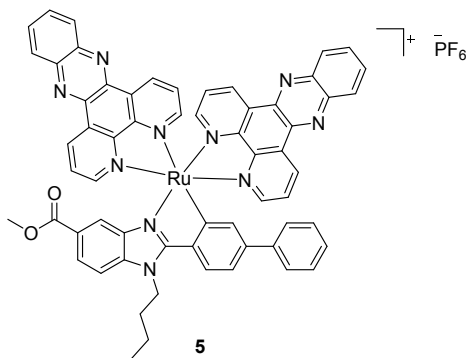
### Complex 4



Dark red powder. Yield = 52%. **<sup>1</sup>H NMR** (401 MHz, CD<sub>3</sub>CN) δ (ppm) = 8.63 (dd, *J* = 8.2, 1.3 Hz, 1H), 8.55 (d, *J* = 5.3 Hz, 1H), 8.38 – 8.31 (m, 4H), 8.27 (d, *J* = 5.3 Hz, 1H), 8.17 (d, *J* = 8.9 Hz, 1H), 8.13 – 8.08 (m, 3H), 8.06 (d, *J* = 8.2 Hz, 1H), 8.02 (d, *J* = 5.4 Hz, 1H), 7.78 – 7.72 (m, 2H), 7.63 – 7.57 (m, 1H), 7.57 – 7.53 (m, 2H), 7.48 (dd, *J* = 8.1, 5.3 Hz, 1H), 7.29 – 7.22 (m, 3H), 7.20 – 7.10 (m, 3H), 6.53 (s, 1H), 6.23 (s, 1H), 4.73 (t, *J* = 7.5 Hz, 2H), 3.66 (s, 3H), 2.07 – 1.96 (m, 2H), 1.53 – 1.36 (m, 2H), 0.96 (t, *J* = 7.4 Hz, 3H). **<sup>13</sup>C NMR** (101 MHz, CD<sub>3</sub>CN) δ (ppm) = 167.1(q), 162.8(q), 156.1, 153.0, 152.2, 151.6, 150.4(q), 150.0(q), 149.0(q), 147.9(q), 142.3, (q) 142.2(q), 140.8(q), 140.6(q), 136.2, 134.77, 133.8, 131.5(q), 131.4(q),

131.4(q), 131.3(q), 129.6, 128.7, 128.6, 128.5, 128.3, 127.7, 126.4, 126.3, 126.2, 126.0, 125.4(q), 124.7, 117.3, 111.4, 52.3, 46.0, 32.4, 20.7, 14.1. IR (KBr) = 1718.91 (C=O) (cm<sup>-1</sup>). Mass spectra: Calc. [M<sup>+</sup>] = 845.2178 (m/z), Exp. [M<sup>+</sup>] = 845.2176 (m/z). Elemental Analysis: C<sub>49</sub>H<sub>39</sub>N<sub>6</sub>O<sub>2</sub>PF<sub>6</sub>Ru Calc.: C = 59.45%, H = 3.97%, N = 8.49%, Exp.: C = 59.53%, H = 3.98%, N = 8.47%

## Complex 5



Dark red powder. Yield = 46 %. <sup>1</sup>H NMR (300 MHz, CD<sub>3</sub>CN) δ (ppm) = 9.61 (dd, *J* = 8.1, 1.4 Hz, 1H), 9.31 – 9.23 (m, 2H), 9.04 (d, *J* = 7.7 Hz, 1H), 8.64 (dd, *J* = 5.4, 1.4 Hz, 1H), 8.50 (dd, *J* = 5.2, 1.4 Hz, 1H), 8.38 – 8.22 (m, 6H), 8.15 (d, *J* = 8.3 Hz, 1H), 8.11 – 8.00 (m, 4H), 7.83 (dd, *J* = 8.2, 5.2 Hz, 1H), 7.74 (dd, *J* = 8.6, 1.5 Hz, 1H), 7.69 – 7.52 (m, 3H), 7.42 – 7.32 (m, 3H), 7.28 (d, *J* = 8.2 Hz, 1H), 7.25 – 7.13 (m, 3H), 6.97 (s, 1H), 6.54 (d, *J* = 1.1 Hz, 1H), 4.77 (t, *J* = 7.4 Hz, 2H), 3.62 (s, 3H), 2.06 – 1.97 (m, 2H), 1.54 – 1.37 (m, 2H), 0.94 (t, *J* = 7.4 Hz, 3H). <sup>13</sup>C NMR (75 MHz, CDCl<sub>3</sub>) δ (ppm) = 167.1(q), 162.9(q), 157.4, 154.1, 153.8, 153.0, 152.7(q), 152.6(q), 151.6(q), 150.6(q), 143.5(q), 143.3(q), 142.3(q), 142.2(q), 141.3(q), 140.8(q), 137.1(q), 135.4(q), 133.3, 133.1, 133.0, 131.5, 131.1(q), 131.0(q), 130.8, 130.6, 130.5, 130.5, 130.3, 129.7, 128.3, 127.9, 127.6, 127.5, 127.2, 127.0(q), 125.9(q), 124.8, 121.5(q), 117.6, 111.6, 52.3, 46.1(CH<sub>2</sub>), 32.5(CH<sub>2</sub>), 20.7(CH<sub>2</sub>), 14.2. IR (KBr) = 1716.22 (C=O) (cm<sup>-1</sup>) Mass spectra: Calc. [M<sup>+</sup>] = 1049.2614 (m/z), Exp. [M<sup>+</sup>] = 1049.2646 (m/z). Elemental Analysis: C<sub>61</sub>H<sub>43</sub>N<sub>10</sub>O<sub>2</sub>PF<sub>6</sub>Ru Calc.: C = 61.36%, H = 3.63%, N = 11.73%, Exp.: C = 61.43%, H = 3.65%, N = 11.72%

## 4. NMR experiments

### Proligand HL3

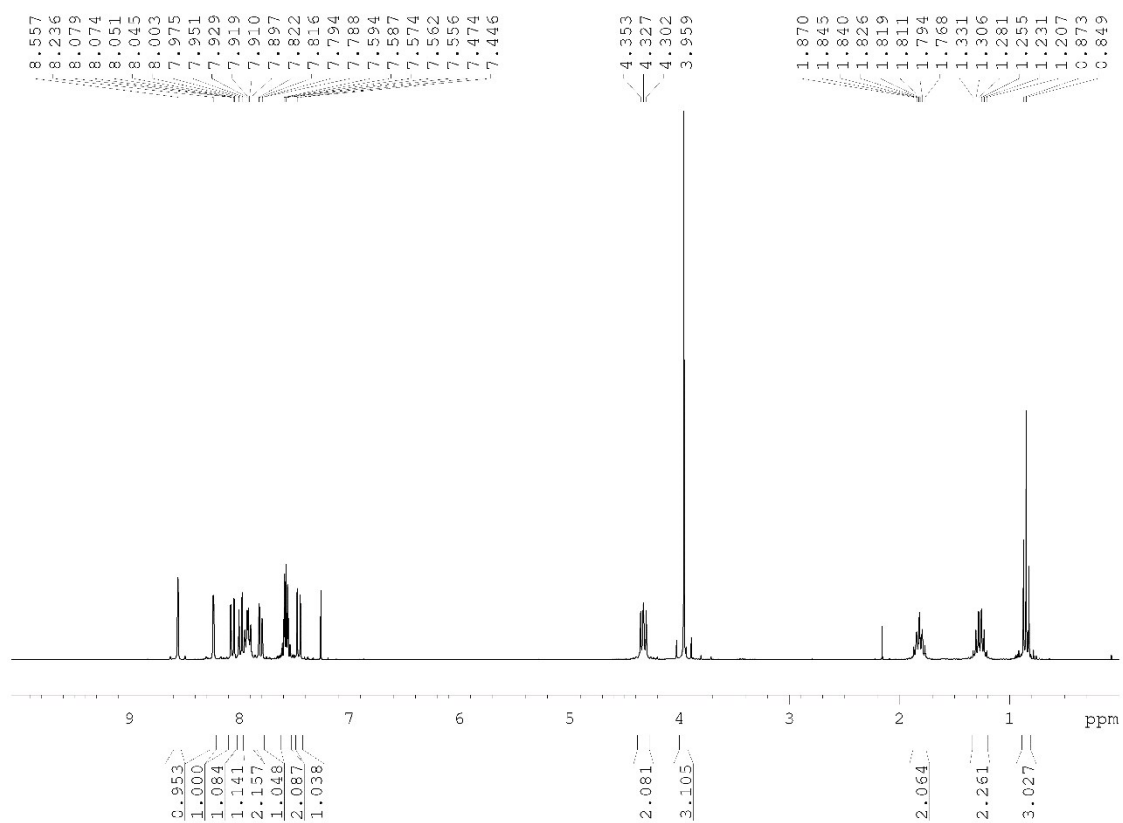


**Figure S4.**  $^1\text{H}$ -NMR spectrum of proligand **HL3** (in  $\text{CDCl}_3$ )



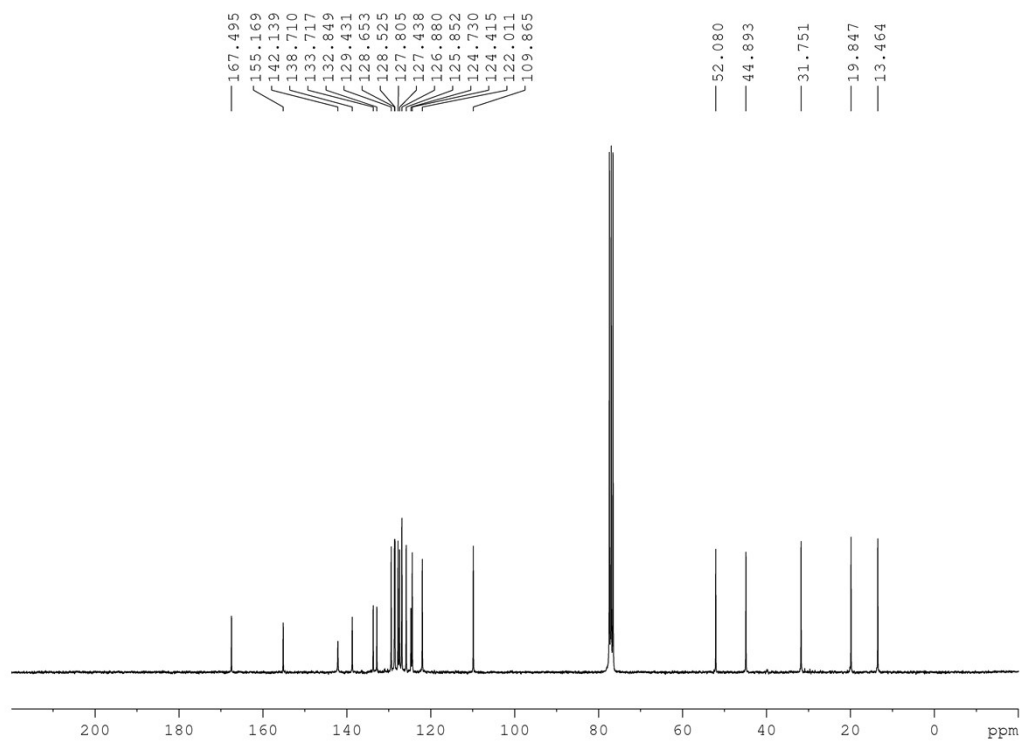


**Figure S5.**  $^{13}\text{C}$ -NMR spectrum of proligand **HL3** (in  $\text{CDCl}_3$ )

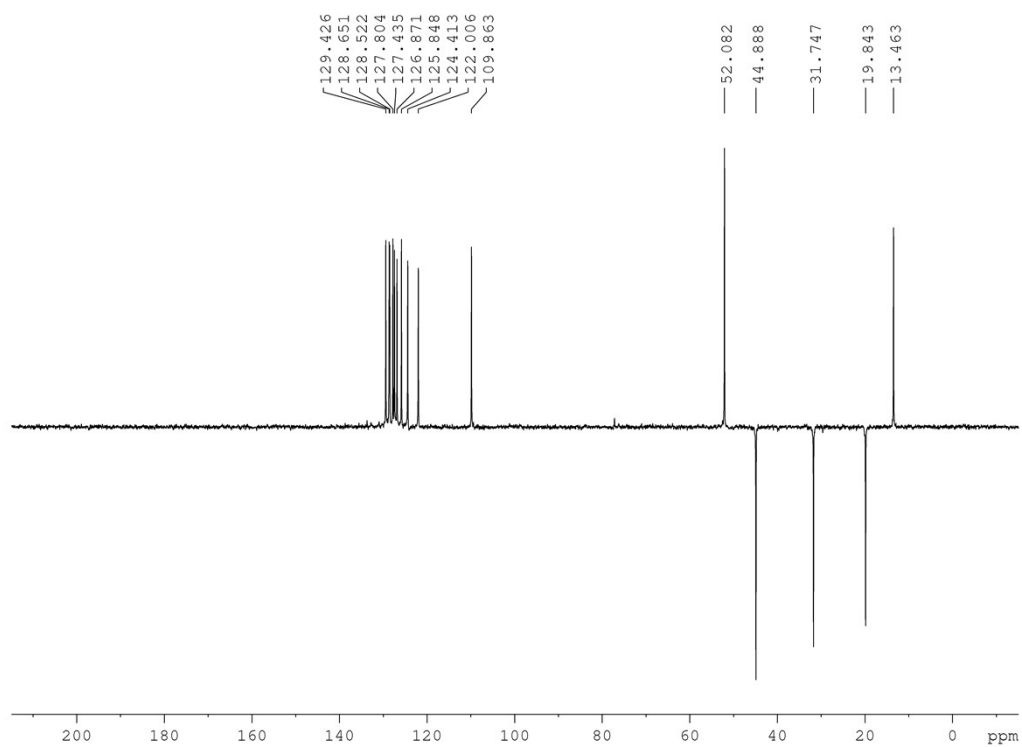


**Figure S6.**  $^{135}\text{-dept}$  NMR spectrum of proligand **HL3** (in  $\text{CDCl}_3$ )

## Compound 1

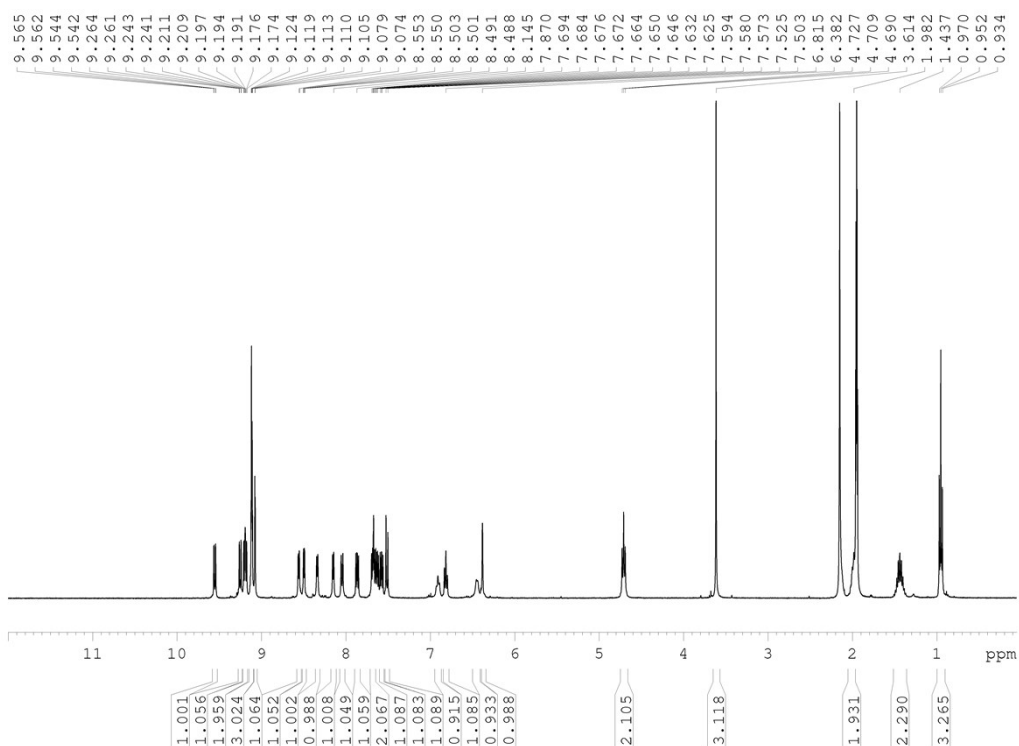


Figure S7. <sup>1</sup>H-NMR spectrum of compound 1 (in CD<sub>3</sub>CN)

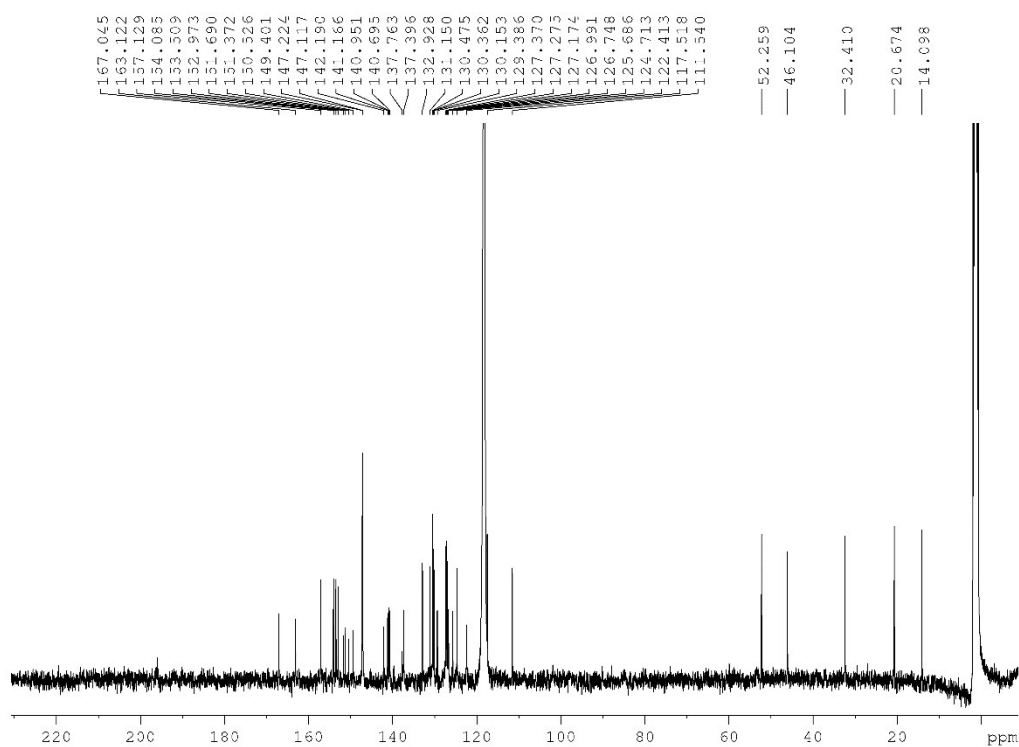


Figure S8. <sup>13</sup>C-NMR spectrum of compound 1 (in CD<sub>3</sub>CN)

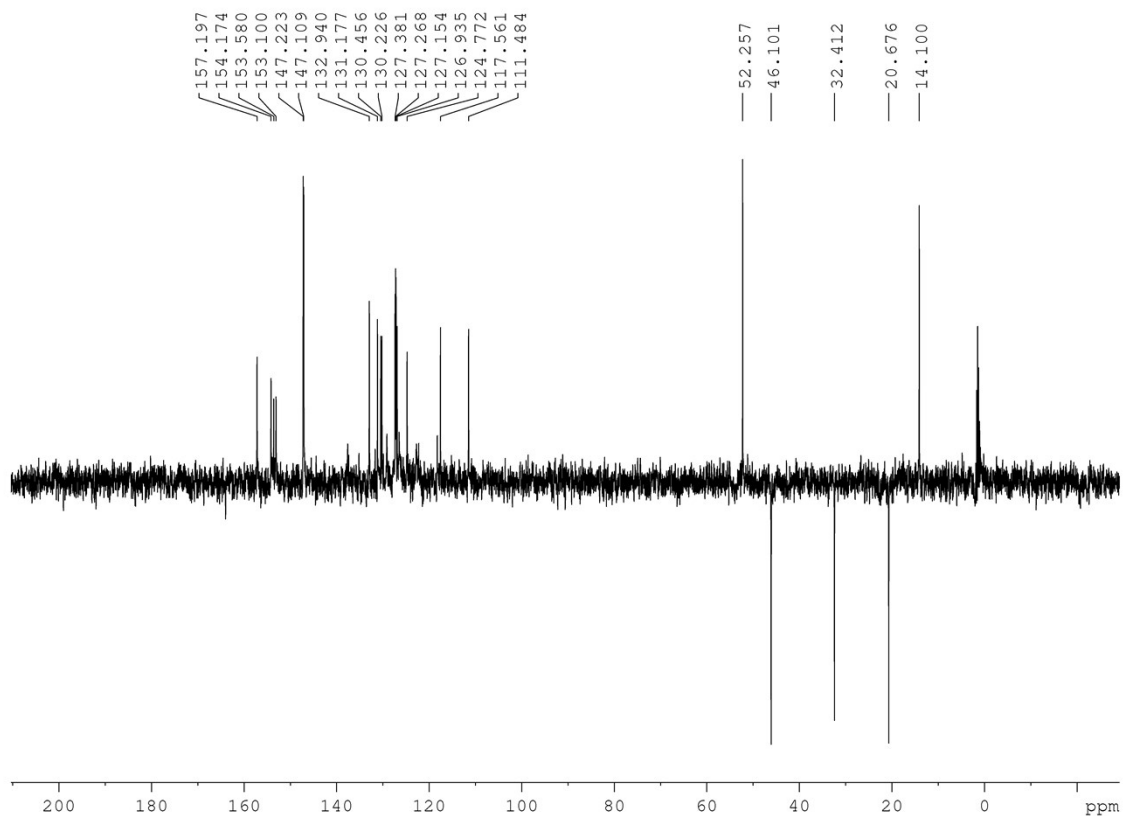


Figure S9. 135-dept NMR spectrum of compound 1 (in CD<sub>3</sub>CN)

### Compound 2

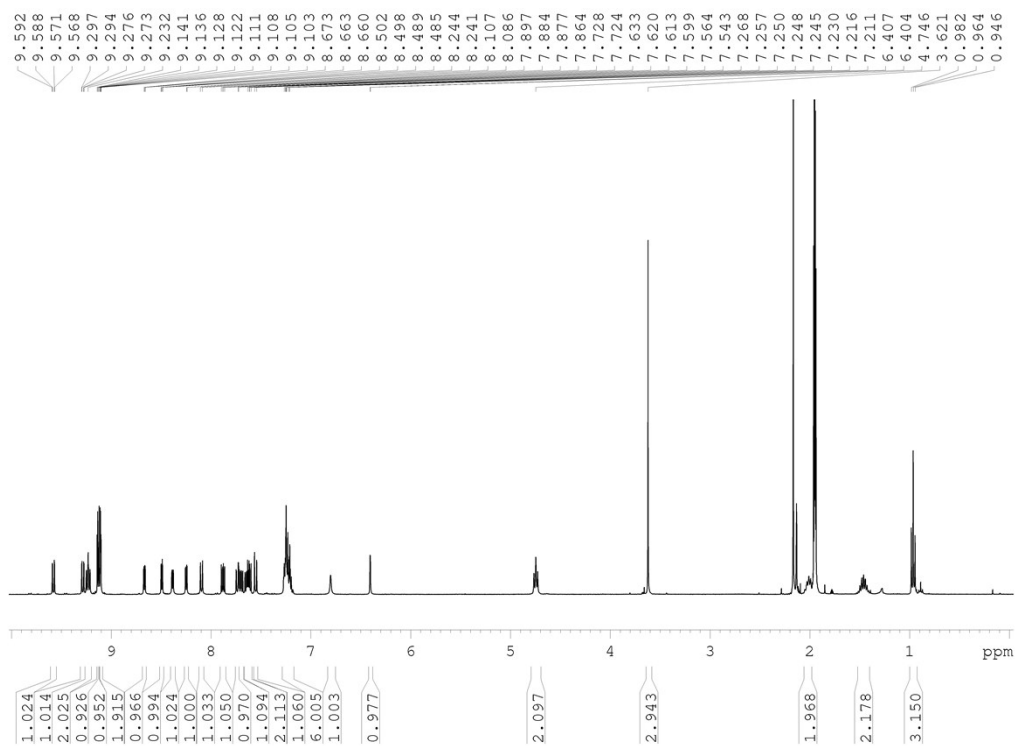


Figure S10. <sup>1</sup>H-NMR spectrum of compound 2 (in CD<sub>3</sub>CN)

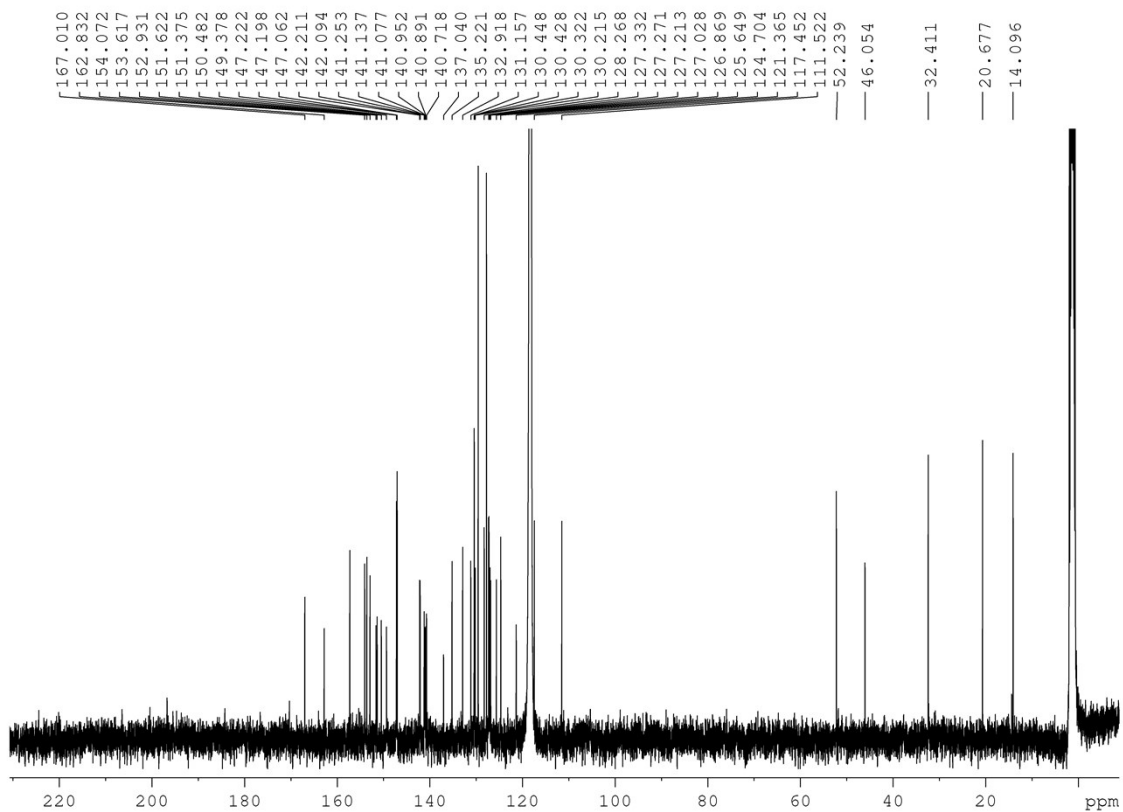


Figure S11.  $^{13}\text{C}$ -NMR spectrum of compound **2** (in  $\text{CD}_3\text{CN}$ )

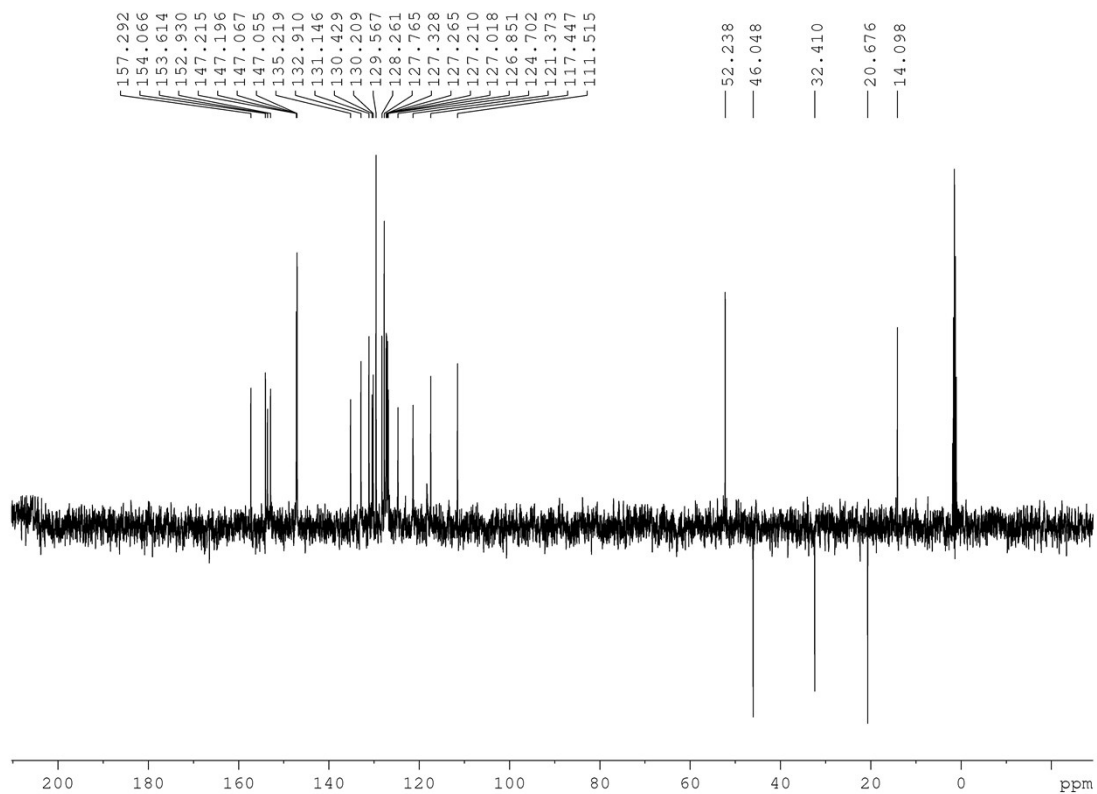


Figure S12.  $^{135}\text{-dept}$  NMR spectrum of compound **2** (in  $\text{CD}_3\text{CN}$ )

### Compound 3

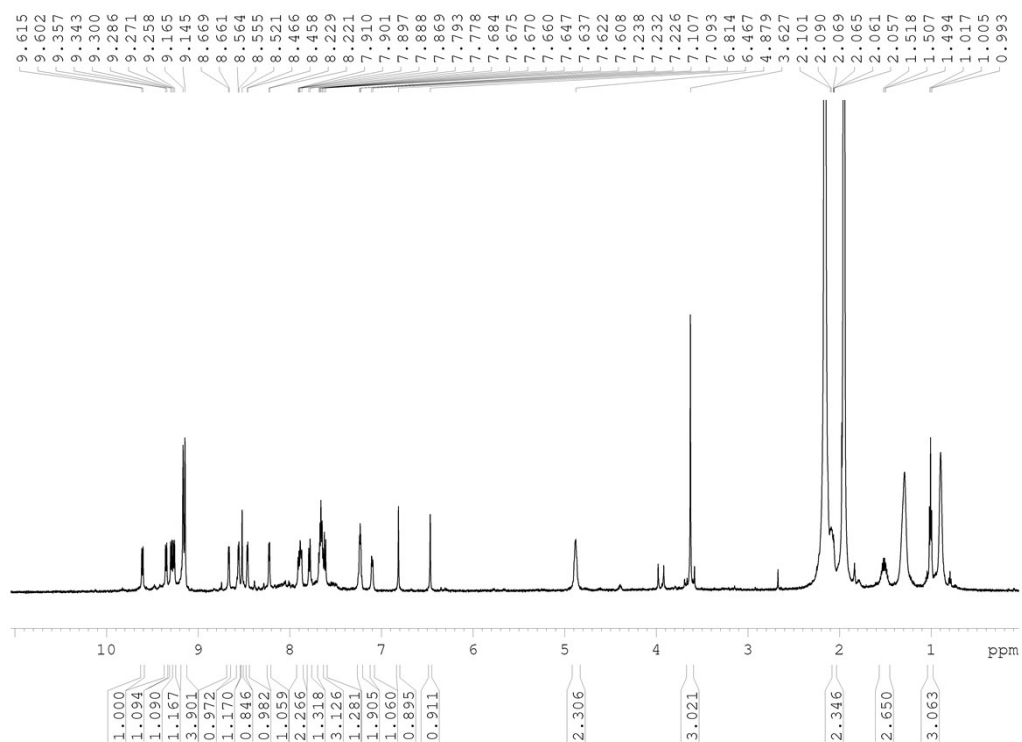


Figure S13. <sup>1</sup>H-NMR spectrum of compound 3 (in CD<sub>3</sub>CN)

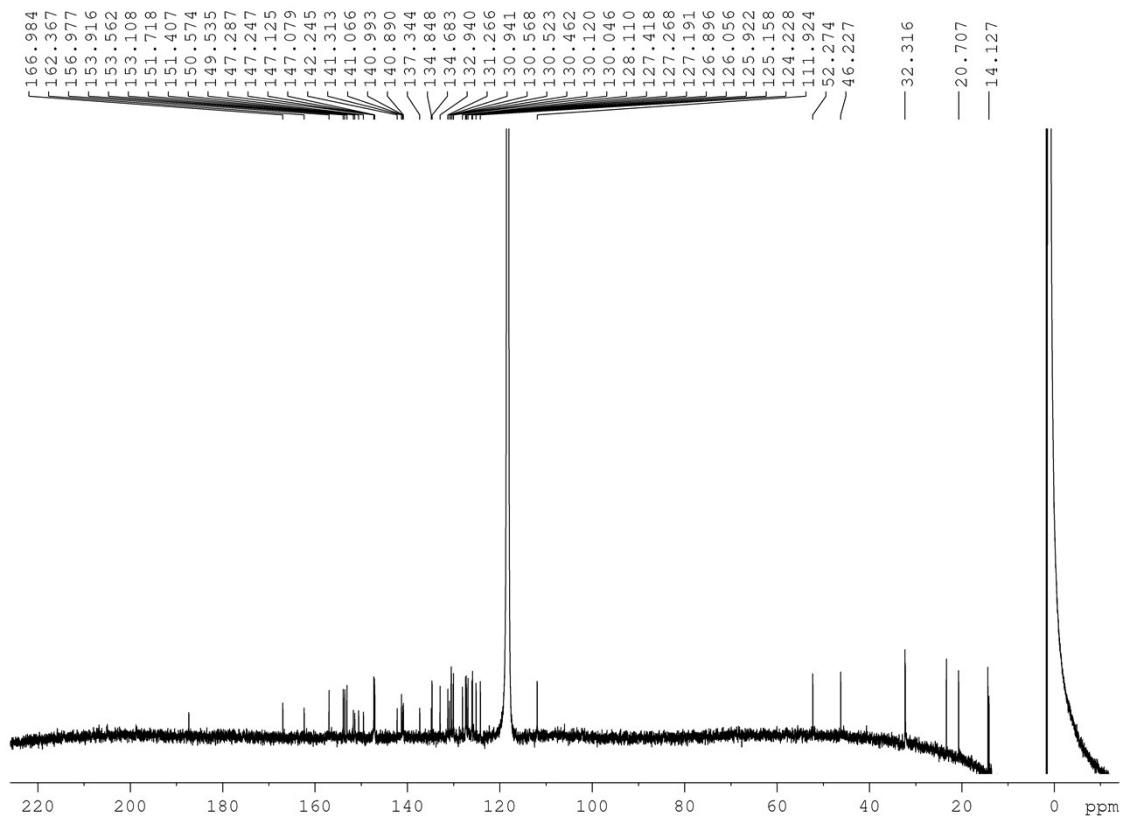
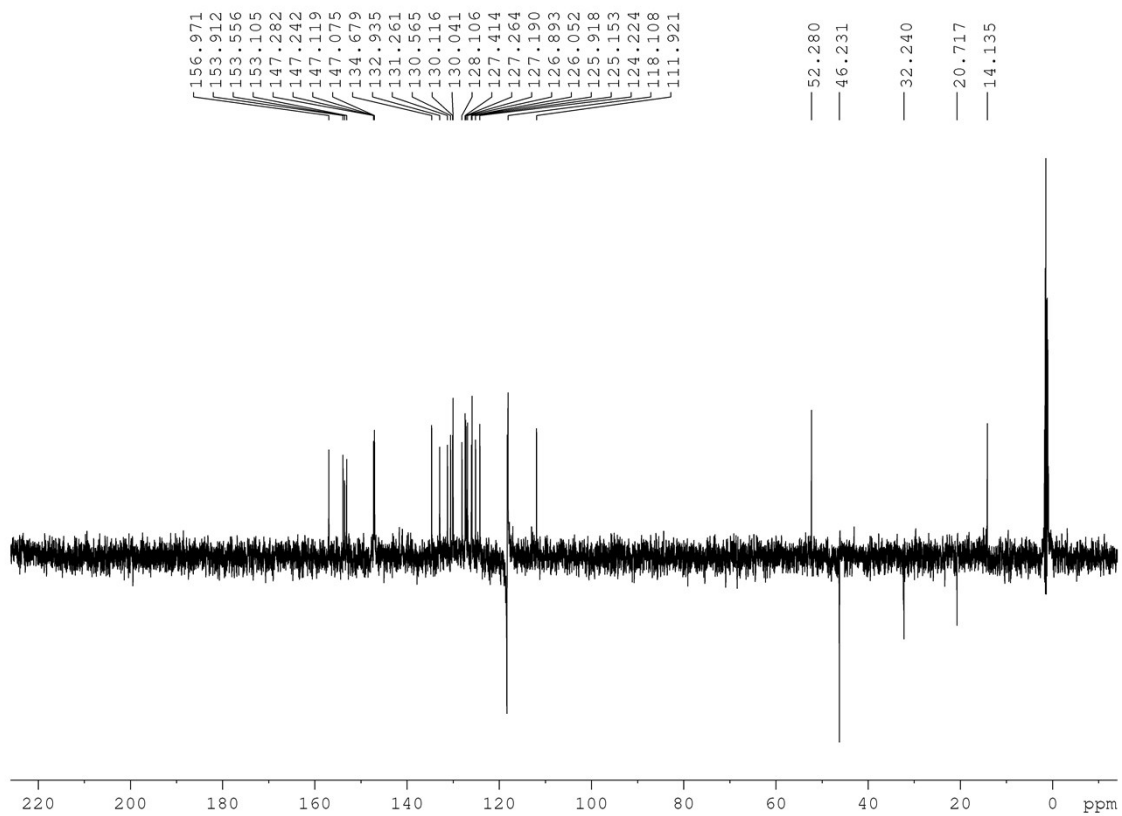


Figure S14. <sup>13</sup>C-NMR spectrum of compound 3 (in CD<sub>3</sub>CN)



**Figure S15.** 135-dept NMR spectrum of compound **3** (in CD<sub>3</sub>CN)

### Compound 4

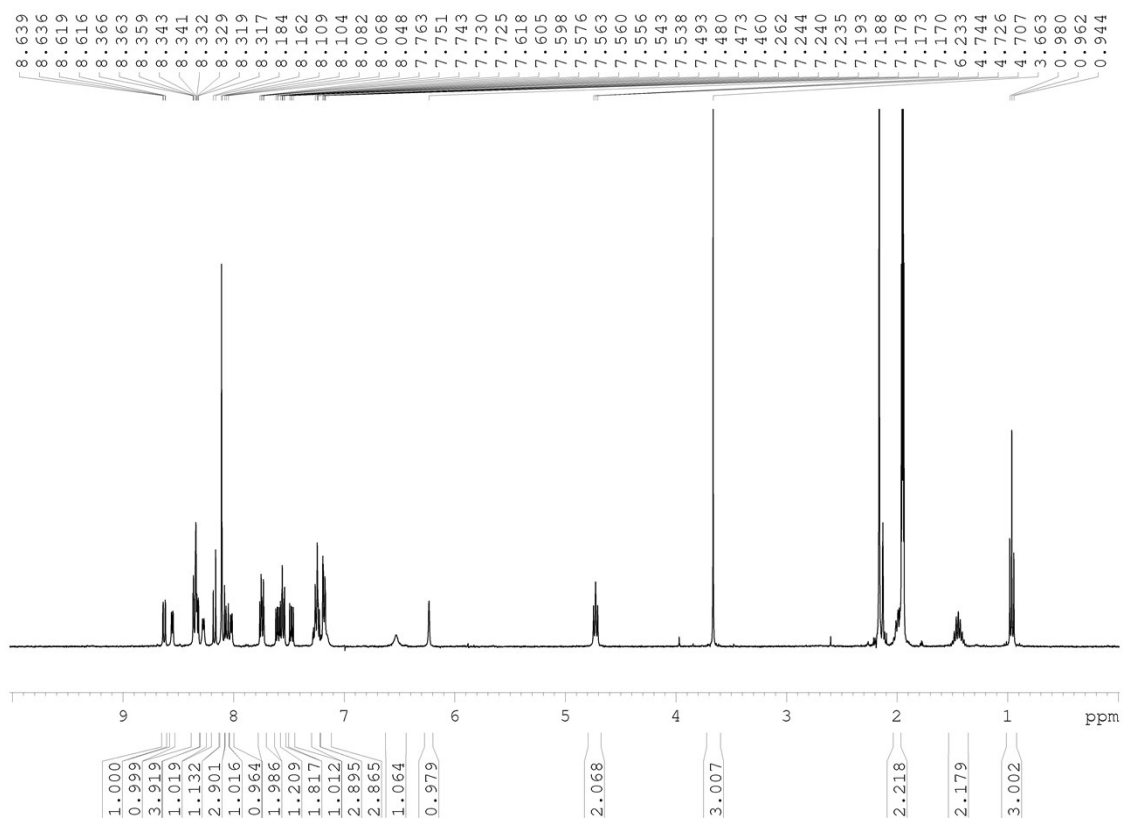


Figure S16.  $^1\text{H-NMR}$  spectrum of compound 4 (in  $\text{CD}_3\text{CN}$ )

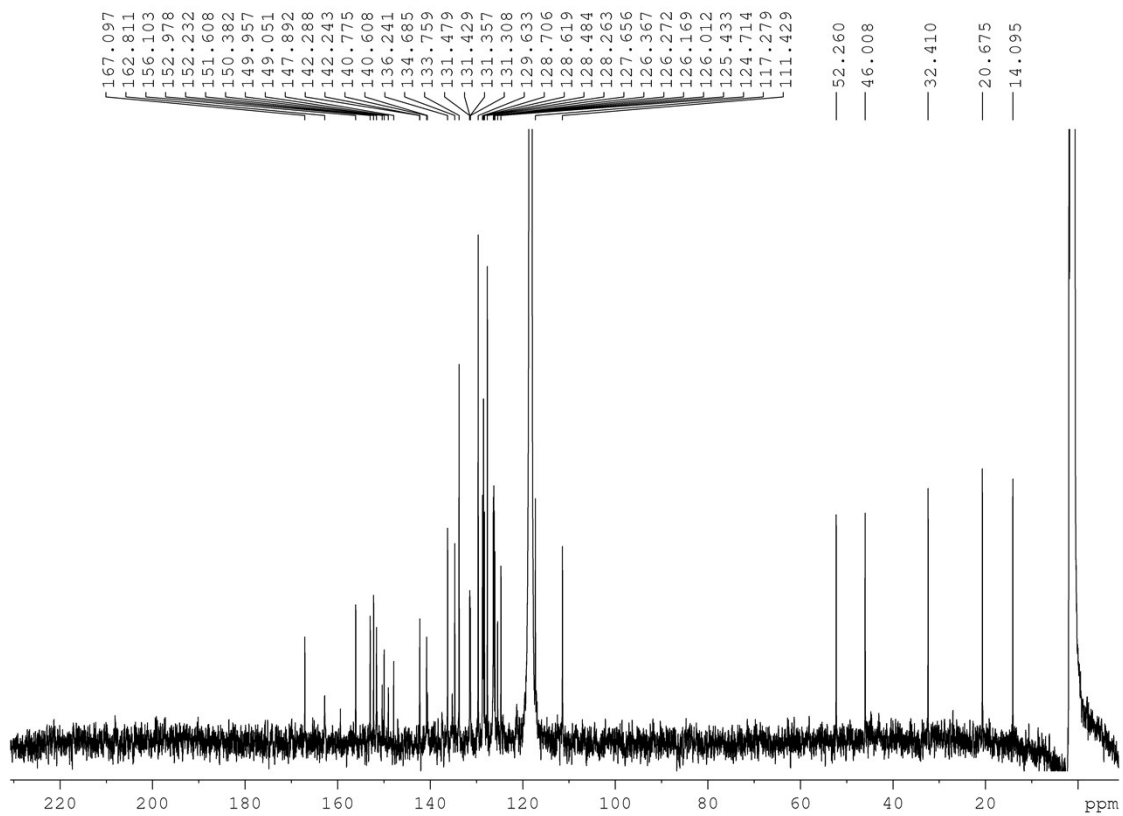
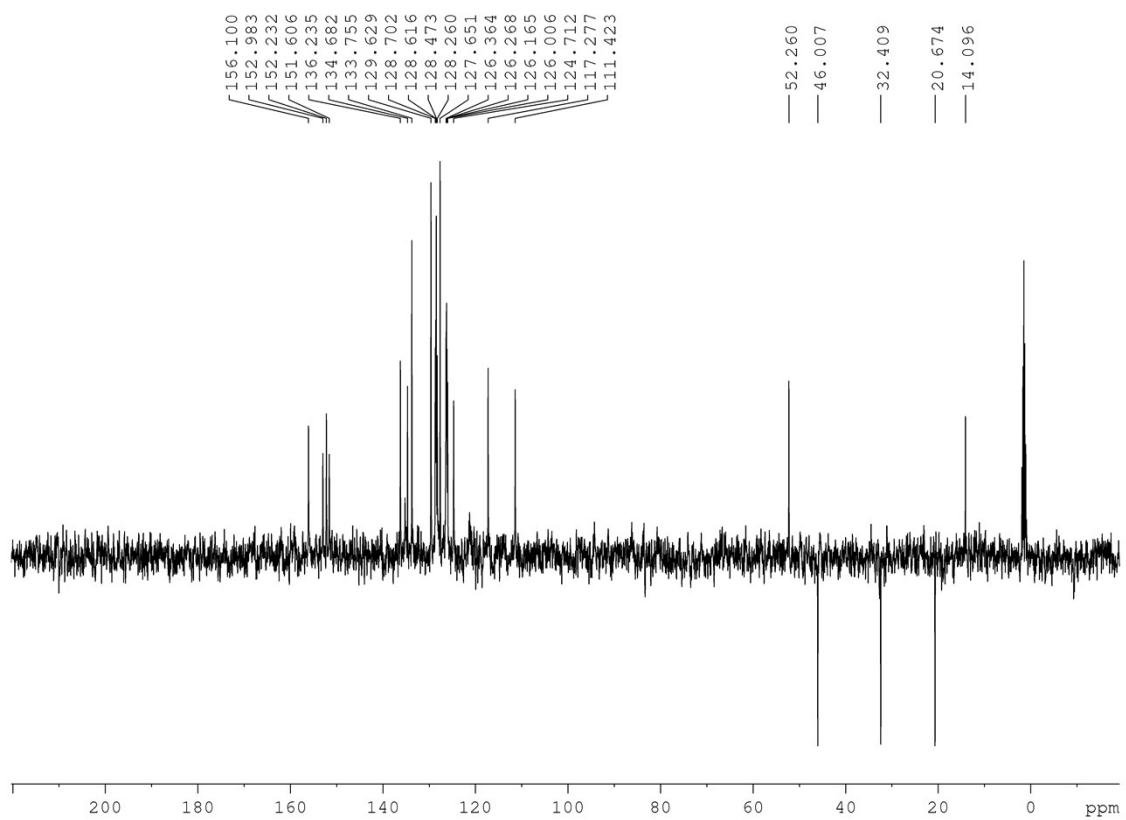


Figure S17.  $^{13}\text{C-NMR}$  spectrum of compound 4 (in  $\text{CD}_3\text{CN}$ )



**Figure S18.** 135-dept NMR spectrum of compound **4** (in CD<sub>3</sub>CN)



### Compound 5

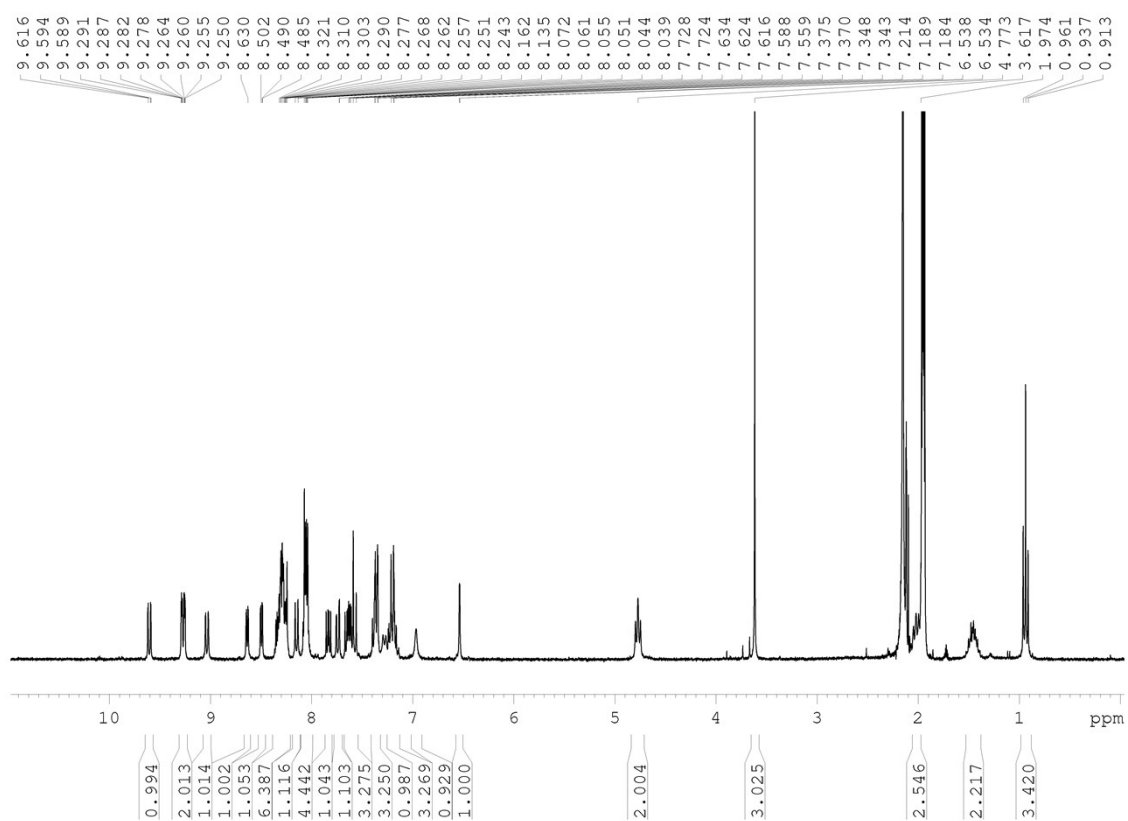


Figure S19.  $^1\text{H-NMR}$  spectrum of compound 5 (in  $\text{CD}_3\text{CN}$ )

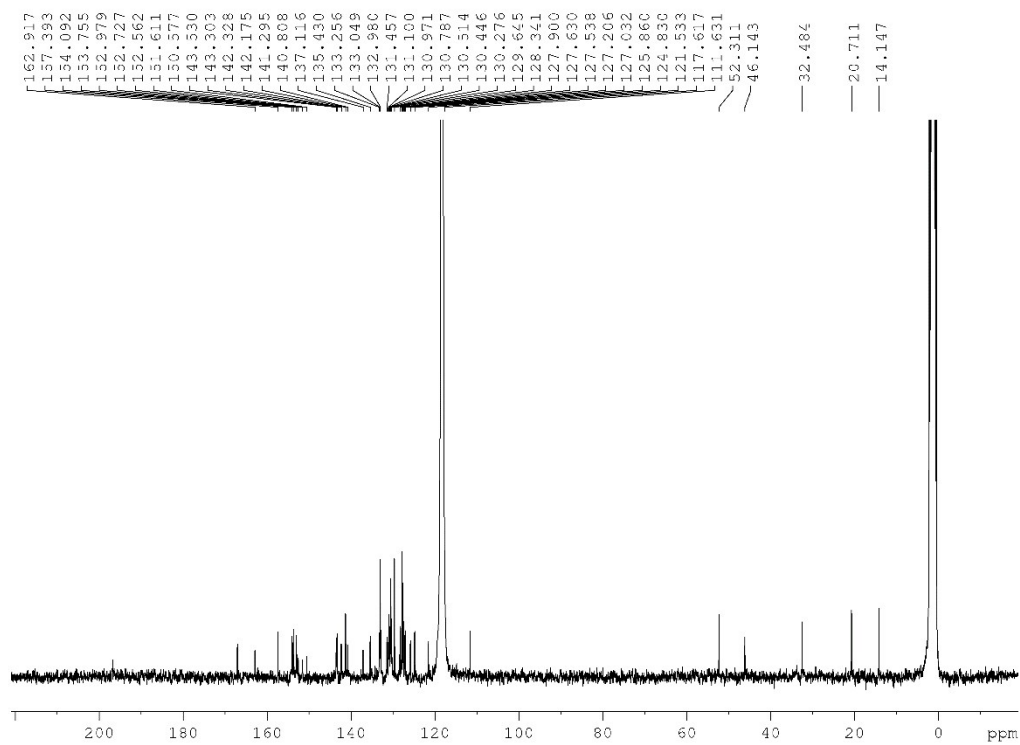
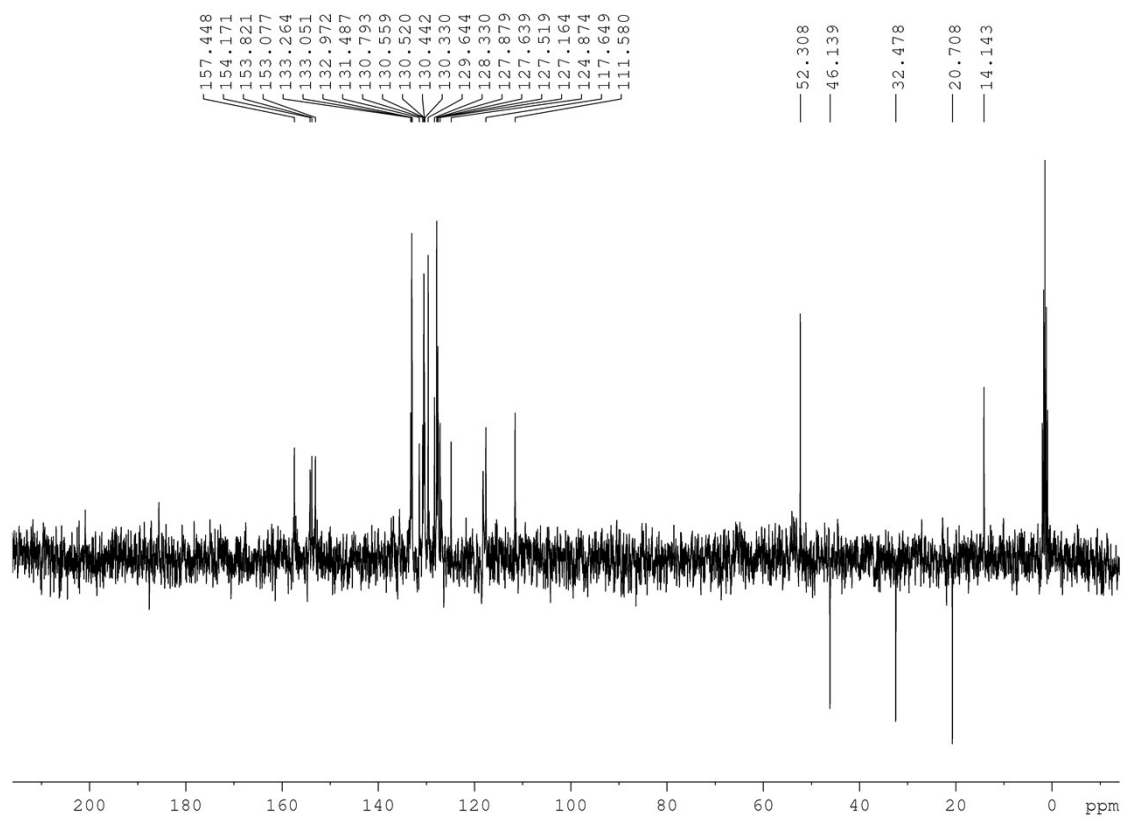


Figure S20.  $^{13}\text{C-NMR}$  spectrum of compound 5 (in  $\text{CD}_3\text{CN}$ )



**Figure S21.** 135-dept NMR spectrum of compound **5** (in CD<sub>3</sub>CN)

## 5. Photophysical properties

**Table S1.** Some photophysical properties of complexes **1** – **5** <sup>[a]</sup>

Complex	$\lambda_{\text{abs}}$ (nm) ( $\epsilon$ , M <sup>-1</sup> cm <sup>-1</sup> )	$\lambda_{\text{exc}}$ (nm)	$\lambda_{\text{em}}$ (nm)	$\tau$ (ns) (%)
(1)	260 (107000), 292 (61000), 490 (13700) 555 (14100)	360	410, 433	-
		560	730	9.5 (55) 55.9 (45)
(2)	262 (111000), 300 (65000), 323 (52300), 503 (16200) 550 (15200)	300	380, 396	-
		560	730	9.0 (57) 57.0 (43)
(3)	260 (114000), 300 (64300), 506 (14100) 560 (13700)	310	374	-
		560	730	8.3 (43) 59.3 (57)
(4)	270 (106000), 324 (49500), 496 (19000) 545 (18300)	295	378, 396	-
		540	730	57.5 (100)
(5)	279 (133000), 323 (63200), 377 (28400) 479 (17700) 528 (17900)	310	384, 396 <sup>[b]</sup>	7.7 (41) 67.9 (59)
		540	-	-

<sup>[a]</sup> Measures were realized in aerated DMSO solutions with concentration of complexes 10  $\mu\text{M}$ . <sup>[b]</sup> Lifetime measured to the most intense band.

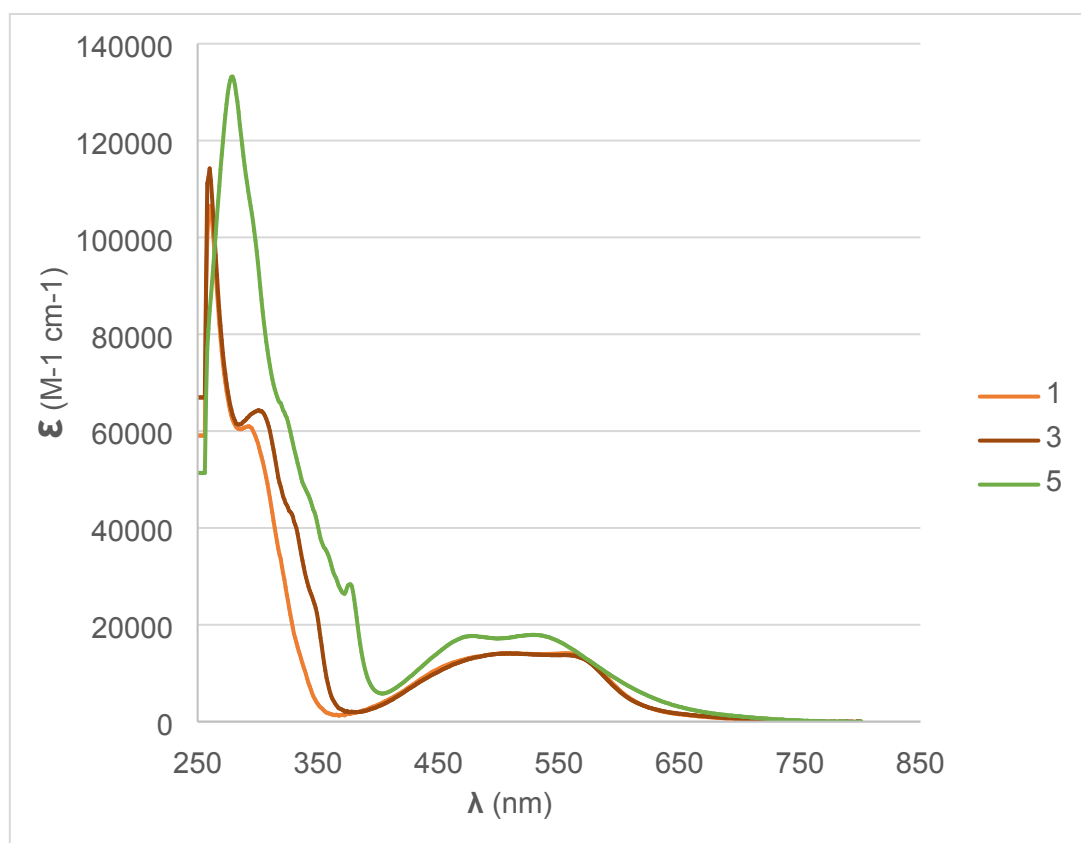


**Figure S22.** Molar extinction coefficient of complexes **1**, **3**, and **5** in DMSO.

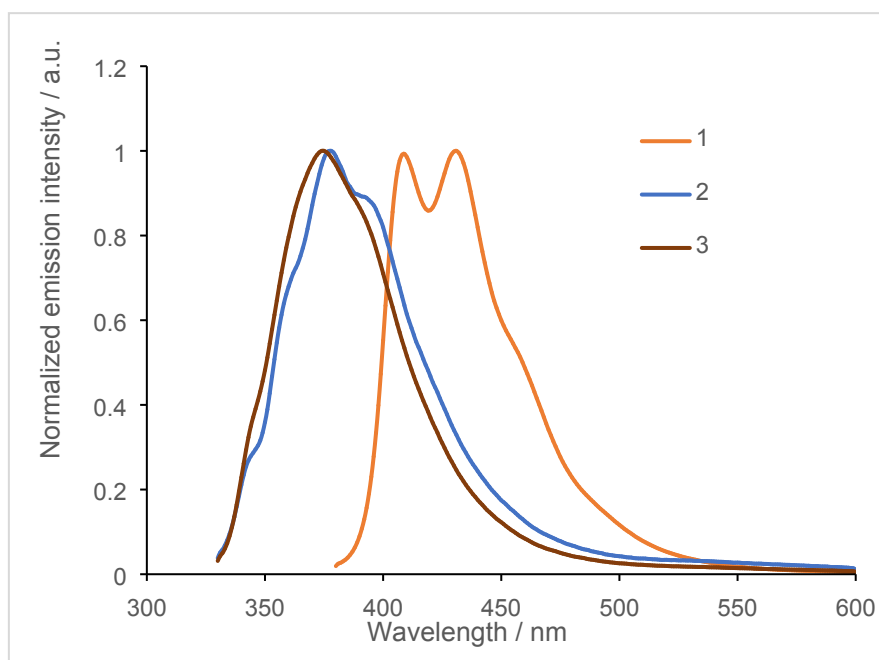


**Figure S23.** Normalized room temperature emission spectra of **1 - 3** in DMSO with  $\lambda_{\text{ex}} = 360$  (**1**),  $\lambda_{\text{ex}} = 300$  (**2**) and  $\lambda_{\text{ex}} = 310$  (**3**) nm.

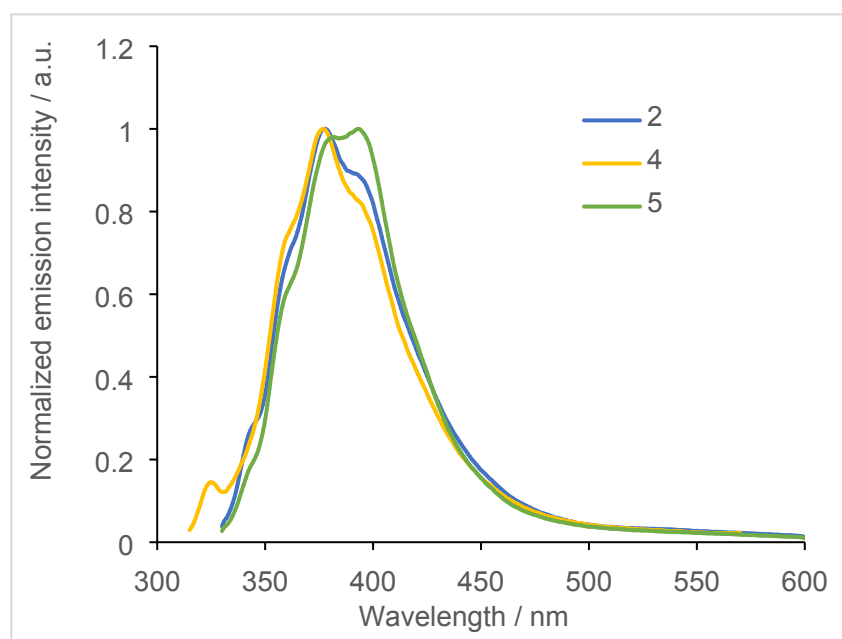


**Figure S24.** Normalized room temperature emission spectra of **2, 4** and **5** in DMSO with  $\lambda_{\text{ex}} = 300$  (**2**),  $\lambda_{\text{ex}} = 295$  (**4**) and  $\lambda_{\text{ex}} = 310$  (**5**) nm.

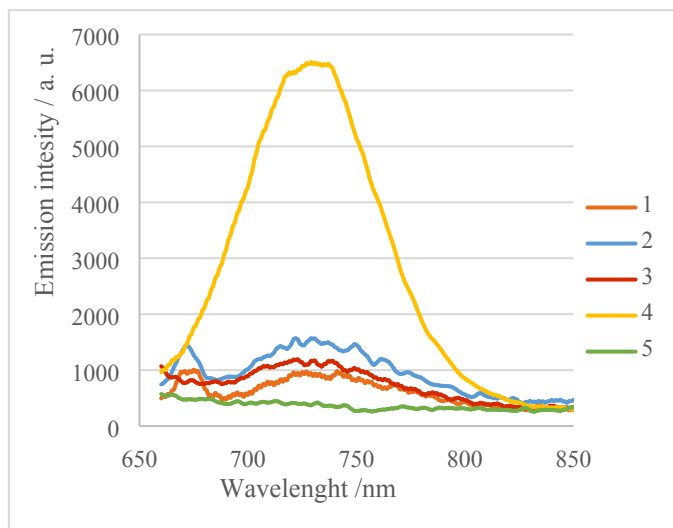


**Figure S25.** Room temperature emission spectra of **1 - 5** in DMSO (10  $\mu$ M) with  $\lambda_{\text{ex}} = 560$  (**1, 2, 3**) and  $\lambda_{\text{ex}} = 540$  (**4, 5**) nm.

## 6. Singlet oxygen quantum yields

Procurement was adapted from literature[5][6]. Samples were prepared in an air-saturated acetonitrile solution. Absorbance of 1,3-diphenylisobenzofuran (DPBF) at 411 nm was plotted against irradiation times. Slope and linear regression were calculated. Singlet oxygen

quantum yield where determined using the equation: 
$$\Phi_{\Delta s} = \Phi_{\Delta r} \left( \frac{m_s}{m_r} \right) \left( \frac{1 - 10^{A_{\lambda r}}}{1 - 10^{A_{\lambda s}}} \right)$$
, where  $\Phi_{\Delta r}$  is the reference singlet oxygen quantum yield ( $[\text{Ru}(\text{bpy})_3](\text{PF}_6)_2$ ,  $\Phi_{\Delta} = 0.57$  in aerated acetonitrile [7]),  $m$  are the slopes of samples and reference, and  $A_{\lambda}$  are the absorbance of compounds and reference at irradiation wavelength.

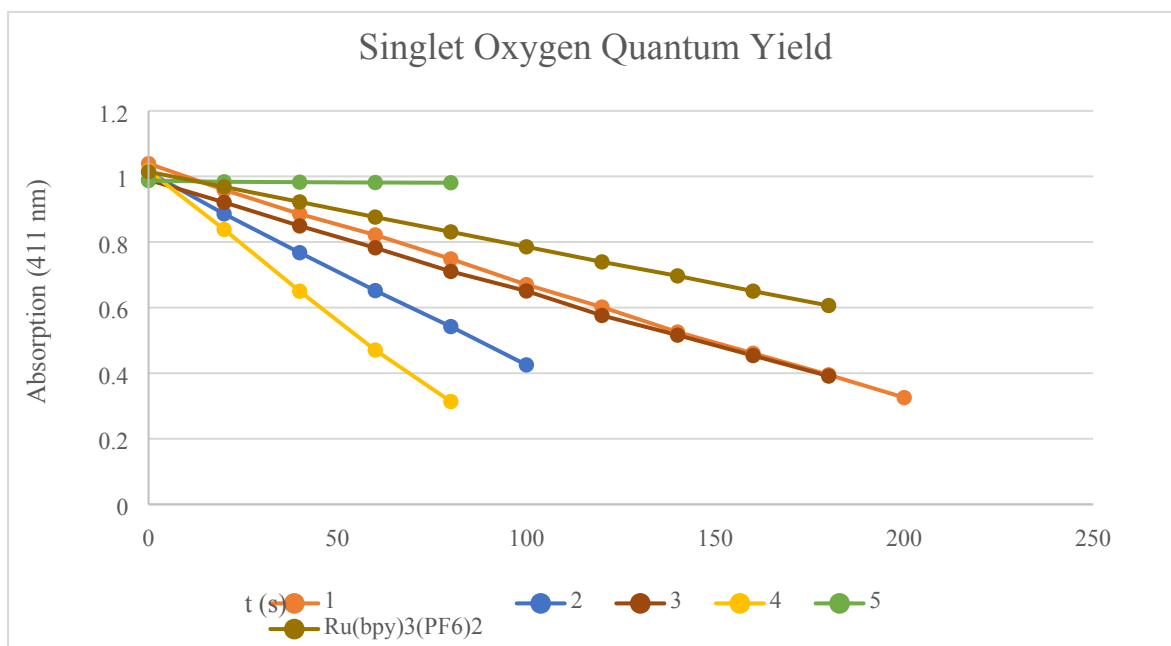


**Figure S26.** Absorbance decrease of DPBF (50  $\mu\text{M}$ ) in presence of complexes **1-5** and  $\text{Ru}(\text{bpy})_3(\text{PF}_6)_2$  (5  $\mu\text{M}$ ) in aerated acetonitrile irradiated with green light (520 nm, 1.3  $\text{mW}/\text{cm}^2$ ).

**Table S2.** Singlet oxygen quantum yields

Compound	1	2	3	4	5
Singlet oxygen quantum yield ( $\Phi_\Delta$ )	0.081	0.078	0.079	0.197	0.001

## 7. Stability of complexes 1-5

To check the stability of the prepared complexes, two experiment were performed using UV-Vis and HPLC-MS.

### UV-Vis

Solutions of the compounds **1-5** were prepared in DMSO at final concentration  $1 \times 10^{-5}$  M. The UV-Vis spectrum of these solutions were registered. Then, the solutions were irradiated under green light (520 nm,  $2.5 \text{ mW/cm}^2$ ) for two hours and then were incubated at  $37 \text{ }^\circ\text{C}$  in the dark for 48 hours. After incubation, the UV-Vis spectra were recorded.

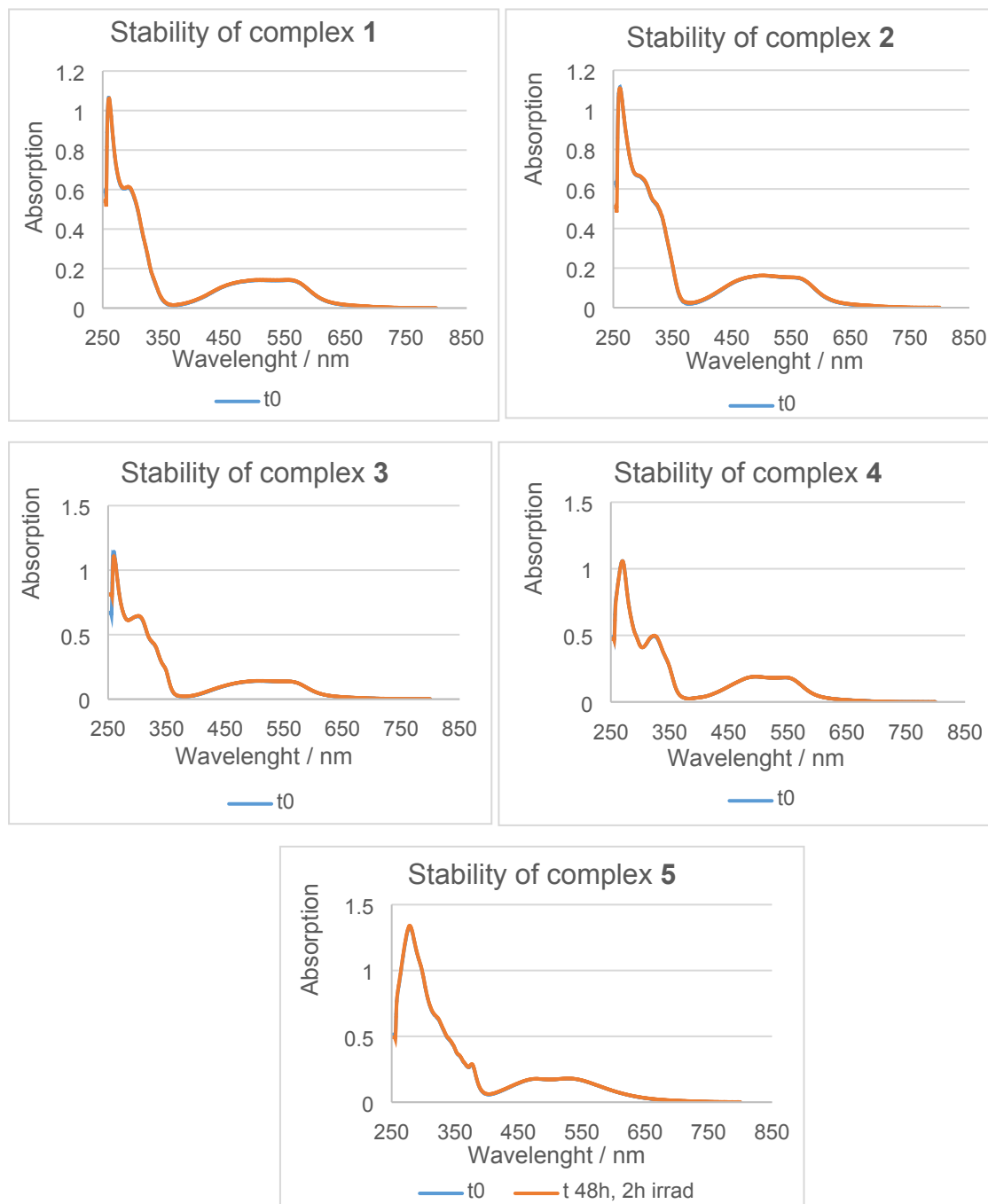


**Figure S27.** UV-Vis spectra of compounds **1-5** in DMSO ( $1 \times 10^{-5}$  M) at  $t = 0$  h and after 2 h of green light irradiation (520 nm,  $2.5 \text{ mW/cm}^2$ ) and 48 h of incubation at  $37 \text{ }^\circ\text{C}$ .

## 7.2. HPLC – MS

Solutions of the compounds **1-5** were prepared in a mixture of RPMI / DMSO 95/5 (v/v) at final concentration  $5 \times 10^{-4}$  M. Solutions were analysed by HPLC-MS.

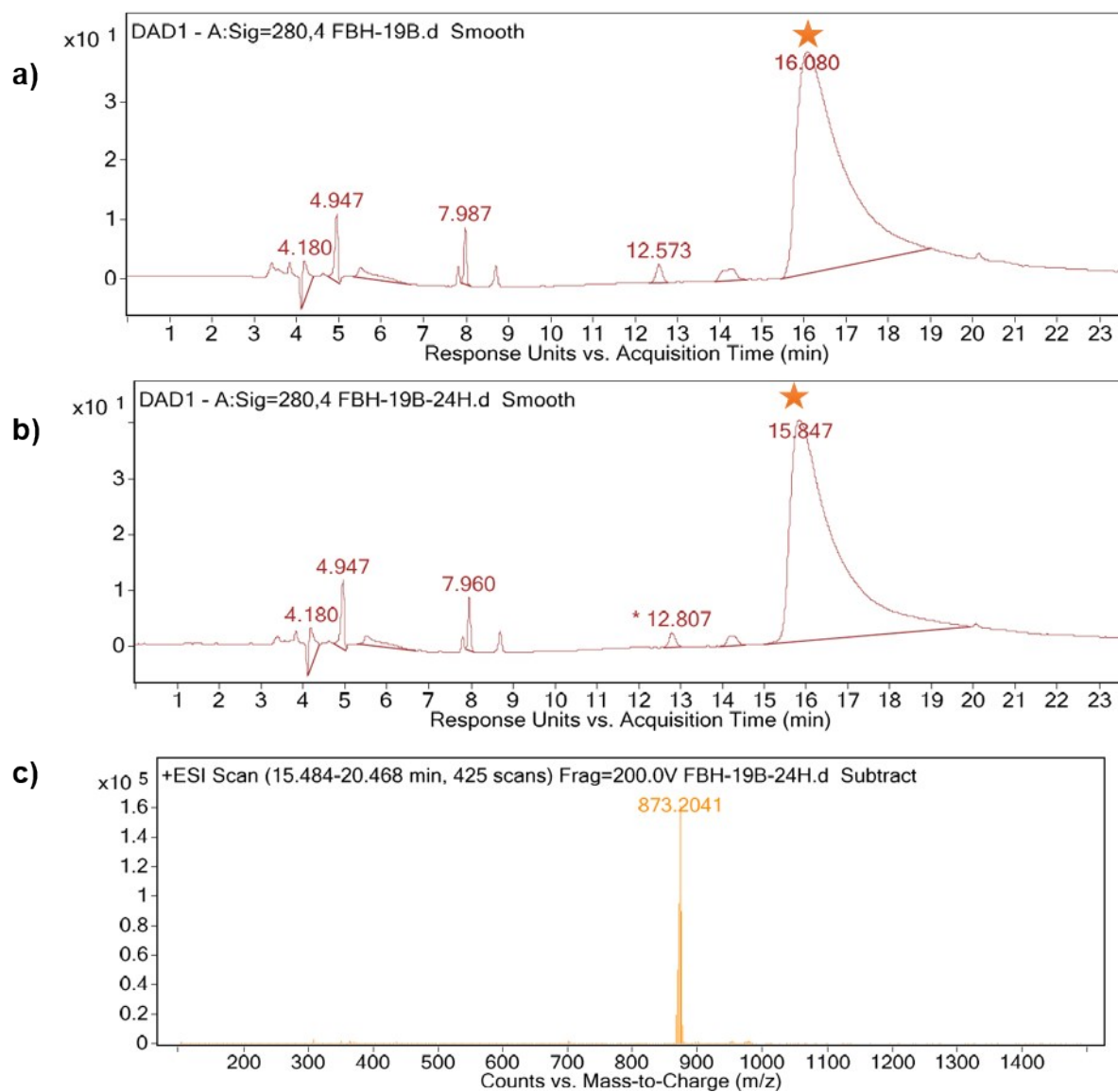


**Figure S28.** HPLC-MS chromatograms of complex **1** ( $5 \times 10^{-5}$  M) in RPMI / DMSO (95/5 v/v) **a)** at  $t = 0$  and **b)** after 1 hour of green light irradiation (520 nm,  $2.5 \text{ mW/cm}^2$ ) and 48 hours of incubation at  $37^\circ \text{C}$ . **C)** ESI-MS (pos ion mode) of complex **1** after irradiation and incubation.



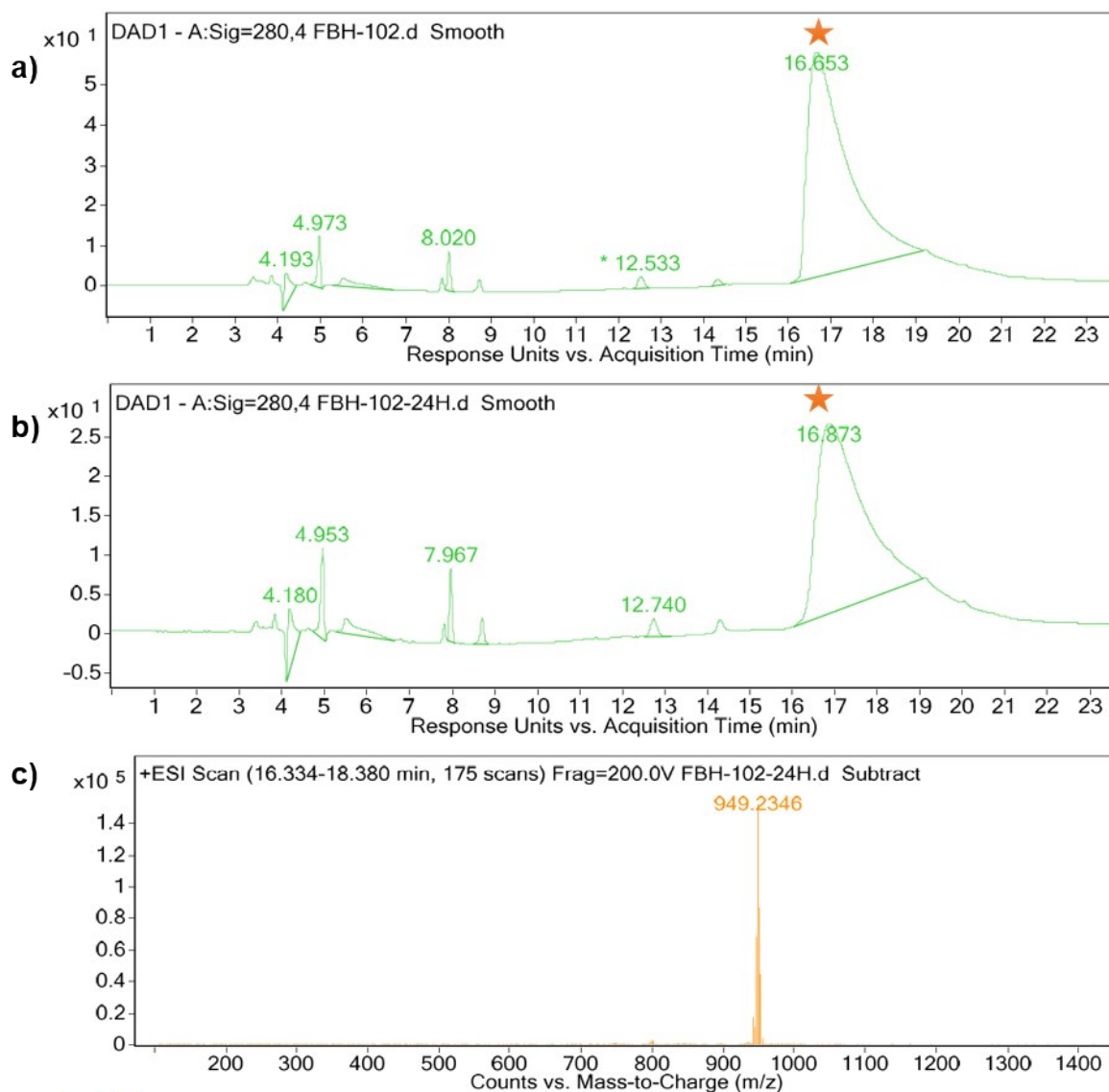


**Figure S29.** HPLC-MS chromatograms of complex **2** ( $5 \times 10^{-5}$  M) in RPMI / DMSO (95/5 v/v) **a)** at  $t = 0$  and **b)** after 1 hour of green light irradiation (520 nm,  $2.5 \text{ mW/cm}^2$ ) and 48 hours of incubation at  $37^\circ \text{C}$ . **c)** ESI-MS (pos ion mode) of complex **2** after irradiation and incubation.

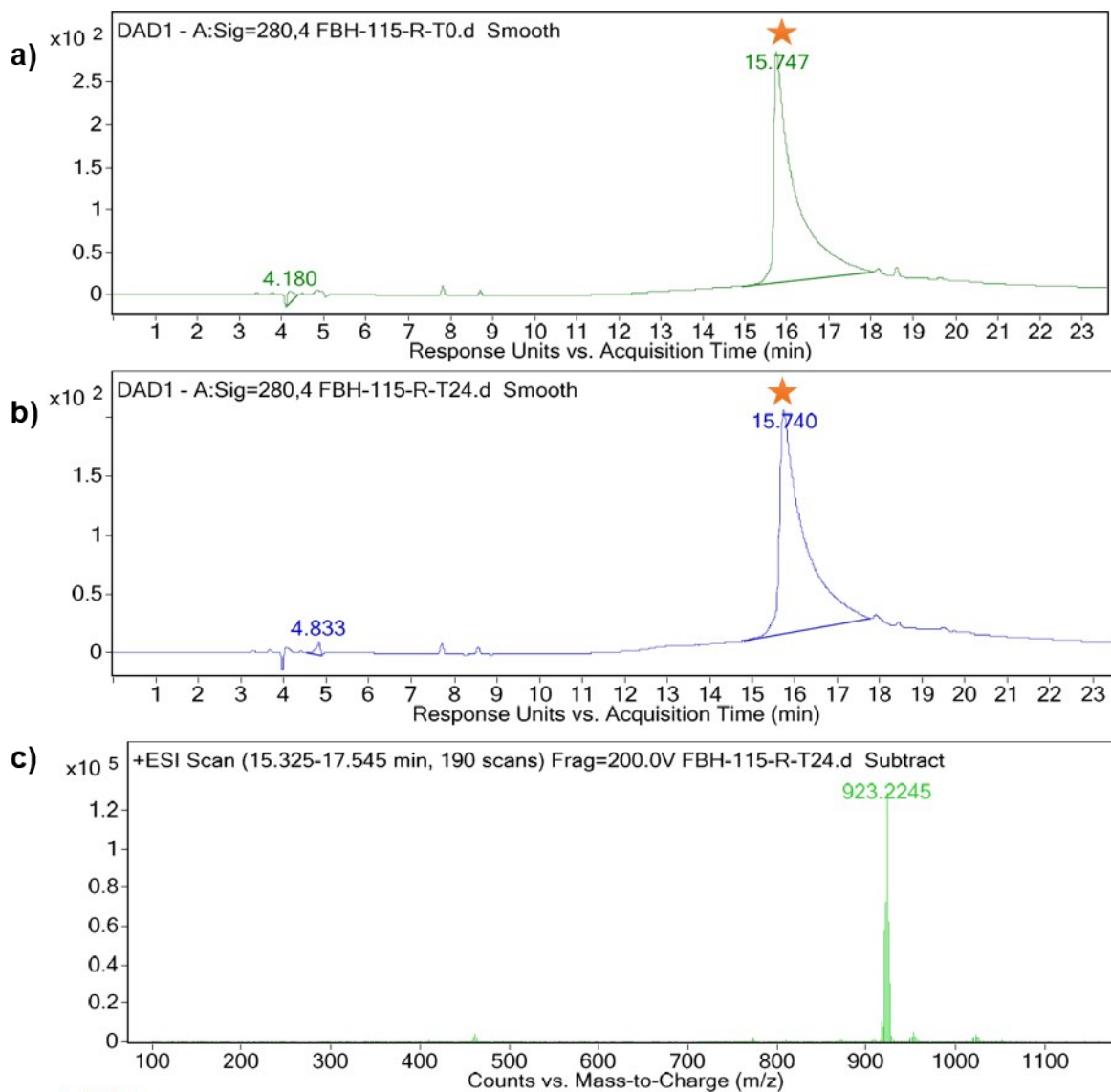


**Figure S30.** HPLC-MS chromatograms of complex **3** ( $5 \times 10^{-5}$  M) in RPMI / DMSO (95/5 v/v) **a)** at  $t = 0$  and **b)** after 1 hour of green light irradiation (520 nm, 2.5 mW/cm<sup>2</sup>) and 48 hours of incubation at 37 °C. **C)** ESI-MS (pos ion mode) of complex **3** after irradiation and incubation.

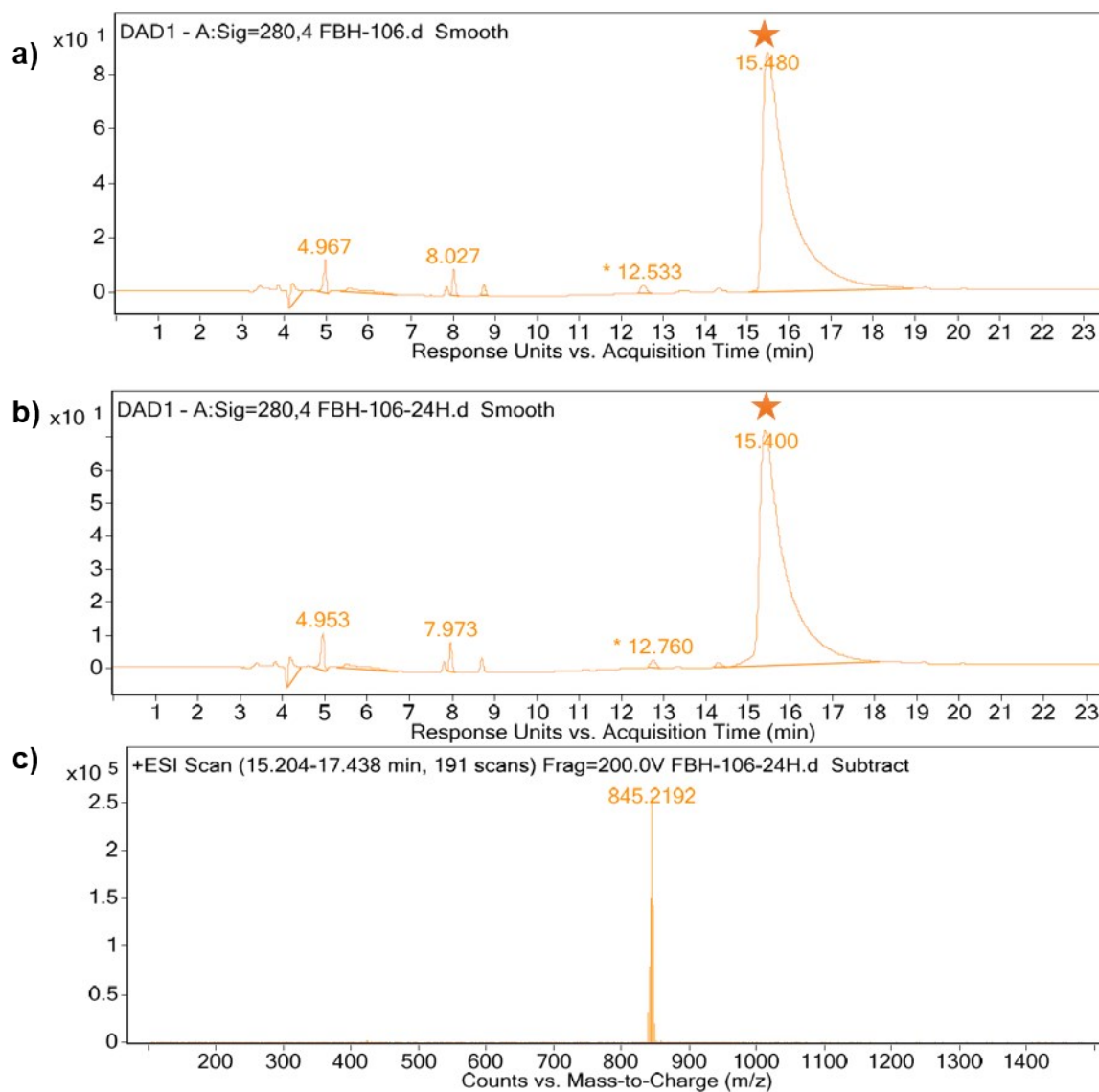


**Figure S31.** HPLC-MS chromatograms of complex **4** ( $5 \times 10^{-5}$  M) in RPMI / DMSO (95/5 v/v) **a)** at  $t = 0$  and **b)** after 1 hour of green light irradiation (520 nm, 2.5 mW/cm<sup>2</sup>) and 48 hours of incubation at 37 °C. **c)** ESI-MS (pos ion mode) of complex **4** after irradiation and incubation.

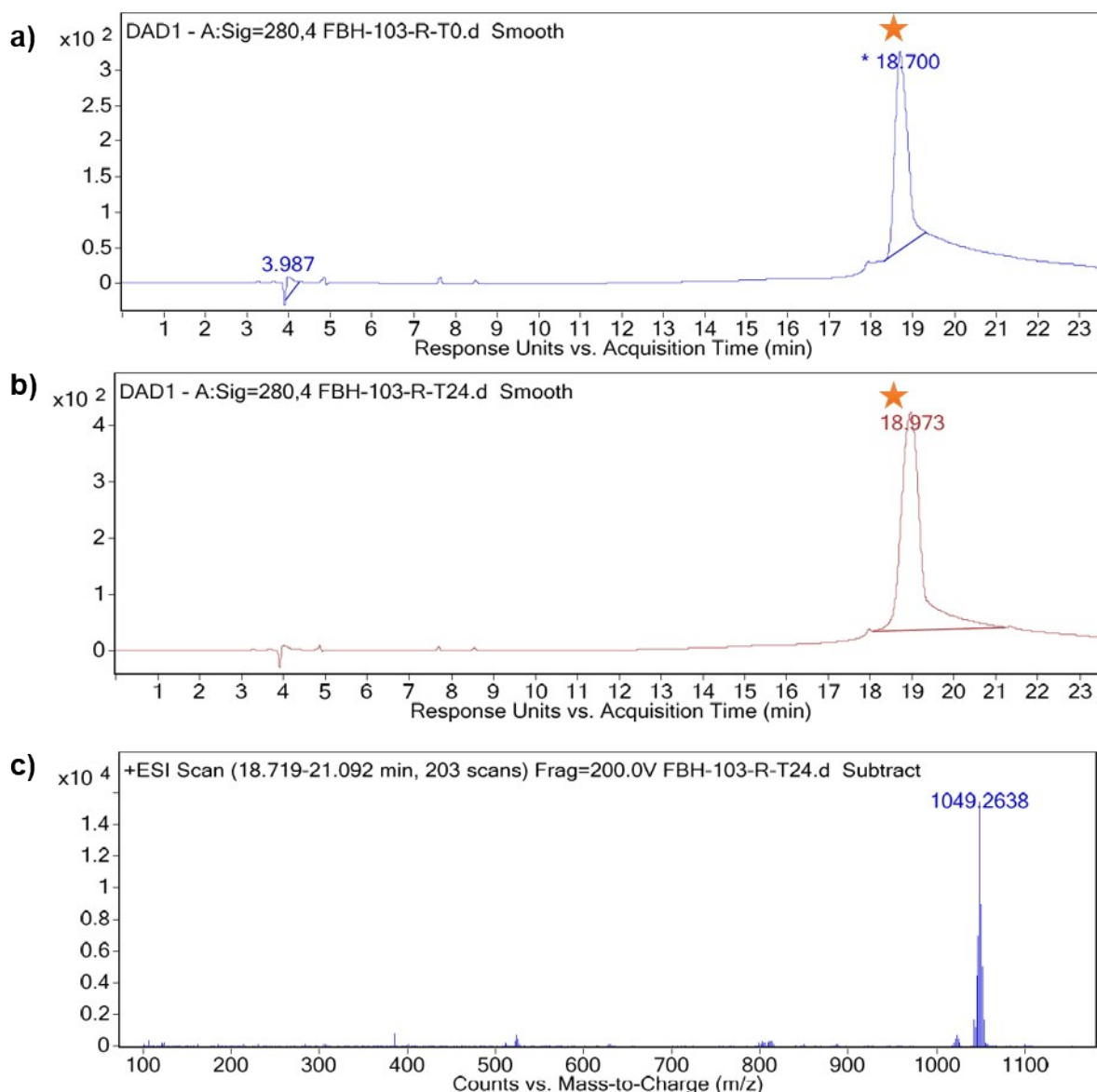


**Figure S32.** HPLC-MS chromatograms of complex **5** ( $5 \times 10^{-5}$  M) in RPMI / DMSO (95/5 v/v) **a)** at  $t = 0$  and **b)** after 1 hour of green light irradiation (520 nm,  $2.5 \text{ mW/cm}^2$ ) and 48 hours of incubation at  $37^\circ \text{C}$ . **C)** ESI-MS (positive ion mode) of complex **5** after irradiation and incubation.

## 8. Octanol- $\text{H}_2\text{O}$ partition coefficient and solubility measures

Partition coefficients were calculated by the “shake-flask” method (adapted from references [6][8]). Compounds were suspended in  $\text{H}_2\text{O}$  in octanol saturated octanol. Suspensions were sonicated for 1 h, shaken for 24 h in an orbital-shaker at 120 r.p.m and there were filtered with a  $0.2 \mu\text{m}$  Nalgene syringe filter (Thermo Fisher Scientific). 4 mL aliquots of the filtered solutions were reserved. Aliquots of the filtered solutions (5 mL) were added to equal volume of octanol saturated  $\text{H}_2\text{O}$ . The mixtures were shaken for 24 h at 298 K. Then, samples were centrifuged to separate the phases. UV-VIS of the organic phases and the reserved aliquots of the filtered solutions were registered.

Cisplatin was suspended in octanol saturated  $\text{H}_2\text{O}$  and the suspension was sonicated for 1 h, shaken for 24 h in an orbital-shaker at 120 r.p.m. and filtered with a  $0.2 \mu\text{m}$  Nalgene syringe filter. 4 mL aliquot of the filtered solution was reserved and 5 mL aliquot was added to

equal volume of H<sub>2</sub>OmQ saturated octanol. The mixture was shaken for 24 h at 298 K and then was centrifuged to separate the phases. UV-Vis spectra of the aqueous phase and the reserved aliquot were registered. Differences in the absorbance at MLCT bands for complexes **1-5** (**1**, 510 nm; **2**, 500 nm; **3**, 510 nm; **4**, 495 nm; **5**, 475 nm) and absorption at 270 nm for cisplatin were used to the determination of LogP<sub>O/W</sub> values.

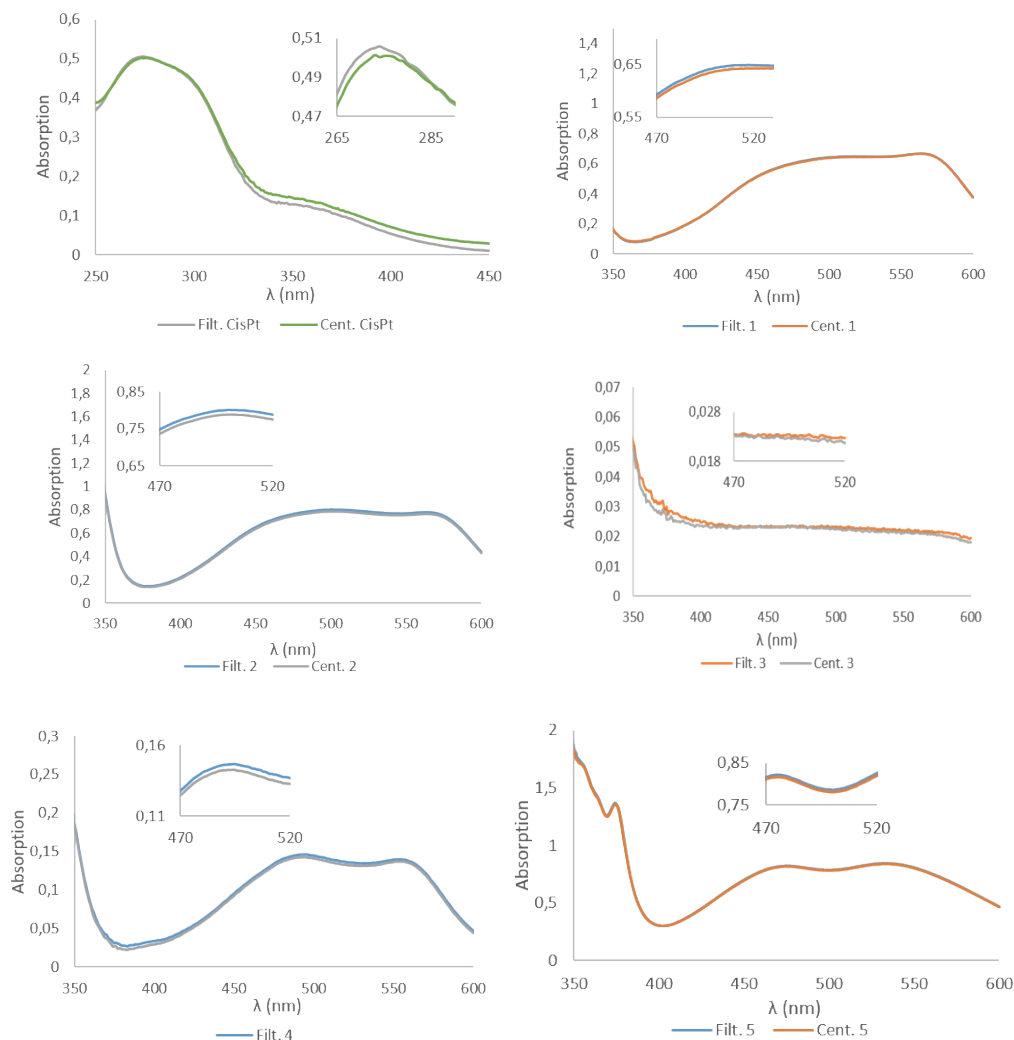


**Figure S33.** UV-Vis spectra of cisplatin and compounds **1-5** used for LogP<sub>O/W</sub> determination.

LogP<sub>O/W</sub> was determined by the following equation for compounds **1-5** (a) and cisplatin (b):

$$\text{a) } \log P_{ow} = \log \left( \frac{As}{Afs - As} \right) \quad \text{b) } \log P_{ow} = \log \left( \frac{Afs - As}{As} \right)$$

“Afs” is the absorbance of the reserved filtered aliquots and “As” is the absorbance of the respective centrifuged phases.

Solubility was determined by the loss of linearity of the Lambert-Beer's law in filtrated solutions[9]. Straight gauge of compounds at different concentrations (0.5, 1, 2.5, 5, 10  $\mu\text{M}$ ) in  $\text{H}_2\text{O}$  with 5% of DMSO were performed. Also, non-linearity behaviour were observed when the solution were filtered with a 0.2  $\mu\text{m}$  Nalgene syringe filter, that accords with the insolubility of the complexes at the higher concentrations and the formation of aggregates.

**Table S3.** Log  $P_{O/W}$  and Solubility of compounds 1-5

Compound	Log $P_{O/W}$	Solubility ( $\mu\text{M}$ )
1	2.02	2.1
2	1.84	1.4
3	1.64	1.0
4	1.59	2.4
5	2.06	0.9
Cis-Pt	-1.96	-

## 9. $^1\text{H-NMR}$ aggregation experiments

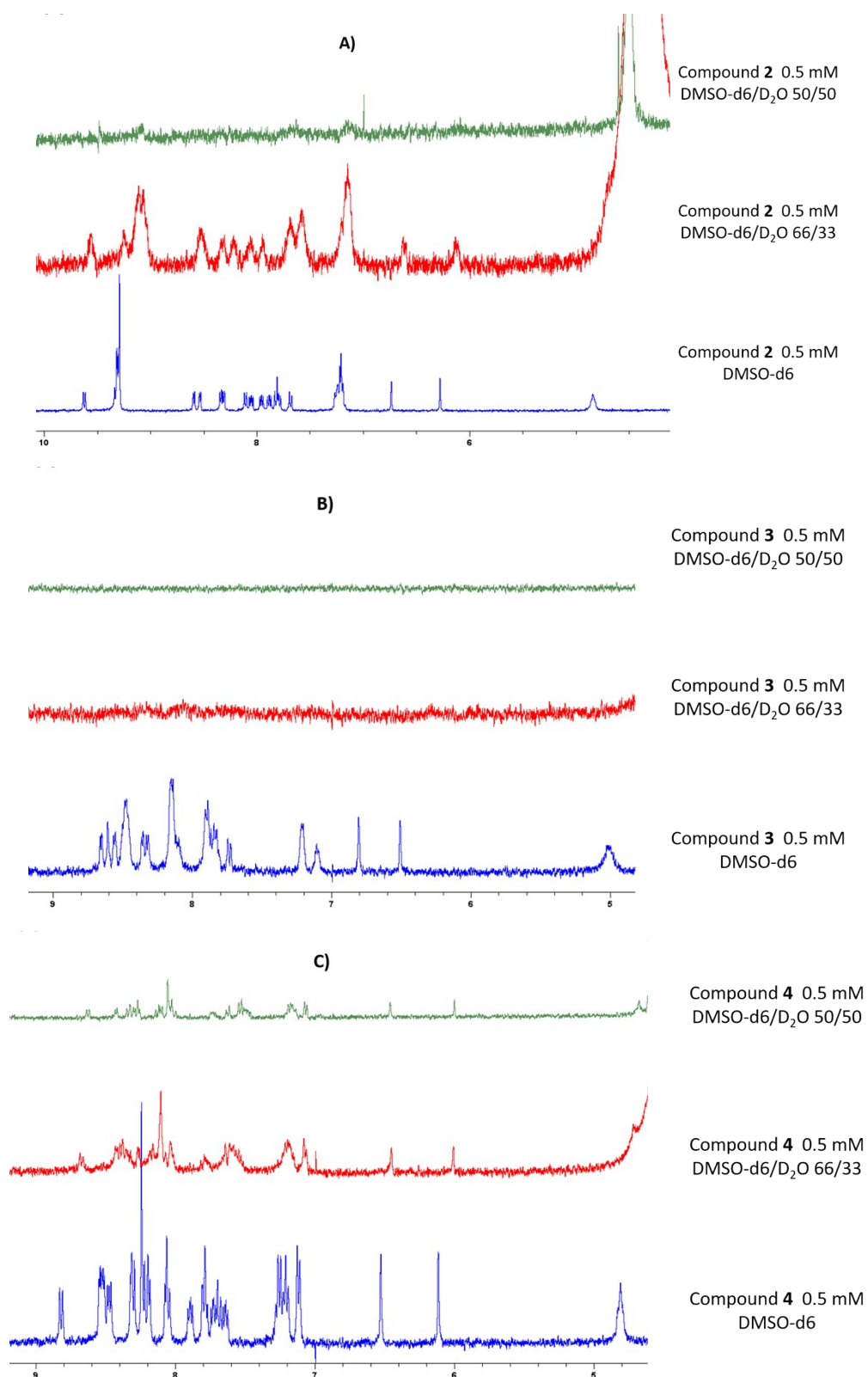


**Figure S34.**  $^1\text{H-NMR}$  spectra of compounds **2** (A), **3** (B), **4** (C) in deuterated DMSO and in different mixtures of DMSO-d<sub>6</sub>/D<sub>2</sub>O.

## 10. Oxidation of NADH

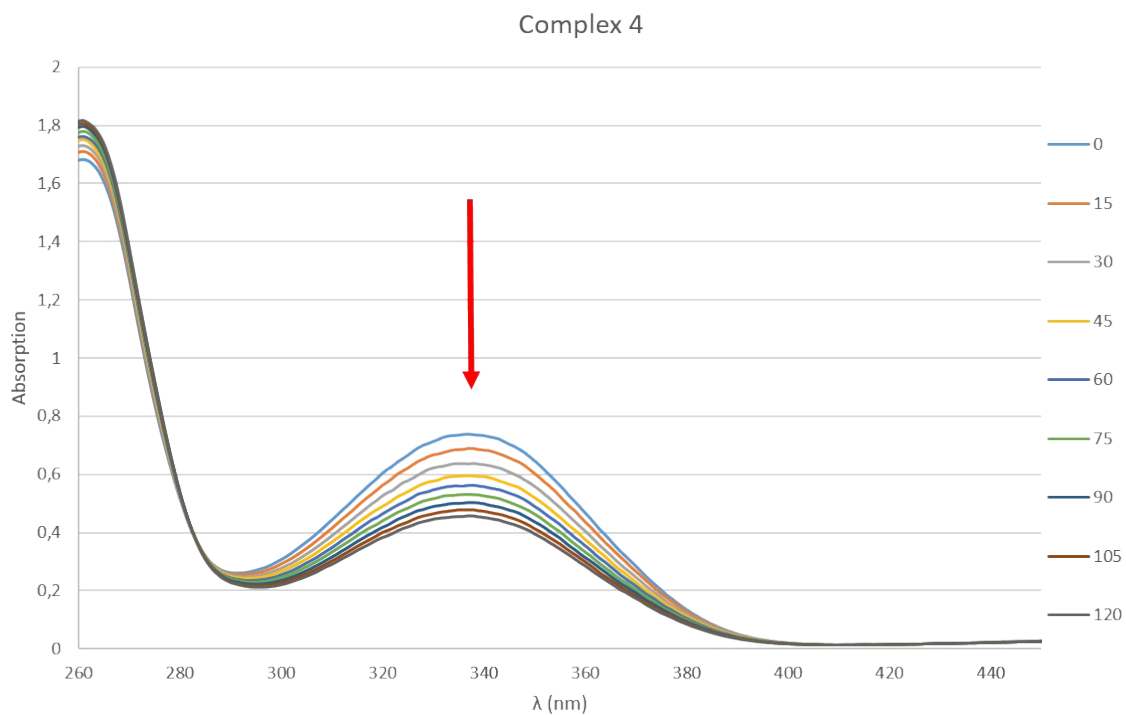


**Figure S35.** UV-Vis spectra of NADH (150 μM) in a mixture of H<sub>2</sub>OmQ/DMF 90/10 (v/v) under green light irradiation (520 nm, 2.0 mW/cm<sup>2</sup>) with 3 μM of complex 4.

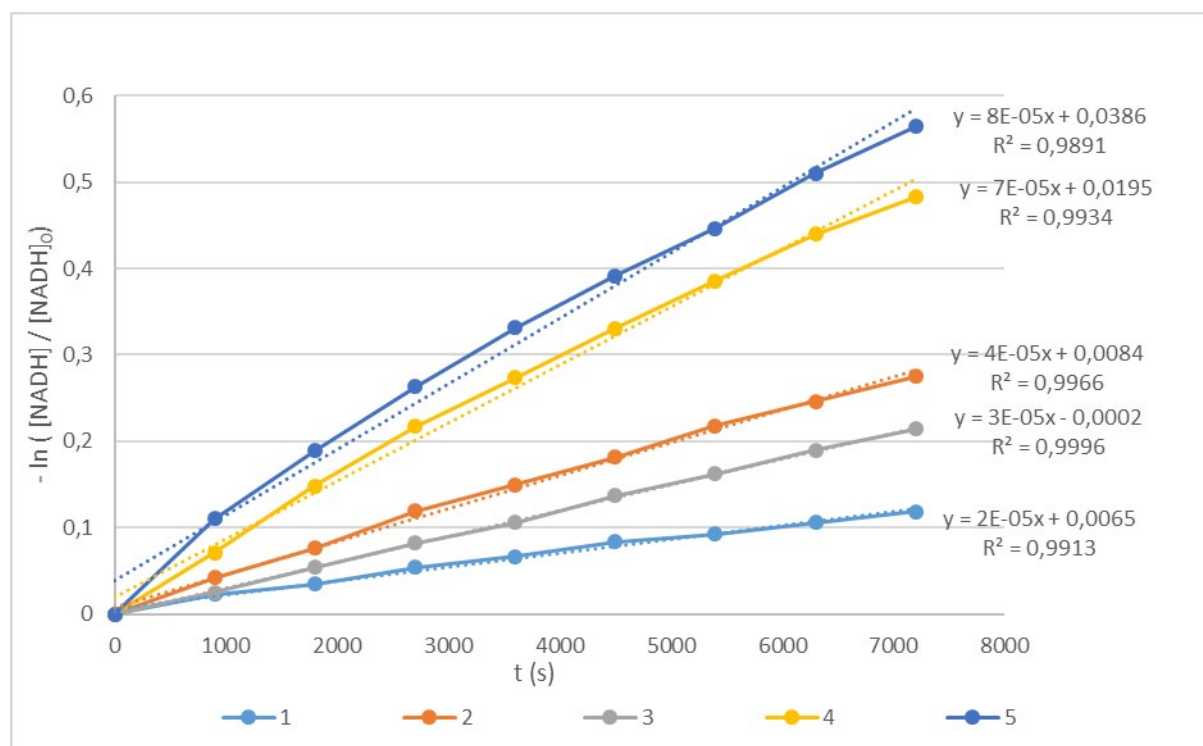




**Figure S36.** First order representation of reaction of oxidation of NADH (150  $\mu\text{M}$ ) with compound **1-5** (3  $\mu\text{M}$ ) in a mixture of  $\text{H}_2\text{OmQ/DMF}$  90/10 (v/v) under green light irradiation (520 nm, 2.0  $\text{mW/cm}^2$ ).

Complex	TON	TOF ( $\text{h}^{-1}$ )
<b>1</b>	3.86	1.93
<b>2</b>	9.38	4.69
<b>3</b>	7.42	3.71
<b>4</b>	15.09	7.55
<b>5</b>	16.53	8.27

Concentration of NADH was obtained using the extinction coefficient at 339 nm ( $6220 \text{ M}^{-1}\text{cm}^{-1}$ )[10]. TON was defined as the number of moles of NADH that compounds **1-5** could convert in 2 h. TOF was calculated from the concentration of oxidized NADH (calculated by the difference of concentration of NADH) after 2 h divided by the concentration of complexes.

**Inhibition of NADH oxidation.** NADH (150  $\mu\text{M}$ ), complexes **2-5** and the respective scavenger were dissolved in a mixture 9/1  $\text{H}_2\text{OmQ/DMF}$  and the solutions were irradiated in a UV-Vis cuvette with green light (520 nm, 2.0  $\text{mW/cm}^2$ ) for 2 h. Reaction performed under  $\text{N}_2$  atmosphere were bubbled for 10 min with  $\text{N}_2$  in a sealed cuvette. Values of inhibition were compared to the same reaction condition without any scavengers and were corrected with a blank without any compound.

ROS	Scavenger
Superoxide anion (O <sub>2</sub> <sup>-</sup> )	Tiron (10 mM)
Hydrogen peroxide (H <sub>2</sub> O <sub>2</sub> )	Sodium pyruvate (10 mM) / NaPyr
Singlet oxygen ( <sup>1</sup> O <sub>2</sub> )	Sodium azide (10 mM) /NaN <sub>3</sub>

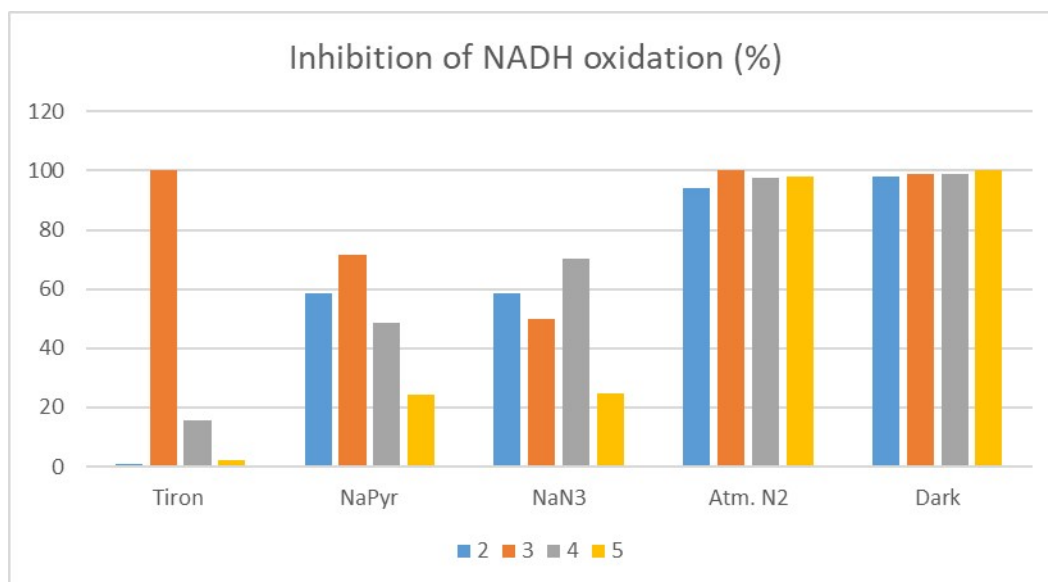


**Figure S37.** Representation of the inhibition of NADH (150  $\mu$ M) oxidation reaction catalysed by compounds **2-5** (3  $\mu$ M) in a mixture 9/1 H<sub>2</sub>O<sub>m</sub>Q/DMF in presence of different ROS scavengers.

## 11. X-ray diffraction

Crystal suitable for X-ray diffraction of **4** was obtained from slow evaporation of a solution of **4** in methanol, and mounted in inert oil on a glass fiber and transferred to the diffractometer. Intensities were registered at low temperature on a Bruker D8QUEST diffractometer using monochromated Mo K $\alpha$  radiation ( $\lambda = 0.71073\text{\AA}$ ). Absorption corrections were based on multi-scans (program SADABS[11]). All non-hydrogen positions were refined with anisotropic temperature factors. Structures were refined anisotropically using SHELXL-2018[12]. Hydrogen atoms were included using rigid methyl groups or a riding model. A summary of crystal data collection and refinement parameters are given in Tables S3-S6.

Special features: There is a poorly-resolved region of residual electron density; this could not be adequately modelled and so was "removed" using the program SQUEEZE, which is part of the PLATON system. The void volume per cell was 487 e $\text{\AA}^3$ , with a void electron count per cell of 143. This additional solvent was not taken account of when calculating derived parameters such as the formula weight, because the nature of the solvent was uncertain. The PF<sub>6</sub> anion is disordered over two positions, ca 56:43%.

**Table S5.** Crystal data and structure refinement for complex **4**.

Identification code	Compound <b>4</b>	
Empirical formula	C <sub>49</sub> H <sub>39</sub> F <sub>6</sub> N <sub>6</sub> O <sub>2</sub> P Ru	
Formula weight	989.90	
Temperature	100(2) K	
Wavelength	0.71073 Å	
Crystal system	Triclinic	
Space group	P-1	
Unit cell dimensions	a = 13.6054(9) Å	α = 66.457(2)°
	b = 13.9682(9) Å	β = 65.954(2)°
	c = 15.6806(10) Å	γ = 81.255(2)°
Volume	2494.7(3) Å <sup>3</sup>	
Z	2	
Density (calculated)	1.318 Mg/m <sup>3</sup>	
Absorption coefficient	0.411 mm <sup>-1</sup>	
F(000)	1008	
Crystal size	0.260 x 0.100 x 0.020 mm <sup>3</sup>	
Theta range for data collection	1.972 to 30.628°	
Index ranges	-19 ≤ h ≤ 19, -19 ≤ k ≤ 20, -22 ≤ l ≤ 22	
Reflections collected	174932	
Independent reflections	15298 [R <sub>int</sub> = 0.0920]	
Completeness to theta = 25.242°	99.9 %	
Absorption correction	Semi-empirical from equivalents	
Max. and min. transmission	0.7461 and 0.6870	
Refinement method	Full-matrix least-squares on F <sup>2</sup>	
Data / restraints / parameters	15298 / 168 / 652	
Goodness-of-fit on F <sup>2</sup>	1.085	
Final R indices [I > 2σ(I)]	R1 = 0.0515, wR2 = 0.1042	
R indices (all data)	R1 = 0.0757, wR2 = 0.1134	
Largest diff. peak and hole	0.665 and -1.014 e.Å <sup>-3</sup>	

**Table S6.** Bond lengths [Å] and angles [°] for complex **4**

Ru(01)-N(1)	2.083(2)	Ru(01)-N(6)	2.0612(19)
Ru(01)-C(15)	2.032(2)	C(15)-Ru(01)-N(1)	78.82(9)
Ru(01)-N(3)	2.047(2)	N(4)-Ru(01)-N(3)	80.22(9)
Ru(01)-N(4)	2.0448(19)	N(6)-Ru(01)-N(5)	78.47(8)
Ru(01)-N(5)	2.143(2)		

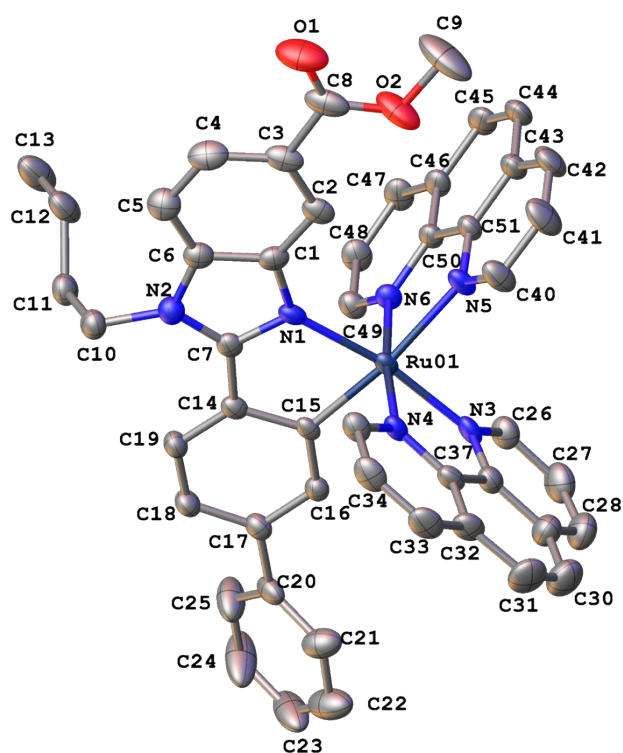


**Figure S38.** X-ray crystal structure of **4**. Ellipsoids are drawn at the 50% probability level. Hydrogen atoms, counterion, and solvent molecules are omitted for clarity

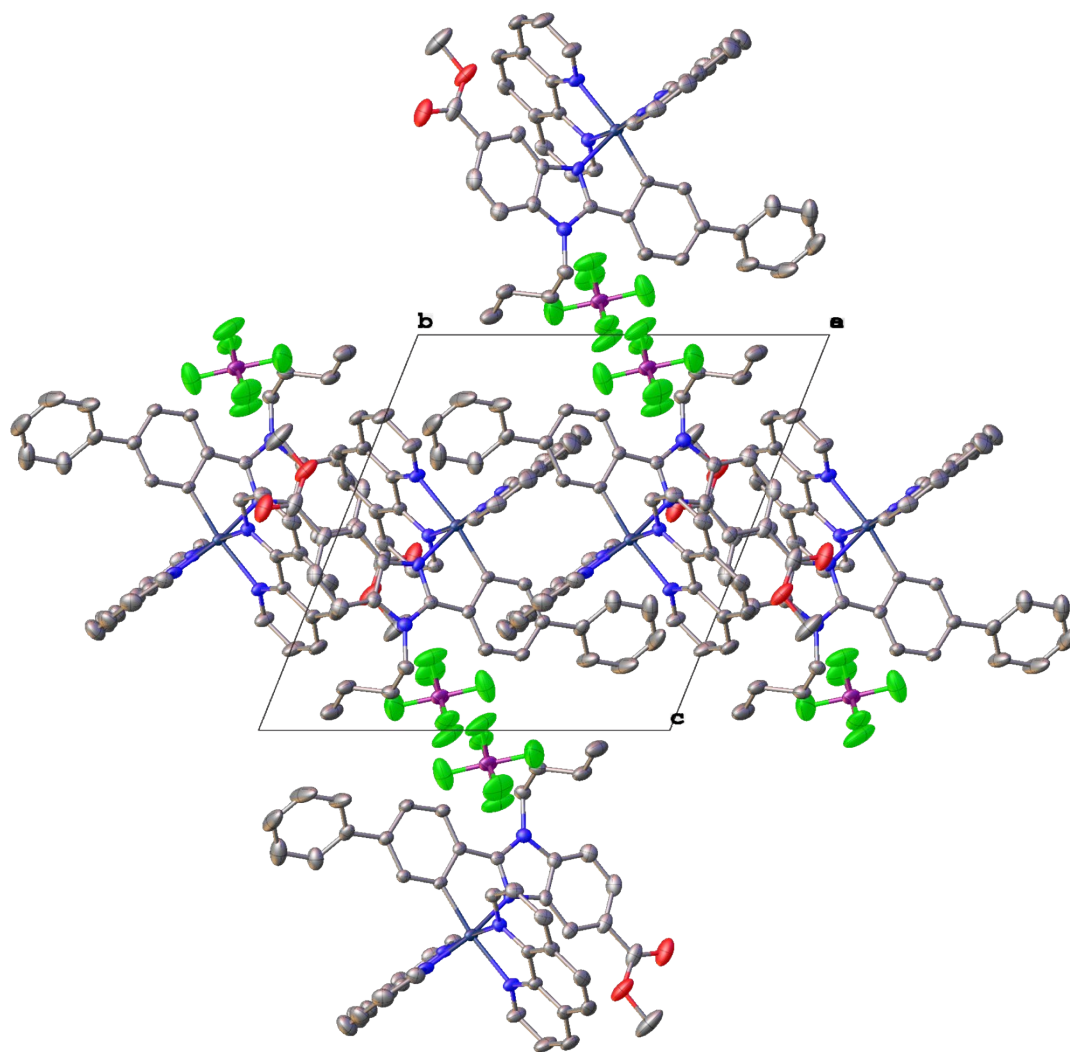


**Figure S39.** Unit cell packing diagram of complex 4.

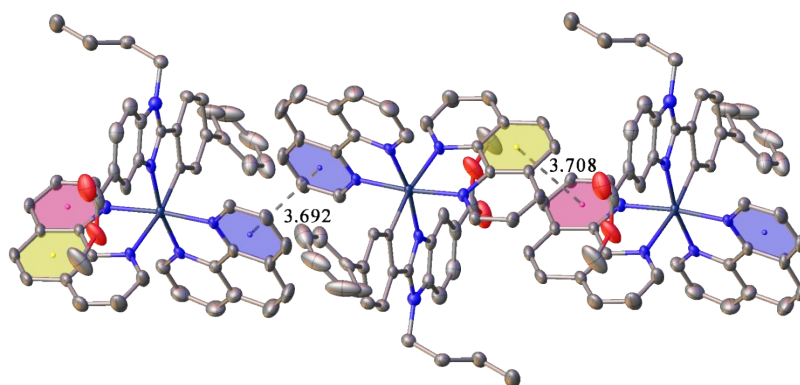


**Figure S40.** Observed  $\pi$ - $\pi$  stacking interactions of complex 4.

## 12. Cell-based assays

### 12.1. Cell culture

Human ovarian carcinoma cell lines, A2780 and A2780cis, were grown in RPMI-1640 supplemented with 10% fetal bovine serum (FBS) and 2 mM L-glutamine, human cervical cancer cells, HeLa, and human triple negative breast cancer cell line, MDA-MB-231, were grown in DMEM supplemented with 10% FBS and 2 mM L-glutamine. Non-tumorigenic chinese hamster ovary cells, CHO, were grown in FK-12 medium supplemented with 10 % FBS and 2mM L-glutamine. The acquired resistance of A2780cis cells was maintained by supplementing the medium with 1  $\mu$ M cisplatin every second passage. All cell lines were cultured in a humidified incubator at 310 K in a 5% CO<sub>2</sub> atmosphere and subcultured 2–3 times a week with an appropriate density for each cell line. The cells lines were confirmed to be mycoplasma-free using Hoechst DNA staining method.[13]

In cell-based assays, a maximum 0.4 % of DMSO (v/v) was used (except for cisplatin, water diluted) which was confirmed to be non-toxic to the cells.

### 12.2. Cytotoxicity assays in the dark

Cell viability was determined using a thiazolyl-blue tetrazolium bromide (MTT)-reagent to assess cell vitality upon exposure of the compounds. In these assays, cells were cultured in 96-well plates at a density of 5000 cells/well in complete medium and incubated for 24 h. Serial dilutions of chemical complexes were added at the final concentrations in the range of 0 to 100  $\mu$ M in a final volume of 100  $\mu$ L per well and incubated for 48 h. The medium was removed and 50  $\mu$ L MTT (1 mg/mL) was added. After incubation of the cells for 4 h, the MTT solution removed and 50  $\mu$ L DMSO was added to solubilize the purple formazan crystals formed in active cells. The absorbance was measured at 570 nm using a microplate reader (FLUOstar Omega) and the IC<sub>50</sub> values were calculated based on the inhibitory rate curves using the next the equation:

$$I = \frac{I_{max}}{1 + \left(\frac{IC_{50}}{C}\right)^n}$$

Where *I* represent the percentage inhibition of viability observed, *I*<sub>max</sub> is the maximal inhibitory effect, IC<sub>50</sub> is the concentration that inhibits 50% of maximal growth, *C* is the concentration of the compound and *n* is the slope of the semi-logarithmic dose-response sigmoidal curves. The non-linear fitting was performed using SigmaPlot 14.0 software. All compounds were tested at least in two independent studies with triplicate points (n=6 biologically independent replicates).

<b>Complexes</b>	<b>A2780</b>	<b>A2780cis</b>	<b>MDA-MB-231</b>	<b>CHO</b>	<b>SF</b>
<b>1</b>	71 ± 2	20 ± 3	72 ± 10	415 ± 33	5.6
<b>2</b>	99 ± 26	27 ± 6	105 ± 8.1	878 ± 11	8.8
<b>3</b>	230 ± 17	46 ± 4	97 ± 22	990 ± 21	4.3
<b>4</b>	77 ± 4	9.2 ± 0.6	61 ± 2	905 ± 11	11.7
<b>5</b>	1170 ± 48	207 ± 17	1319 ± 47	2604 ± 372	2.2
<b>Cisplatin</b>	2251 ± 144	19 041 ± 1167	-	6322 ± 505	3.2

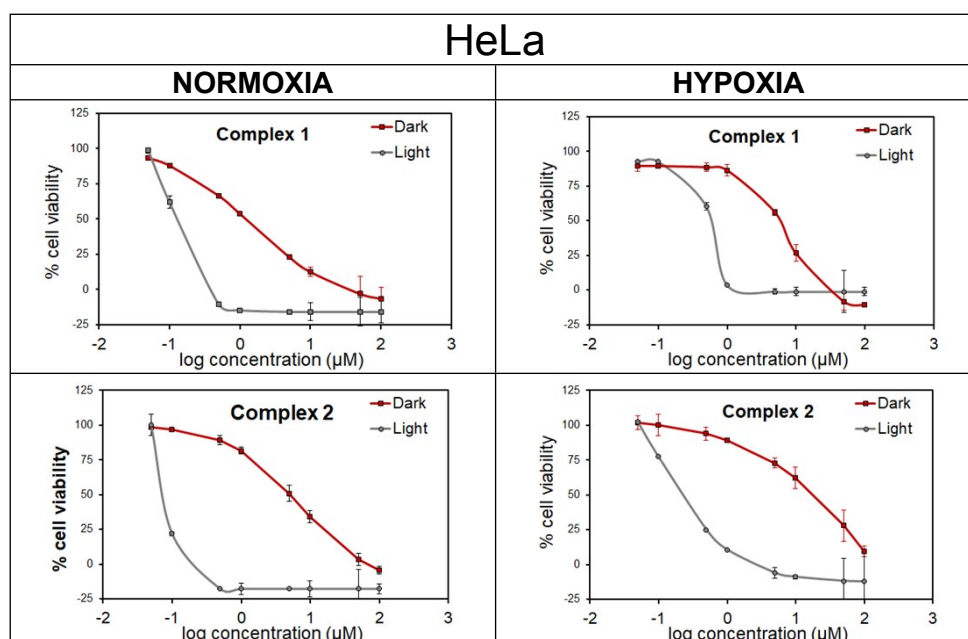
Selectivity factor (SF) defined as IC<sub>50</sub>(CHO normal cells)/IC<sub>50</sub>(A2780 cancer cells).

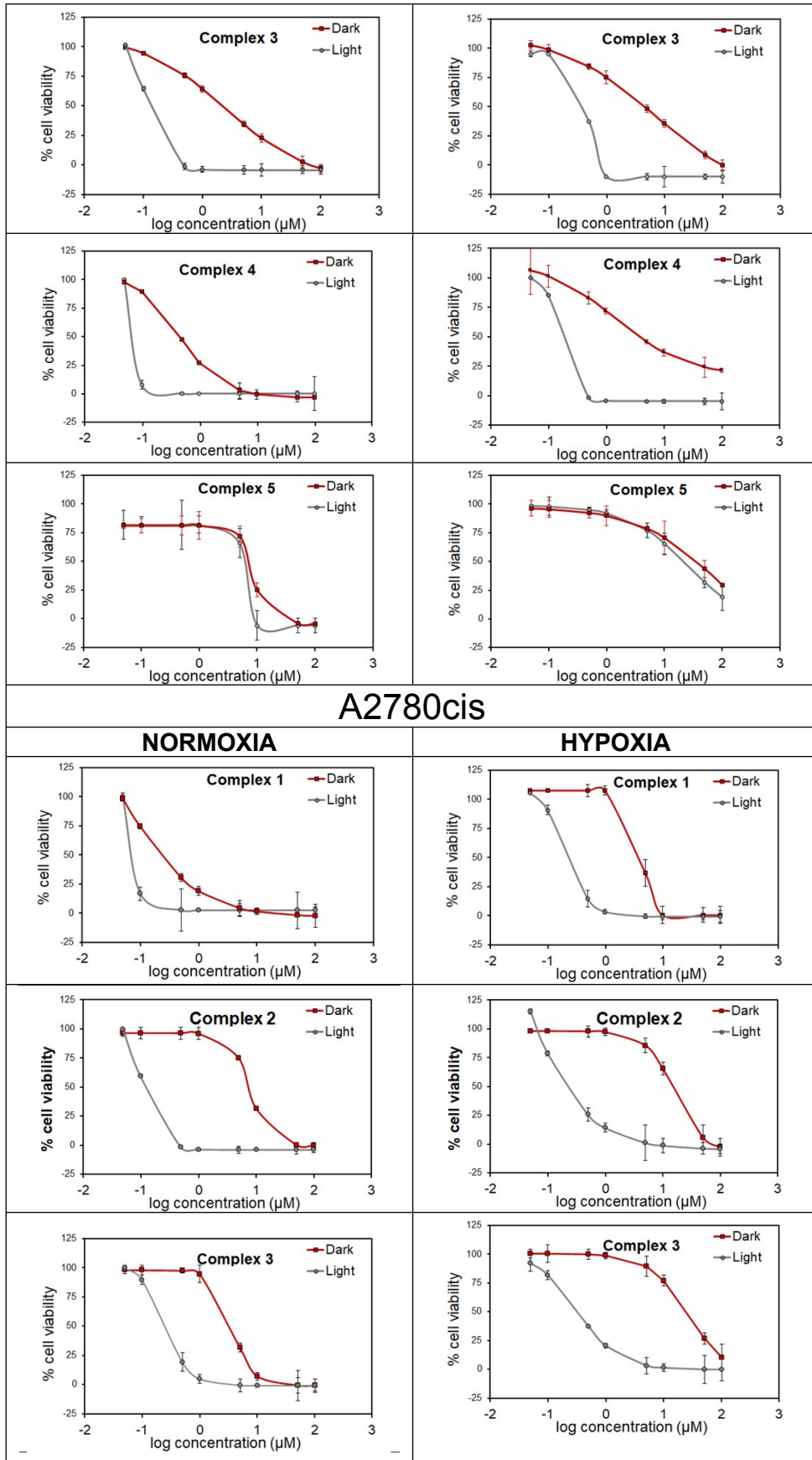
**Table S8.** IC<sub>50</sub> values (μM) obtained for A2780cis cells treated with the investigated Ru complexes in the dark or after irradiation by green light. <sup>[a]</sup>

Complex		Dark	Green light	(PI) <sup>[b]</sup>
<b>1</b>	Normoxia	0.53 ± 0.008	0.083 ± 0.003	6.4
	Hypoxia	3.8 ± 0.7	0.207 ± 0.02	18.3
<b>2</b>	Normoxia	7.5 ± 0.4	0.105 ± 0.004	71.4
	Hypoxia	11.2 ± 0.6	0.022 ± 0.005	509
<b>3</b>	Normoxia	1.91 ± 0.06	0.18 ± 0.02	10.9
	Hypoxia	10.7 ± 0.9	0.316 ± 0.05	33.8
<b>4</b>	Normoxia	0.66 ± 0.07	0.087 ± 0.007	7.6
	Hypoxia	14 ± 2	0.042 ± 0.004	333
<b>5</b>	Normoxia	9.2 ± 0.4	7.1 ± 0.4	1.3
	Hypoxia	>100	>100	1

<sup>[a]</sup> Cells were treated for 2 h (1 h of incubation and 1 h of irradiation at doses of 1.3 mW/cm<sup>2</sup> of green light) followed by 46 h of incubation in drug-free medium.

<sup>[b]</sup> PI (phototoxic index) is defined as the ratio of the toxic effect in the dark and upon light irradiation; PI = [IC<sub>50</sub>]<sub>dark</sub>/[IC<sub>50</sub>]<sub>520 nm</sub>.







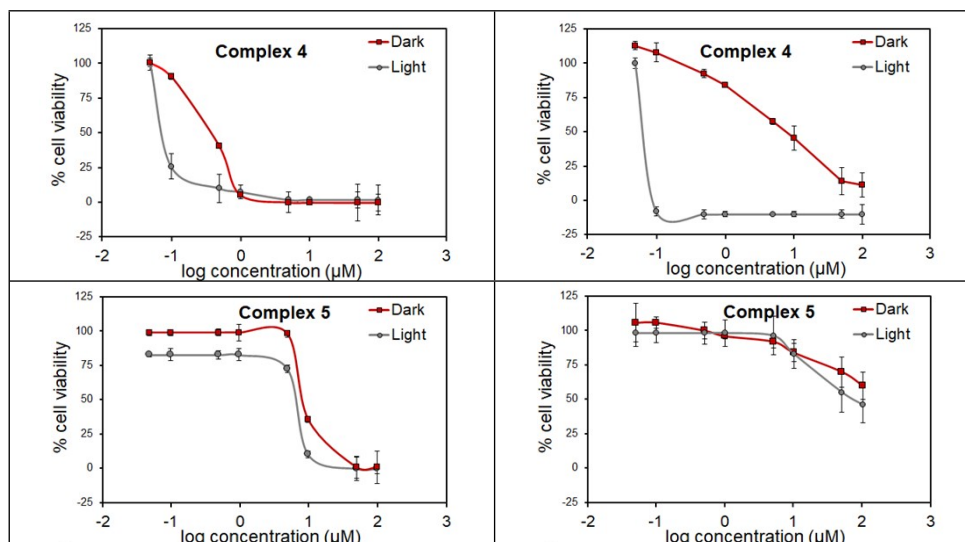


**Figure S41.** Dose-response curves for dark- and photo-cytotoxicity of Ru complexes against HeLa and A2780cis cells under normoxia (21% O<sub>2</sub>) and hypoxia (2% O<sub>2</sub>). All the experiments were performed as duplicates of triplicates (n=6 biologically independent replicates) and data represented mean ± SD.

### 12.3. Photocytotoxicity assays

HeLa and A2780cis cells were used to determine photocytotoxicity of the tested complexes. Cells were cultured in 96-well plates at a density of 5000 cells/well in complete medium and incubated for 24 h. Serial dilutions of chemical complexes were added at the final concentrations in the range of 0 to 100 μM in a final volume of 100 μL per well. Hypoxic conditions were induced by nitrogen atmosphere in a CO<sub>2</sub>/O<sub>2</sub> controlled humidified incubator and were kept under these conditions during the whole experiment. The treatment schedule was performed as follows: 1 h of incubation in the dark followed by 1 h incubation under irradiation conditions by placing the Photoreactor EXPO-LED from Luzchem (Canada) fitted with LED Vis lamps (green led lamps ( $\lambda_{\text{max}} = 520 \text{ nm}$ , at a final light intensity applied of 1.3 mW/cm<sup>2</sup>) inside the CO<sub>2</sub> incubator. The temperature throughout the experiment was 37 °C. Control samples were placed in the dark and then incubated again for 1 h in the humidified CO<sub>2</sub> incubator. Drug-containing medium was then removed by suction, cells washed with saline PBS buffer and loaded with complete cell culture medium. Cells were then incubated for 46 h in this drug-free medium. After the cell recovery period, the medium was removed and 50 μL MTT (1 mg/mL) was added for additional 4 h, then removed and 50 μL DMSO was added to solubilize the purple formazan crystals formed in active cells. The absorbance was measured at 570 nm using a microplate reader (FLUOstar Omega) and the IC<sub>50</sub> values were calculated based on the inhibitory rate curves using the above equation. All compounds were tested at least in two independent experiments with triplicate points (n=6 biologically independent replicates).

### 12.4. Metal accumulation in isolated DNA and in whole cells

The HeLa cells were seeded at 5·10<sup>5</sup> cells/well in 6-well plates in 1.8 mL of complete growth medium and incubated 48 h. Alternatively, cells were seeded in T25 cm<sup>2</sup> flasks at high density and allowed to reach 80 % confluence over 48 h. Cells were then treated with 10 μM of the tested compounds for 2 h. For whole-cells accumulation, cells were trypsinized and counted. For the DNA accumulation, genomic DNA was isolated using DNAzol® reagent (Merck)

following manufacturer instructions and the extracted DNA was quantified using NanoDrop-1000. Both whole cell pellets and isolated DNA samples were digested using Suprapur® nitric acid 30 % for 24 h. The amount of metal elements ruthenium and platinum was determined using Inductively Coupled Plasma Mass Spectrometry (ICP-MS).

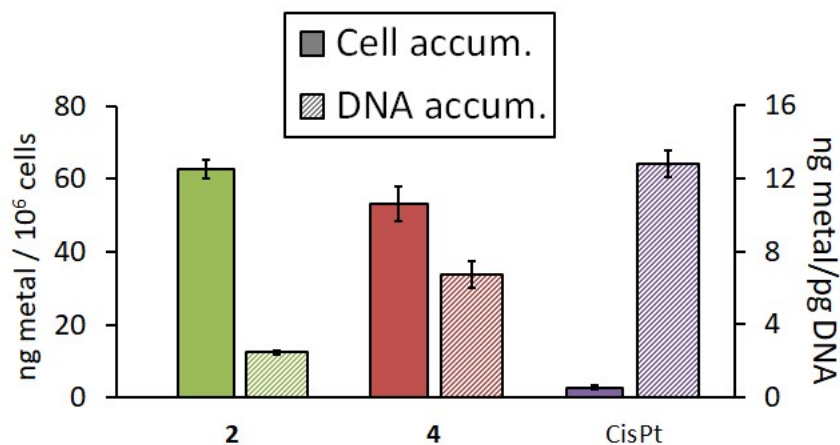


**Figure S42.** Metal accumulation in whole HeLa cells and in isolated DNA determined by ICP-MS analysis after treatment with Ru complexes **2** and **4** and cisplatin (10  $\mu$ M). Data expressed as mean amount of <sup>99</sup>Ru or <sup>194</sup>Pt  $\pm$  SD (from two independent experiences, n=2 replicates).

### 12.5. Determination of ROS generation in HeLa cells under hypoxia after the treatment with the Ru complexes using selective scavengers

Reactive oxygen species were determined using the 2'-7'-dichlorofluorescein diacetate (DCFH-DA) reagent. HeLa cells were seeded onto 96-well plates at  $2 \cdot 10^4$  cells/well for 24 h under normoxic (21% O<sub>2</sub>) or hypoxic conditions (2% O<sub>2</sub>) in the humidified CO<sub>2</sub> incubator. Cells were then cotreated with selective ROS scavengers and with 5  $\mu$ M of the tested complexes for 1 h. Formation of <sup>1</sup>O<sub>2</sub> was prevented by sodium azide (NaN<sub>3</sub>) at a final concentration of 5 mM[14]; hydroxyl radicals ( $\bullet$ OH) were scavenged by D-Mannitol (Mann) at 50 mM[14,15] superoxide anion ( $\bullet$ O<sub>2</sub><sup>-</sup>) production was reduced by tiron scavenger (5 mM)[16,17]; generation hydrogen peroxide was prevented by sodium pyruvate (NaPyr) at 10 mM[14]; and peroxy radical (ROO $\bullet$ ) species were eliminated by 0.1 mM of trolox[18]. The ROS scavengers remained throughout the experiment. After treatment application, cells were incubated for 1 h in the dark followed by 1 h of irradiation with green light 520 nm; 1.3 mW/cm<sup>2</sup>. After irradiation, the cells were stained by using 10  $\mu$ M of DCFH-DA for 30 min. Cells were then trypsinized to allow cell capture by the flow cytometer (Fortessa X20) using the 96-well platen adaptation and analyzed using FlowingSoftware version 2.5.1. The assay was performed in two independent experiences (n= 3 per replicate).

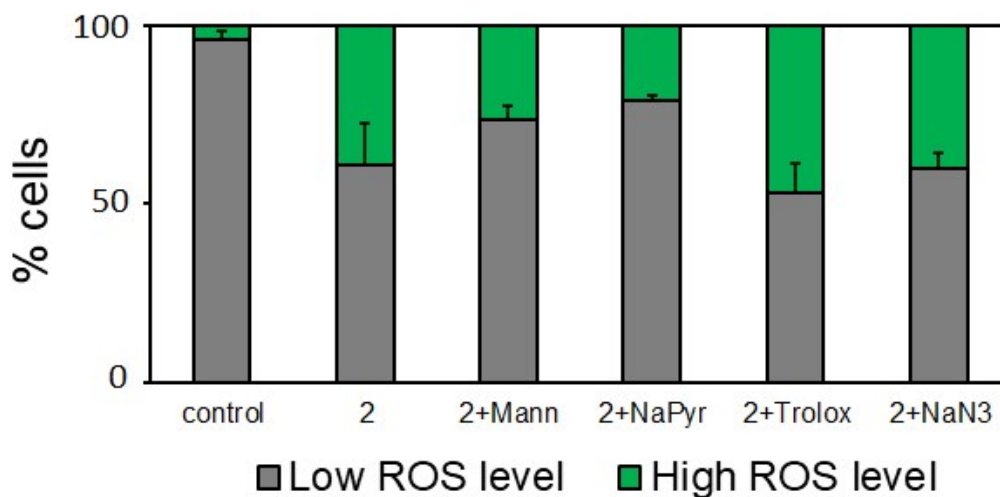
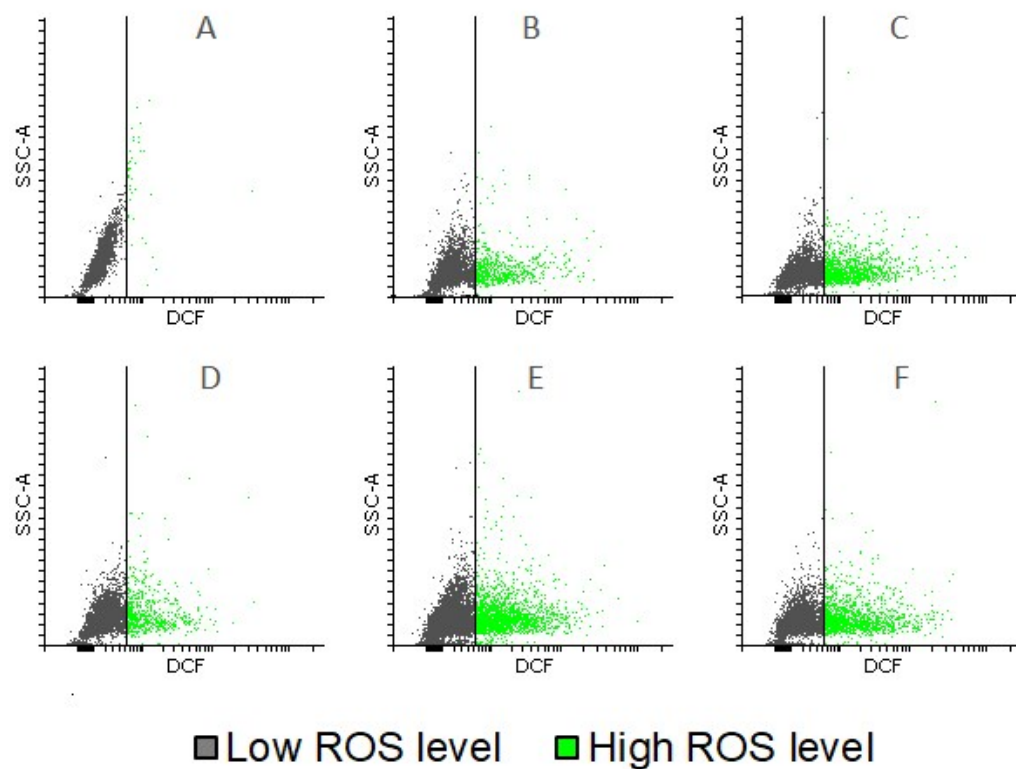


**Figure S43.** FACS analysis for determination of ROS in HeLa cells by flow cytometry after the irradiation with green light under normoxia (SSC-A: cell complexity and DCF: dichlorofluorescein product fluorescence). Cells were incubated with specific ROS scavengers and then treated with Ru(II) complexes (1h in the dark followed by 1h under light irradiation). Untreated, irradiated cells were used as a negative control (A); cells treated with **2** without scavengers was used as a positive control (B); incubation with specific ROS scavengers: D-mannitol or Mann [50 mM] (C), sodium pyruvate or NaPyr [10 mM] (D), trolox [0.1 mM] (E) and sodium azide or NaN<sub>3</sub> [5 mM] (F). Scavengers remained throughout the experiment. Data are representative of two independent experiments with n=3 replicates

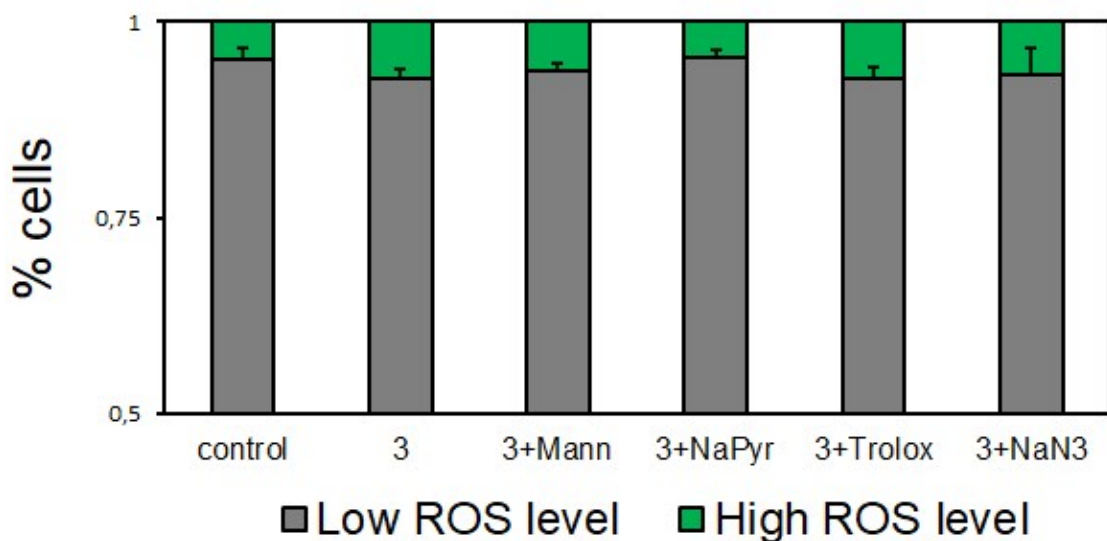
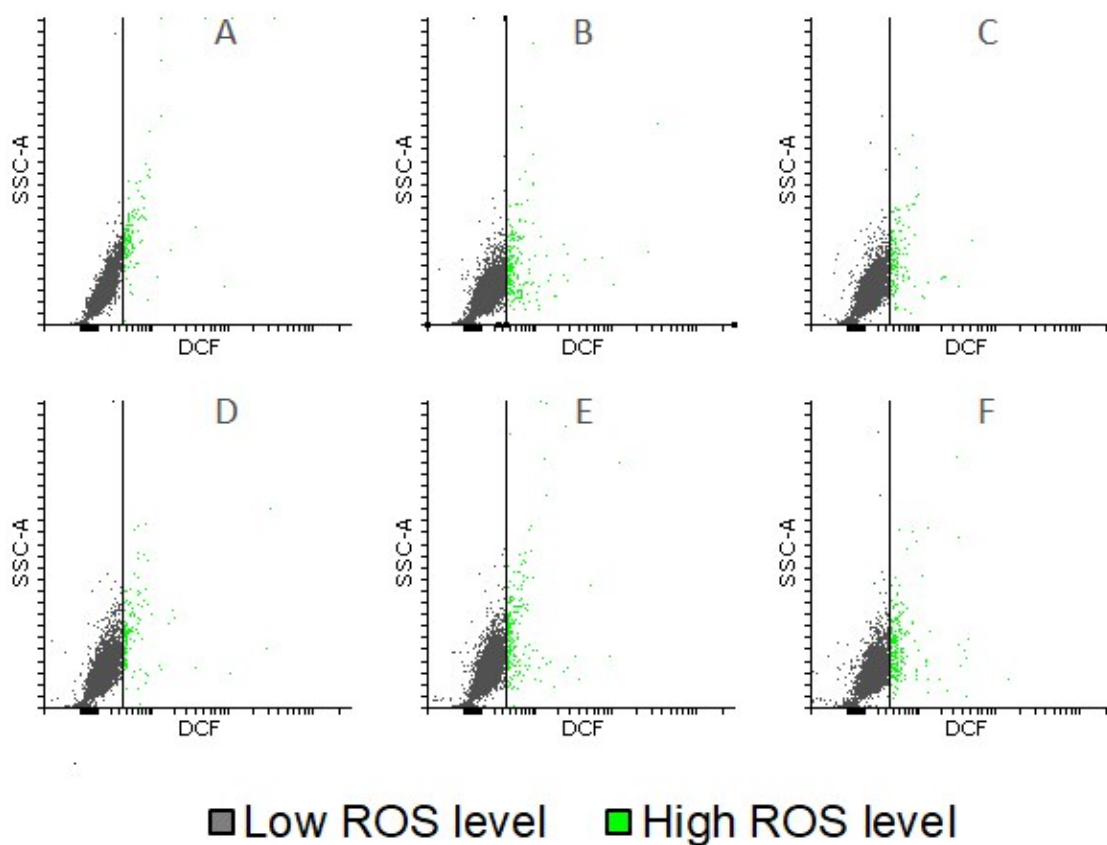


**Figure S44.** FACS analysis for determination of ROS in HeLa cells by flow cytometry after the irradiation with green light under normoxia (SSC-A: cell complexity and DCF: dichlorofluorescein product fluorescence). Cells were incubated with specific ROS scavengers and then treated with Ru(II) complexes (1h in the dark followed by 1h under light irradiation). Untreated, irradiated cells were used as a negative control (A); cells treated with **3** without scavengers was used as a positive control (B); incubation with specific ROS

scavengers: D-mannitol or Mann [50 mM] (C), sodium pyruvate or NaPyr [10 mM] (D), trolox [0.1 mM] (E) and sodium azide or NaN<sub>3</sub> [5 mM] (F). Scavengers remained throughout the experiment. Data are representative of two independent experiments with n=3 replicates

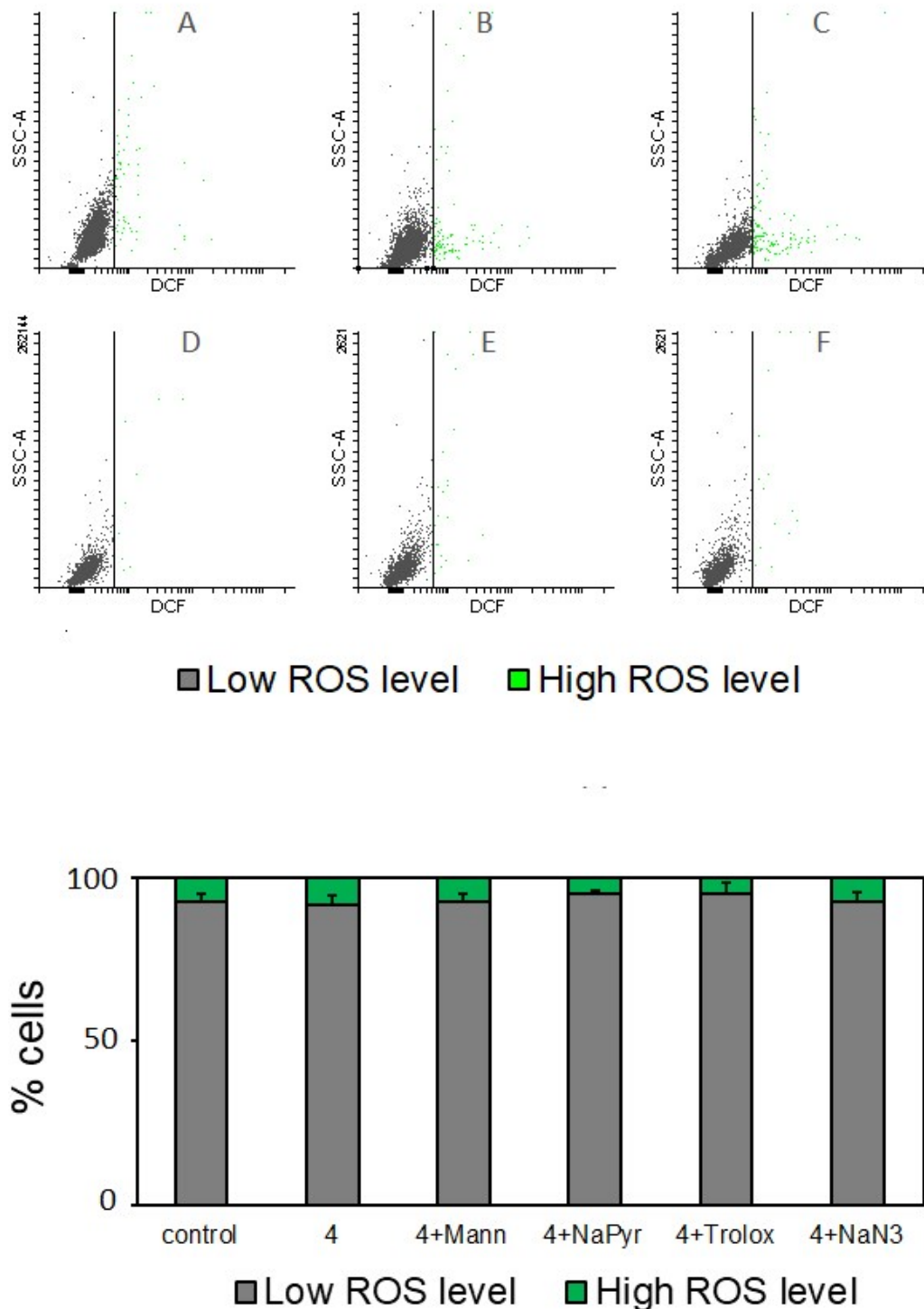


**Figure S45.** FACS analysis for determination of ROS in HeLa cells by flow cytometry after the irradiation with green light under normoxia (SSC-A: cell complexity and DCF: dichlorofluorescein product fluorescence). Cells were incubated with specific ROS

scavengers and then treated with Ru(II) complexes (1h in the dark followed by 1h under light irradiation). Untreated, irradiated cells were used as a negative control (A); cells treated with 4 without scavengers was used as a positive control (B); incubation with specific ROS scavengers: D-mannitol or Mann [50 mM] (C), sodium pyruvate or NaPyr [10 mM] (D), trolox [0.1 mM] (E) and sodium azide or NaN<sub>3</sub> [5 mM] (F). Scavengers remained throughout the experiment. Data are representative of two independent experiments with n=3 replicates

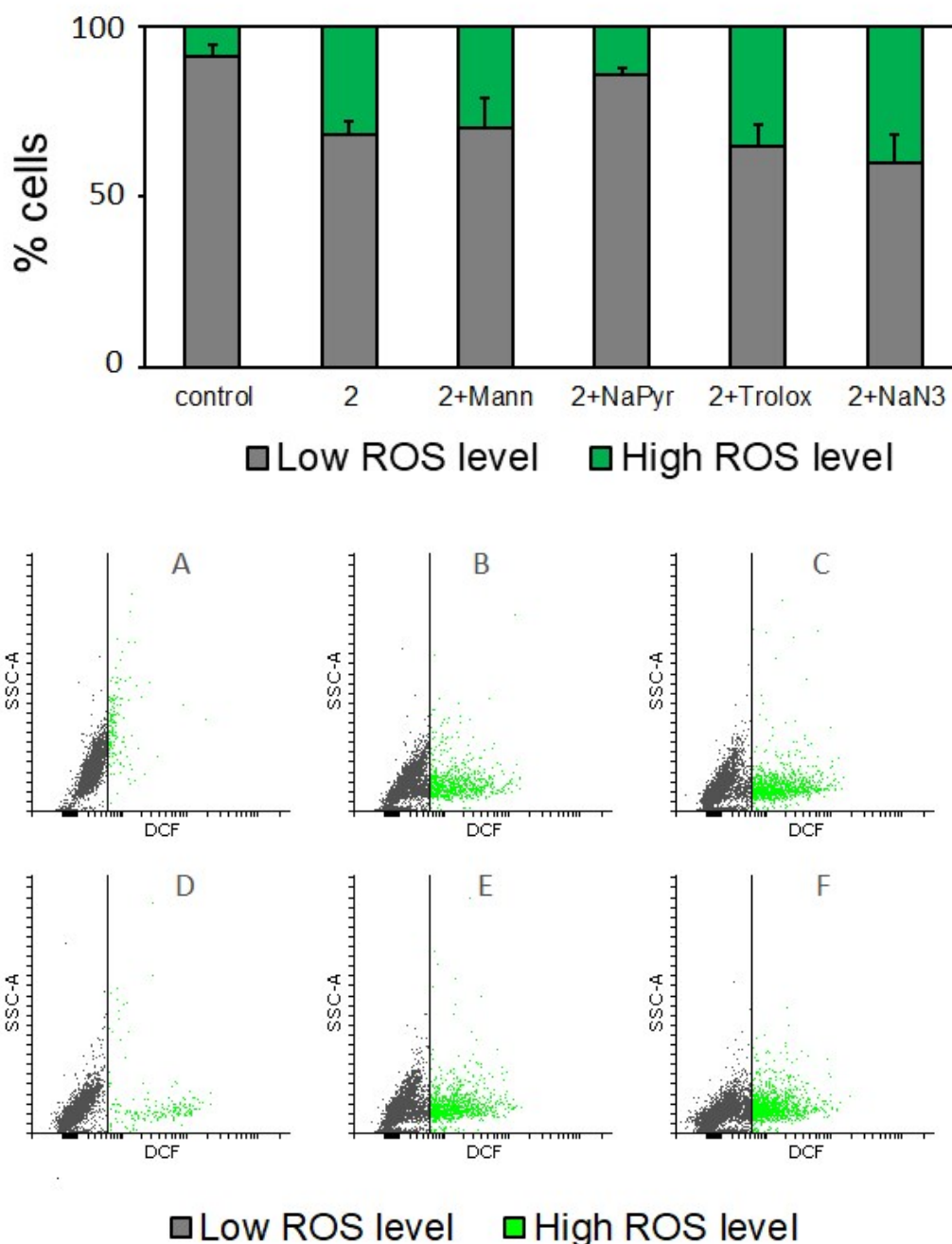


**Figure S46.** FACS analysis for determination of ROS in HeLa cells by flow cytometry after the irradiation with green light under hypoxia (SSC-A: cell complexity and DCF: dichlorofluorescein product fluorescence). Cells were incubated with specific ROS scavengers and then treated with Ru(II) complexes (1h in the dark followed by 1h under light

irradiation). Untreated, irradiated cells were used as a negative control (A); cells treated with **2** without scavengers was used as a positive control (B); incubation with specific ROS scavengers: D-mannitol or Mann [50 mM] (C), sodium pyruvate or NaPyr [10 mM] (D), trolox [0.1 mM] (E) and sodium azide or NaN<sub>3</sub> [5 mM] (F). Scavengers remained throughout the experiment. Data are representative of two independent experiments with n=3 replicates.

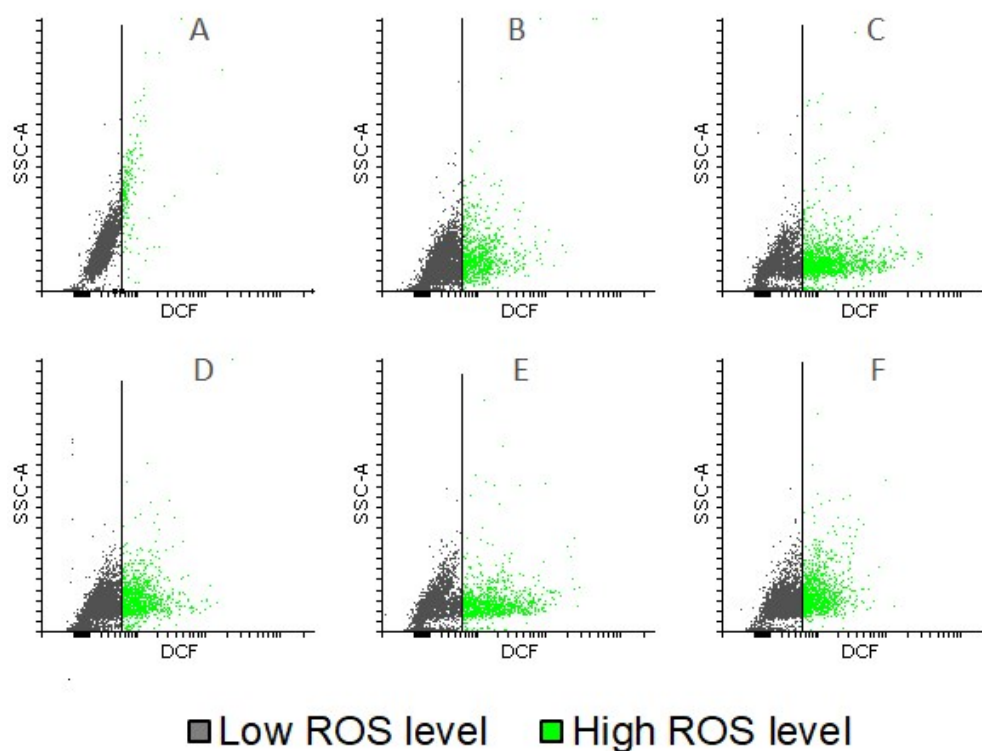
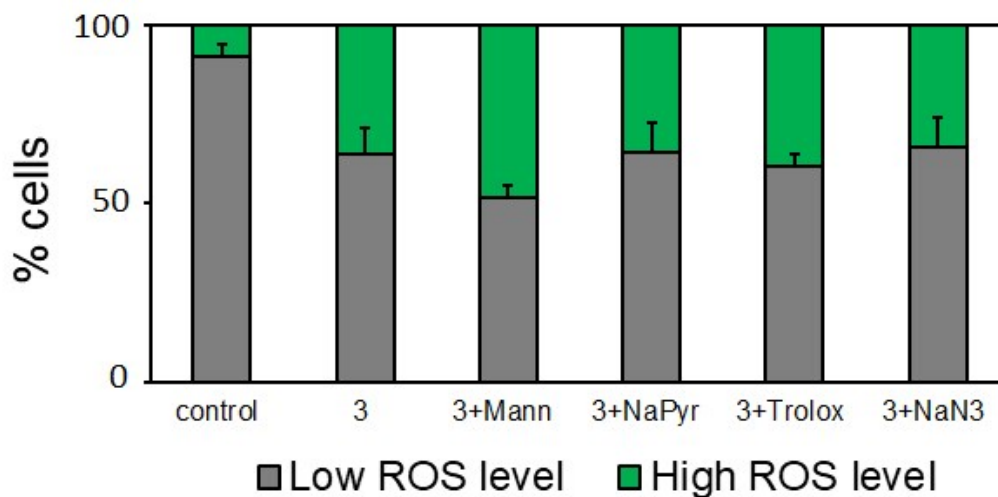


**Figure S47.** FACS analysis for determination of ROS in HeLa cells by flow cytometry after the irradiation with green light under hypoxia (SSC-A: cell complexity and DCF: dichlorofluorescein product fluorescence). Cells were incubated with specific ROS scavengers and then treated with Ru(II) complexes (1h in the dark followed by 1h under light irradiation). Untreated, irradiated cells were used as a negative control (A); cells treated with

**3** without scavengers was used as a positive control (B); incubation with specific ROS scavengers: D-mannitol or Mann [50 mM] (C), sodium pyruvate or NaPyr [10 mM] (D), trolox [0.1 mM] (E) and sodium azide or NaN<sub>3</sub> [5 mM] (F). Scavengers remained throughout the experiment. Data are representative of two independent experiments with n=3 replicates.

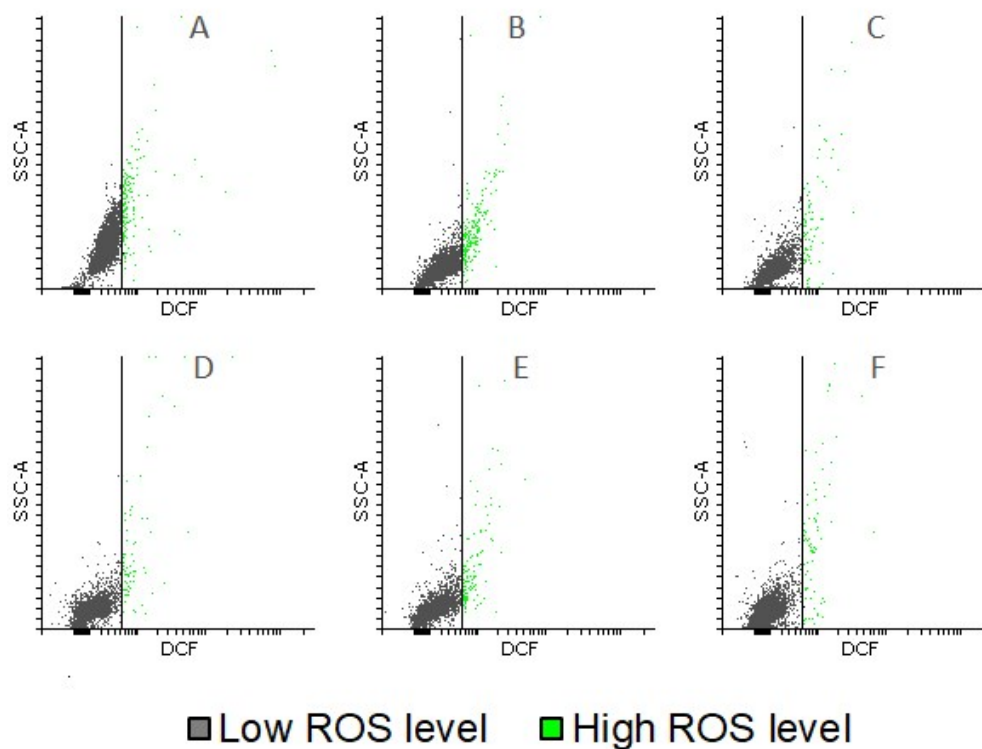
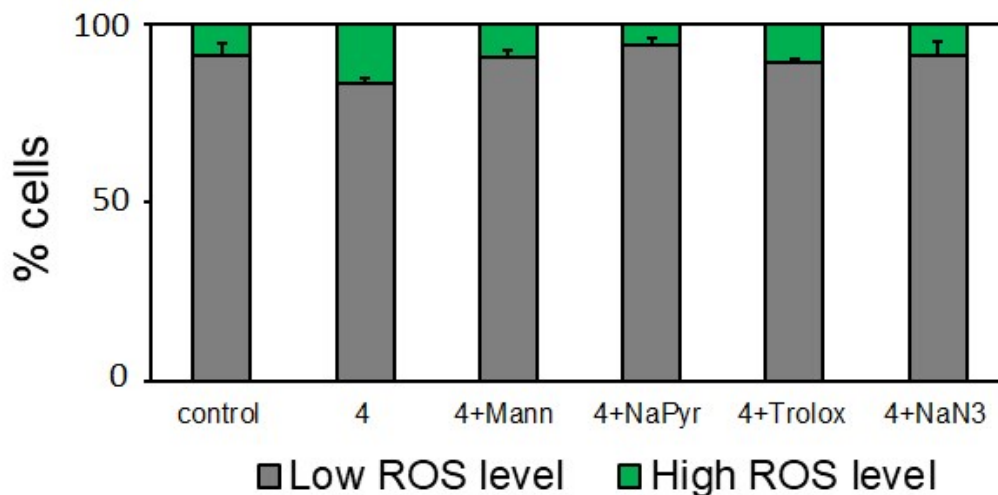


**Figure S48.** FACS analysis for determination of ROS in HeLa cells by flow cytometry after the irradiation with green light under hypoxia (SSC-A: cell complexity and DCF: dichlorofluorescein product fluorescence). Cells were incubated with specific ROS scavengers and then treated with Ru(II) complexes (1h in the dark followed by 1h under light irradiation). Untreated, irradiated cells were used as a negative control (A); cells treated with **4** without scavengers was used as a positive control (B); incubation with specific ROS scavengers: D-mannitol or Mann [50 mM] (C), sodium pyruvate or NaPyr [10 mM] (D), trolox



[0.1 mM] (E) and sodium azide or NaN<sub>3</sub> [5 mM] (F). Scavengers remained throughout the experiment. Data are representative of two independent experiments with n=3 replicates.

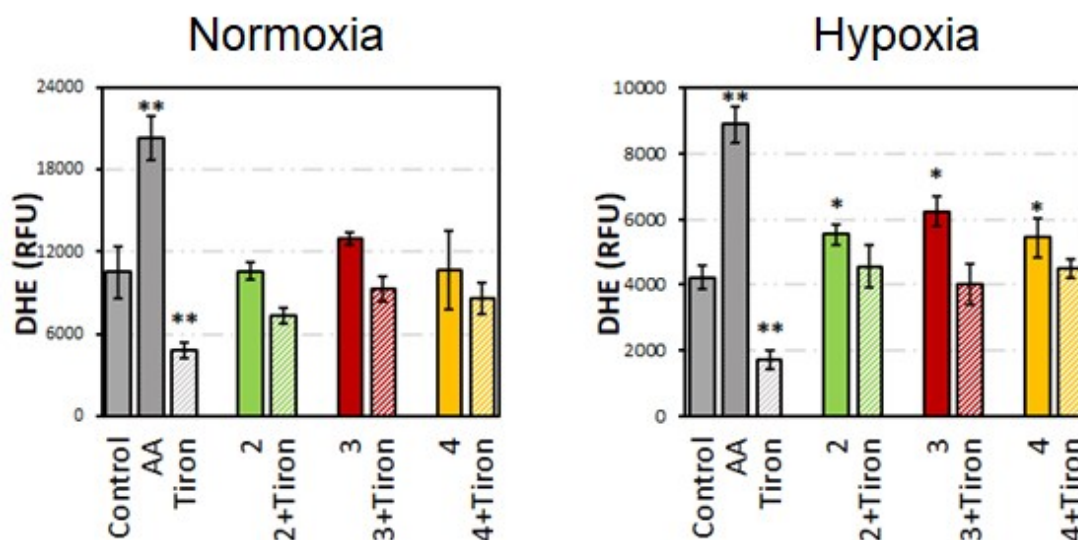


**Figure S49.** Dihydroethidium fluorescence (DHE) analysis for determination of superoxide anion levels after treatments with Ru complexes (1 h incubation and 1 h irradiation) Data represented as mean  $\pm$  SD from three independent experiments. Statistical significance from control cells based on \* $p < 0.05$  and \*\* $p < 0.01$  using unpaired t-test.

## 12.6. Inhibition of global protein synthesis assay in cancer cells

Nascent protein synthesis was assayed using the Click-iT Plus O-propargyl-puromycin (OPP) Protein Synthesis Assay Kit (Invitrogen™) according to manufacturer instructions. Briefly, A2780 cells were incubated at  $2 \cdot 10^4$  cells/well in 96-well plates for 24 h and treated with the ruthenium complexes or cycloheximide for 12 hours. Then 20  $\mu$ M Click-iT OPP reagent for 30 min, fixed with 3.7% formaldehyde in PBS, permeabilized with 0.5% Triton X-100 and then stained with the Click-iT Plus OPP reaction cocktail containing Alexa Fluor 488 picolyl azide as instructed. Cells were then washed, counterstained with NuclearMask blue stain and imaged by confocal fluorescence microscopy. Alternatively, quantification of OPP labeling was measured in 96 well-plates by High-Throughput screening flow cytometry (Fortessa X20) following the protocol above and adding a trypsinization step to allow cell capture by the cytometer. Prior to the assay, fluorescence intensities of both Alexa Fluor 488 and NuclearMask stain was measured in a ClarioStar™ microplate reader. The fluorescence intensity ratio between Alexa Fluor 488 (protein synthesis) and nuclear staining (cell vitality) was used as an indicator for actual global protein synthesis. Experiments were repeated in duplicate using triplicate points per concentration level (n=6 biological independent replicates).

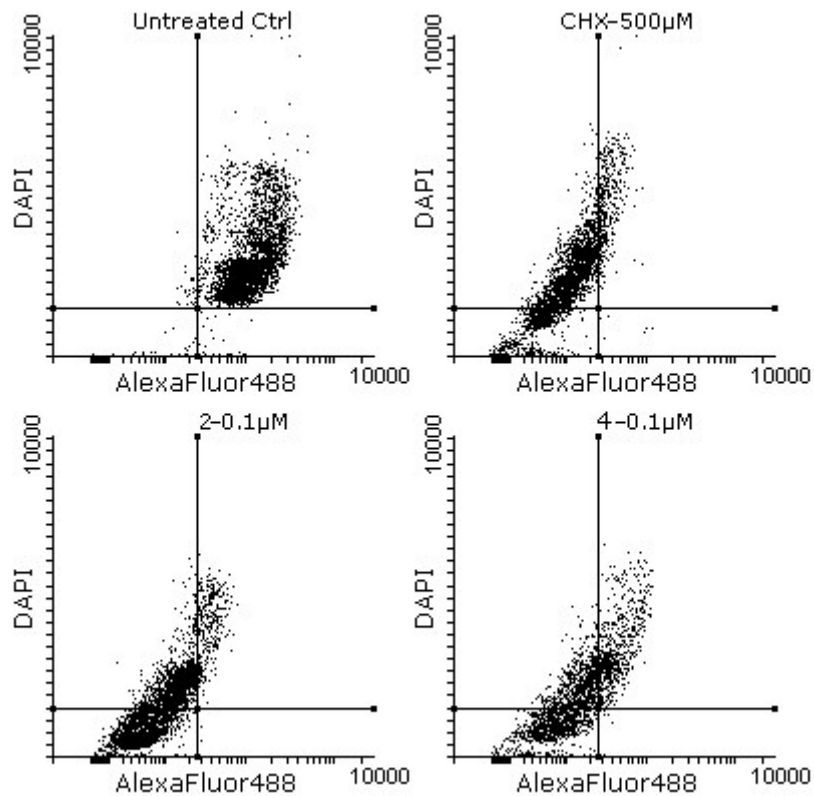


**Figure S50.** Representative dot plots of A2780 cells after 12h treatment with complexes **2** and **4** or cycloheximide (CHX) at indicated concentrations determined using OPP-incorporation Protein Synthesis Assay Kit by HTS-flow cytometry. NucelarMask/DAPI (cell nuclei staining) vs AlexaFluor488 (nascent peptides tagging) fluorescence were used to determine both cell vitality and in-cell global protein synthesis.

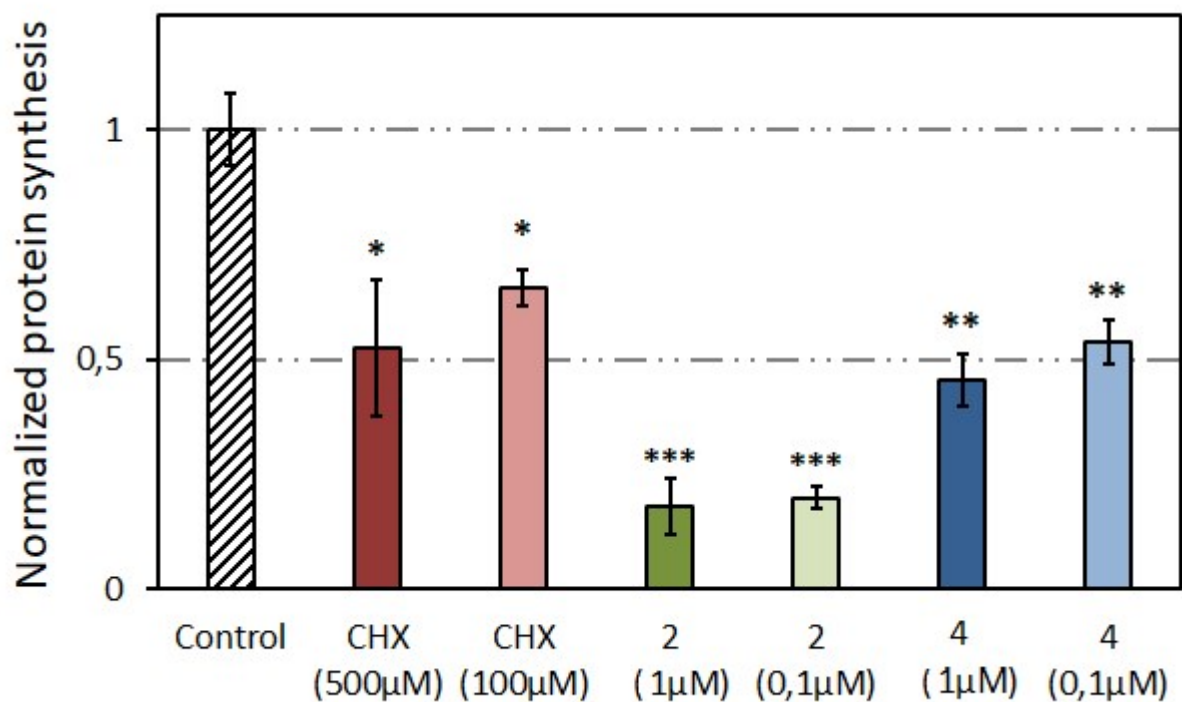
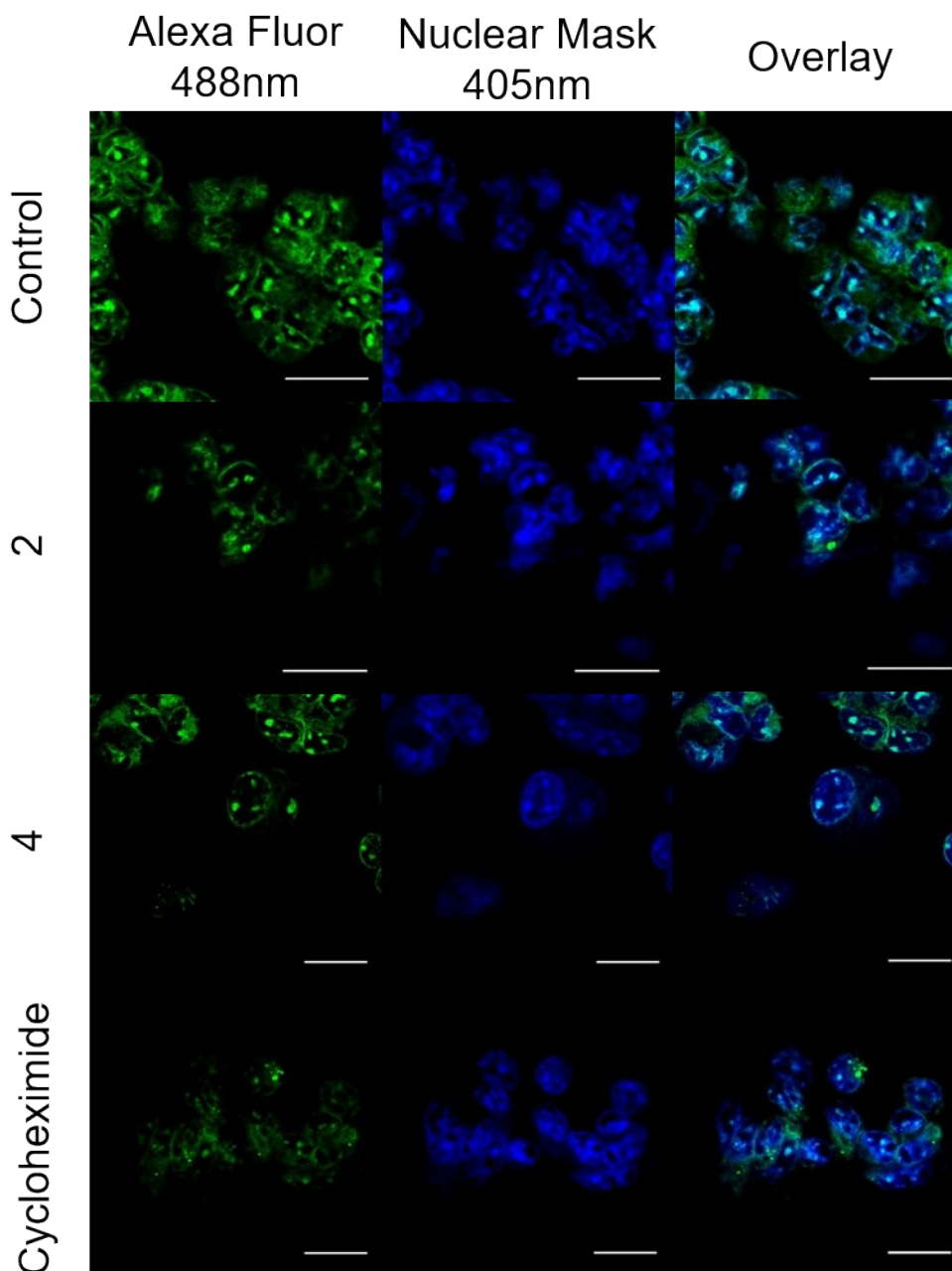


**Figure S51.** Normalized translation levels measured by O-propargyl-puromycin incorporation in nascent proteins using Click-iT Alexa Fluor-OPP Kit (Thermofisher) after treatment for 12 h with either ruthenium complexes or cycloheximide (CHX) as a positive control for proteosynthesis inhibition. Data are representative of two independent experiments and represented as mean  $\pm$  SD (n=6 biological independent replicates),  $p$  values: \* $p$ <0.05, \*\* $p$ <0.01 and \*\*\* $p$ <0.001(unpaired t-test).



**FigureS52.** Detection of protein synthesis on A2780 cells after 12 h treatment with ruthenium complexes (0.1  $\mu$ M) or cycloheximide (500  $\mu$ M) using Click-iT Alexa Fluor-OPP by confocal microscopy. NuclearMask was used for co-staining cell nuclei. Scale bar = 25  $\mu$ m.

## 12.7. Cell death induction determination by flow cytometry

The impact on cell death induction of the ruthenium complexes on A2780 cells was evaluated using the FITC-Annexin V/Propidium Iodide (PI) labelling method. Briefly, A2780 cells were seeded in 12-well plates at a density of  $2 \cdot 10^5$  cells/well and incubated overnight. Testing complexes were added at indicated concentrations for 24 h and cisplatin was used as a positive control for apoptosis induction. After treatment, cells were harvested by trypsinization, washed with PBS, centrifuged and the pellets were resuspended in 185  $\mu$ L binding buffer. Then, 5  $\mu$ L Annexin-V-FLUOS and 10  $\mu$ L PI were added and the resuspended cell solution was left at room temperature in the dark for 15 min. Cells were analyzed by flow cytometry (Beckman CoulterEpics XL) and a total of 10 000 events were acquired in each sample, registering at 620 and 525 nm for PI and Annexin V, respectively,  $\lambda_{exc} = 488$  nm. Data were analyzed using FlowingSoftware version 2.5.1. The assay was performed in two independent experiences (n= 2 per replicate) yielding similar results.

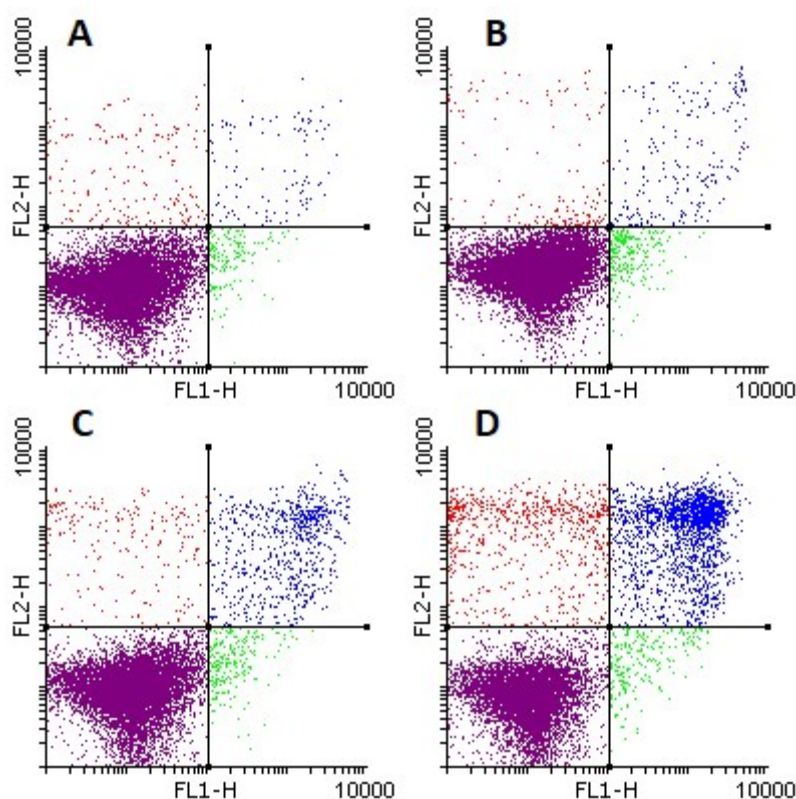


**Figure S53.** Representative dot plots of A2780 cells after 24 h treatment with complexes **2** (C), **4** (D) or cisplatin (B) at 1  $\mu$ M determined using Annexin V/PI by flow cytometry. Control cells (A) contained maximal DMSO concentration used in treatments (0.4%). FL1-H channel indicates Annexin V-FLUOS stained cells whereas FL2-H channel measures PI-positive cells.

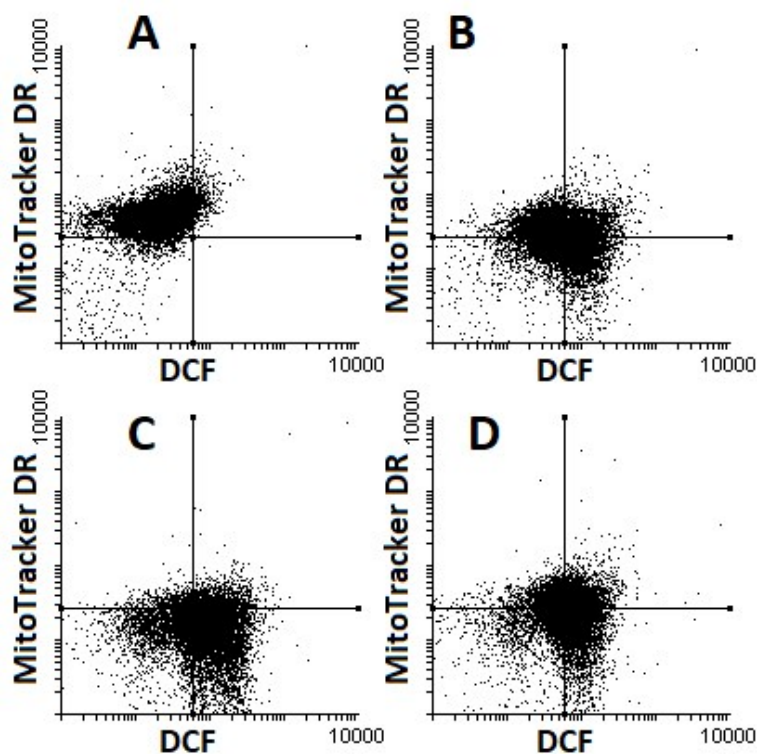


**Figure S54.** Representative flow cytometry diagrams of dual dichlorofluorescein (DCF) and Mitotracker Deep Red staining in A2780 cells after treatment with 1  $\mu$ M of Ru complexes for 8 h. Cisplatin (1  $\mu$ M) was used as a positive control. (A) Control cells, (B) Cisplatin, (C) Complex 2, (D) Complex 4.

### 13. References

- [1] C. Wang, L. Lystrom, H. Yin, M. Hetu, S. Kilina, S.A. McFarland, W. Sun, Dalton Trans. 45 (2016) 16366–16378.
- [2] J. Yellol, S.A. Pérez, A. Buceta, G. Yellol, A. Donaire, P. Szumlas, P.J. Bednarski, G. Makhloufi, C. Janiak, A. Espinosa, J. Ruiz, J. Med. Chem. 58 (2015) 7310–7327.
- [3] E. Ferrer Flegeau, C. Bruneau, P.H. Dixneuf, A. Jutand, J. Am. Chem. Soc. 133 (2011) 10161–10170.
- [4] B. Boff, M. Ali, L. Alexandrova, N.Á. Espinosa-Jalapa, R.O. Saavedra-Díaz, R. Le Lagadec, M. Pfeffer, Organometallics 32 (2013) 5092–5097.
- [5] Z. Lv, H. Wei, Q. Li, X. Su, S. Liu, K.Y. Zhang, W. Lv, Q. Zhao, X. Li, W. Huang, Chem. Sci. 9 (2018) 502–512.
- [6] J. Karges, F. Heinemann, M. Jakubaszek, F. Maschietto, C. Subecz, M. Dotou, R. Vinck, O. Blacque, M. Tharaud, B. Goud, E. Viñuelas Zahinos, B. Spingler, I. Ciofini, G. Gasser, J. Am. Chem. Soc. 142 (2020) 6578–6587.
- [7] G. Ghosh, H. Yin, S.M.A. Monro, T. Sainuddin, L. Lapoot, A. Greer, S.A. McFarland, Photochem. Photobiol. 96 (2020) 349–357.
- [8] J. Karges, P. Goldner, G. Gasser, Inorganics 7 (2019) 4.
- [9] A. Notaro, G. Gasser, A. Castonguay, ChemMedChem 15 (2020) 345–348.
- [10] H. Huang, S. Banerjee, K. Qiu, P. Zhang, O. Blacque, T. Malcomson, M.J. Paterson, G.J. Clarkson, M. Staniforth, V.G. Stavros, G. Gasser, H. Chao, P.J. Sadler, Nat. Chem. 11 (2019) 1041–1048.
- [11] G.M. Sheldrick, Acta Crystallogr. Sect. C Struct. Chem. 71 (2015) 3–8.

- [12] G.M. Sheldrick, *Acta Crystallogr. A* 64 (2008) 112–122.
- [13] T.R. Chen, *TCA Man. Tissue Cult. Assoc.* 1 (1975) 229–232.
- [14] X. Zhang, B.S. Rosenstein, Y. Wang, M. Lebowitz, H. Wei, *Free Radic. Biol. Med.* 23 (1997) 980–985.
- [15] X. Ding, Q. Xu, F. Liu, P. Zhou, Y. Gu, J. Zeng, J. An, W. Dai, X. Li, *Cancer Lett.* 216 (2004) 43–54.
- [16] C.M. Krishna, J.E. Liebmann, D. Kaufman, W. DeGraff, S.M. Hahn, T. McMurry, J.B. Mitchell, A. Russo, *Arch. Biochem. Biophys.* 294 (1992) 98–106.
- [17] J. Yamada, S. Yoshimura, H. Yamakawa, M. Sawada, M. Nakagawa, S. Hara, Y. Kaku, T. Iwama, T. Naganawa, Y. Banno, S. Nakashima, N. Sakai, *Neurosci. Res.* 45 (2003) 1–8.
- [18] V. Novohradsky, A. Rovira, C. Hally, A. Galindo, G. Viguera, A. Gandioso, M. Svitelova, R. Bresolí-Obach, H. Kostrhunova, L. Markova, J. Kasparkova, S. Nonell, J. Ruiz, V. Brabec, V. Marchán, *Angew. Chem. Int. Ed Engl.* 58 (2019) 6311–6315.